EXHIBIT D

Exponent®

Expert Report of
Lawrence E. Eiselstein, Ph.D., P.E.

In the matter of

California Sportfishing Protection Alliance (Plaintiff)

v.

Pacific Bell Telephone Company (Defendant)

Case No.
2:21-CV-00073-MCE-JDP

Exponent®

Expert Report of
Lawrence E. Eiselstein, Ph.D., P.E.

California Sportfishing Protection Alliance (Plaintiff)
v.
Pacific Bell Telephone Company (Defendant)
Case No. 2:21-CV-00073-MCE-JDP

Prepared For:

Paul Hastings LLP
101 California Street
San Francisco, CA 94111

Prepared By:

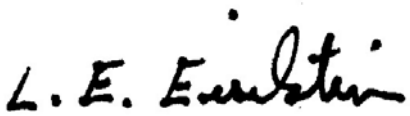

Lawrence E. Eiselstein, Ph.D., P.E.
Exponent, Inc.
149 Commonwealth Drive
Menlo Park, CA 94025

September 9, 2024

Contents

Qualifications and Personal Background of Dr. L.E. Eiselstein

I, Dr. Lawrence Eiselstein, am a Principal Engineer at Exponent, Inc. (Exponent) specializing in failure analysis, accident reconstruction, risk analysis, and materials science (corrosion and metallurgy) as applied to product design, manufacture, intellectual property issues, and materials testing and evaluation.

I have over 40 years of experience assisting clients in design and failure analysis of a wide range of commercial and civil structures. I have experience regarding the underground, atmospheric, and aqueous corrosion of piping, tanks, sewers, and other structures (including overhead, buried, and submerged structures). I also have experience related to corrosion of implantable medical devices. My work has included designing and protecting devices. I have considerable experience analyzing and measuring the corrosion rate of various materials in a wide variety of corrosive environments from highly corrosive environments such as highly acidic, highly basic, and highly oxidizing environments to environments such as soil, natural waters, atmospheric corrosion, as well as in-vivo conditions such as simulated physiological solutions. I also have experience measuring the release of metal ions (Fe, Ni, Cr, Co, Mo, and W) into the body from long-term passivating metal alloy implants.

I have experience with the corrosion and mechanical properties of lead and lead alloys used in battery and electrowinning of copper and its use in plumbing and soldering.

I hold a Ph.D., and am a Registered Professional Engineer in California in both metallurgy and corrosion engineering. My résumé is included in Appendix A.

Appendix B contains my recent deposition and trial testimony experience. My hourly billing rate, as set by my employer, Exponent, is $710 in 2024.

Introduction

This matter relates to lead-clad cables located in Lake Tahoe. The lead-clad cables were installed and used by Defendant Pacific Bell Telephone Company (Pacific Bell) for telecommunications services and are no longer in service.

Plaintiff California Sportfishing Protection Alliance (CSPA) brought a civil suit against Pacific Bell in 2021. The CSPA Complaint alleges that "Lake Tahoe water contacts the lead sheathing in the Cables and dissolves the lead, and then distributes the lead throughout Lake Tahoe and its larger environment."[1]

The CSPA Complaint also states that, "Plaintiff has obtained a portion of one of the Cables and has tested it to determine whether the Cables are likely to leach lead into Lake Tahoe."[2] Plaintiff claims that their testing results indicate that "lead in the Cables is being disseminated into the aquatic environment of Lake Tahoe."[3]

Paul Hastings, LLP (Paul Hastings) requested that I review the CSPA Complaint and evaluate the issues that it raises related to metallurgy and materials science, including lead corrosion in freshwater environments such as Lake Tahoe. I summarize my opinions related to these issues in the next section of this report, followed by a Background section with more detailed discussion of the issues. The bases for my opinions are discussed subsequently in the report.

1 Second Amended Complaint. (August 20, 2021). ¶23.

2 Second Amended Complaint. (August 20, 2021). ¶7.

3 Second Amended Complaint. (August 20, 2021). ¶7.

Executive Summary

Corrosion occurs when metals are exposed to certain environments. Corrosion processes for lead and other metals require a conductive environment such as water (or air with water vapor), among other factors. If coatings, or other protective layers, prevent lead from contacting the environment, corrosion does not occur.

Even without an externally applied protective layer or coating being present, lead exposed to environments containing water will form its own protective layer. This protective film or "passivating layer" of corrosion product can build up on the surface of the metal and act as a barrier between the metal and the environment. For lead, the passivation process tends to make it less susceptible to further corrosion and the corrosion rate is significantly reduced as this barrier film develops. Natural waters, such as those in Lake Tahoe, promote the development of a passivating layer. Based on my education, experience, and training, as well as the extensive scientific literature related to lead and lead corrosion processes, I have reached the following opinions in this matter:

Opinion 1: Lead has been used in many industries and for many applications, including as cladding for telecommunication cables, because it is durable and corrosion resistant.

Opinion 2: The subject cables in Lake Tahoe have multiple protective layers between the lead cladding and environment (i.e., water and lakebed). I have not seen any evidence of lead release from locations where the external tar-impregnated protective layers and steel rod armor around the lead cladding are intact. Based on photographs and cable survey data, the tar-impregnated protective layers appear to be intact along almost the full length of the subject cables.

Opinion 3: Where the lead cladding from the cables is in direct contact with Lake Tahoe water (e.g., due to cable damage or cut ends), a passivating layer forms that limits the lead corrosion rate (and therefore the rate at which lead can be released to the environment). If the passivating layer is disturbed such that lead again becomes exposed to the environment, the passivating layer re-forms again slowing lead release to the environment.

Opinion 4: Based on the available measurements, there is no statistically significant difference between lead concentrations a few inches away from the cable and in control locations far from the cable.

Opinion 5: The cable segment testing conducted in a "plastic container" described in Plaintiff's Complaint is not representative of the conditions in Lake Tahoe. Plaintiff's testing likely overestimated the release rate of lead because cutting and removing the test article from Lake Tahoe would have disturbed the passivating layer. The

passivating layer generally acts to slow the corrosion rate, so disturbing the passivating layer during removal and handling of the test article is likely to produce an artificially high corrosion rate (compared to the corrosion rate that would have occurred had the test article been left in its original environment).

Background

Introduction to Lake Tahoe

Lake Tahoe is a remote subalpine lake situated at an elevation of 1.90 km above sea level and surrounded by mountains including the Carson Range and the Sierra Nevada.[4] It has a large lake surface area (490 km^2) and volume (150 km^3).[5] Lake Tahoe water is relatively clear so the subject cables are visible from the surface in some locations.

Table 1 provides a summary of information about Lake Tahoe water, including certain parameters that are relevant to corrosion processes and rates.

Table 1. Lake Tahoe summary information and other information relevant to corrosion.

Parameter	Description	Reference
Temperature	Ranges from 0 to 23°C	Rowe, Saleh et al. 2002[4]
Conductance	13 to 900 (µS/cm) at 25°C	Rowe, Saleh et al. 2002[4]
pH	7.71–8.07 7.63–7.75 7.58 ± 0.30 (avg ± stdev) 8.34 ± 0.41 (avg ± stdev)	Imboden 1977[6] Haley & Aldrich 2024[7] Unpublished data referenced in Tracy 2011[8] Tracy 2011[8]
Dissolved Inorganic Carbon (DIC)	9.89 ± 0.44 mg/L (avg ± stdev)	Tracy 2011[8]
Dissolved Oxygen	Lake Tahoe: 5.2 to 12.6 mg/L	Rowe, Saleh et al. 2002[4]
Total Alkalinity as $CaCO_3$	Truckee River water: 36 to 76 mg/L in 2014 to 2016	California Water Board[9]
Phosphorus	The soluble reactive phosphorus is a measure of phosphate in the water: Median values ranged from 0.002 to 0.090 mg/L	Rowe, Saleh et al. 2002[4]

4 Rowe, T. G., Saleh, D. K., Watkins, S. A., & Kratzer, C. R. (2002). *Streamflow and water-quality data for selected watersheds in the Lake Tahoe basin, California and Nevada, through September 1998* (Water-Resources Investigations Report No. 02-4030). U.S. Geological Survey.

5 Chien, C. T., Allen, B., Dimova, N. T., Yang, J., Reuter, J., Schladow, G., & Paytan, A. (2019). Evaluation of atmospheric dry deposition as a source of nutrients and trace metals to Lake Tahoe. *Chemical Geology, 511*.

6 Imboden, D. M., Weiss, R. F., Craig, H., Michel, R. L., & Goldman, C. R. (1977). Lake Tahoe geochemical study. 1. Lake chemistry and tritium mixing study. *Limnology and Oceanography*, *22*(6).

7 Haley & Aldrich Inc. (June 2024). *Supplemental Report on Lake Tahoe Field Sampling and Analysis of Impacts of Legacy Telecommunication Cables on Water Quality, South Lake Tahoe, California*. p. 7.

8 Tracy, B. (2011). *Carbon Fluxes and Carbon Loading at Lake Tahoe, California-Nevada* [Master's thesis, University of California, Davis]. See PDF p. 96 for pH values and PDF p. 81 for DIC values.

9 California State Water Resources Control Board. *Lahontan Regional Board - Water Quality Monitoring Dashboard.* Retrieved July 2, 2024, from Lahontan Regional Board - Water Quality Dashboard (ca.gov)

Parameter	Description	Reference
Chloride	Lake Tahoe: 0.4 to 5.3 mg/L in 1968 to 1972 Lake Tahoe: 1.6 to 1.8 mg/L in the mid-1970s Truckee River: 3.36 to 16.7 mg/L	Heyvaert, Reuter, 2013 [10] Heyvaert, Reuter, 2013[10] California Water Board[9]
Silica/Silicate	14 mg/L	Nathenson 1989[11]
Bicarbonate	52 mg/L HCO_3	Nathenson 1989[11]
Dimensions	Maximum length and width: 35.4 x 19.3 km	Rowe, Saleh et al. 2002[4]
Depth	Average: 305 m; Maximum: 499 m	Rowe, Saleh et al. 2002[4]
Surface Area	490 km^2	Chien, Allen et al. 2019[5]
Water Volume	150 km^3	Chien, Allen et al. 2019[5]

[This space deliberately left blank.]

[10] Heyvaert, A. C., Reuter, J. E., Chandra, S., Susfalk, R. B., Schladow, S. G., & Hackley, S. (2013). *Lake Tahoe nearshore evaluation and monitoring framework*. Final Report prepared for the USDA Forest Service Pacific Southwest Research Station. Lake_Tahoe_Nearshore_Evaluation_and_Monitoring_Framework.pdf (sacriver.org)

[11] Nathenson, M. (1989). *Chemistry of Lake Tahoe, California-Nevada, and nearby springs* (Open File Report 88-641). Department of the Interior, US Geological Survey. See Table 2, p. 13.

The Subject Cables

Plaintiff's Complaint describes two cables that lie submerged along the west shore of Lake Tahoe and at the mouth of Emerald Bay.[12] Figure 1 is a map reproduced from the expert report in this matter of Tiffany Thomas, Ph.D., which indicates the locations of Cable A and Cable B.[13]

Figure 2 and Figure 3 show photographs of the cables as they appeared in 2021 and 2023 (see figure captions for photograph references). Figure 2 shows submerged sections of the cables.[14,15] Figure 3 shows a cut end of Cable A and an example of weathering on Cable B.[16]

Marine Taxonomic Services (MTS) removed and disassembled a section of Cable from Lake Tahoe in or around 2018.[17] MTS described the cable as follows:

> *The cable is composed of multiple layers of varying substances. The outside layer appears to be a petroleum-based tar-impregnated fiber. The layer below that is a protective layer composed of 27 strands of 0.25-inch thick solid steel rod. There are three layers of tar-impregnated twine under the steel rods. The core is separated from these outer protective layers with a rolled 0.188-inch layer of lead. Inside the lead the core is wrapped in paper. There are 13 rolled-paper elements and 24 pairs of paper wrapped solid-copper wire inside the core. Each of the paper-wrapped wire pairs is bundled with the use of a light string.*

MTS reported that that there were 3.39 lbs of lead per foot of cable.[18] Photographs of the cable from the same MTS document are shown in Figure 4.[19]

Plaintiff provided a similar description of the cables in the Complaint but described the outer coating as being jute impregnated with tar/bitumen.[20]

---

12 Second Amended Complaint. (August 20, 2021). ¶18.

13 Expert Report of Dr. Tiffany Thomas.

14 Ramboll US Consulting, Inc. (August 2023). *Lake Tahoe Water Lead Study*. Figure 3-7.

15 Haley & Aldrich Inc. (October 2021). *Investigation shows legacy telecommunication cables are not affecting water quality in Lake Tahoe, California*. p. 1.

16 Haley & Aldrich Inc. (October 2021). *Investigation shows legacy telecommunication cables are not affecting water quality in Lake Tahoe, California*. p. 1.

17 BTBMTS0015770.

18 BTBMTS0015770.

19 BTBMTS0015770.

20 Second Amended Complaint. (August 20, 2021). ¶5.

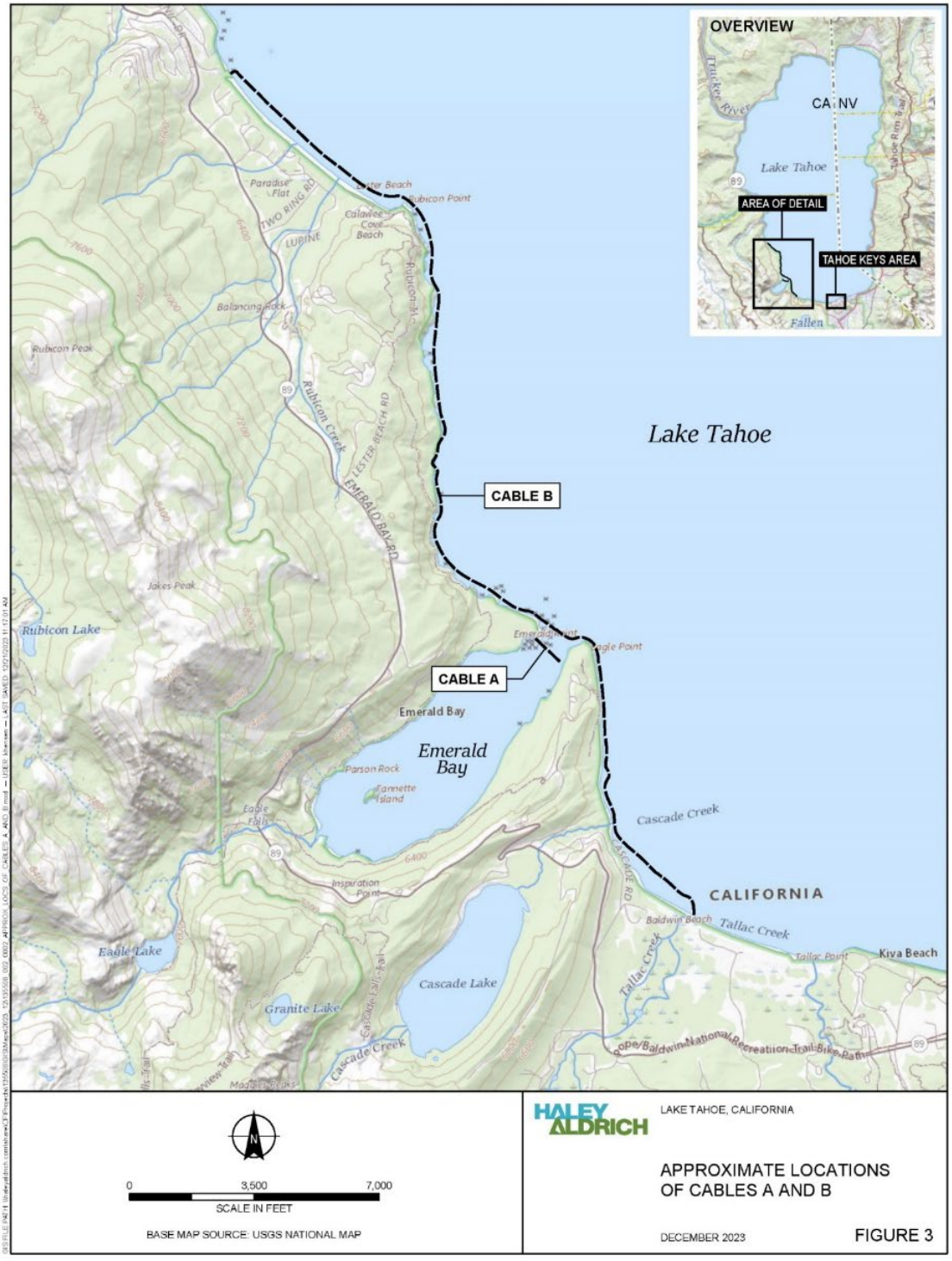

Figure 1. Map showing the locations of Cables A and B in Lake Tahoe. This map was reproduced from the expert report in this case by Dr. Thomas.[21]

[21] Expert Report of Dr. Tiffany Thomas.

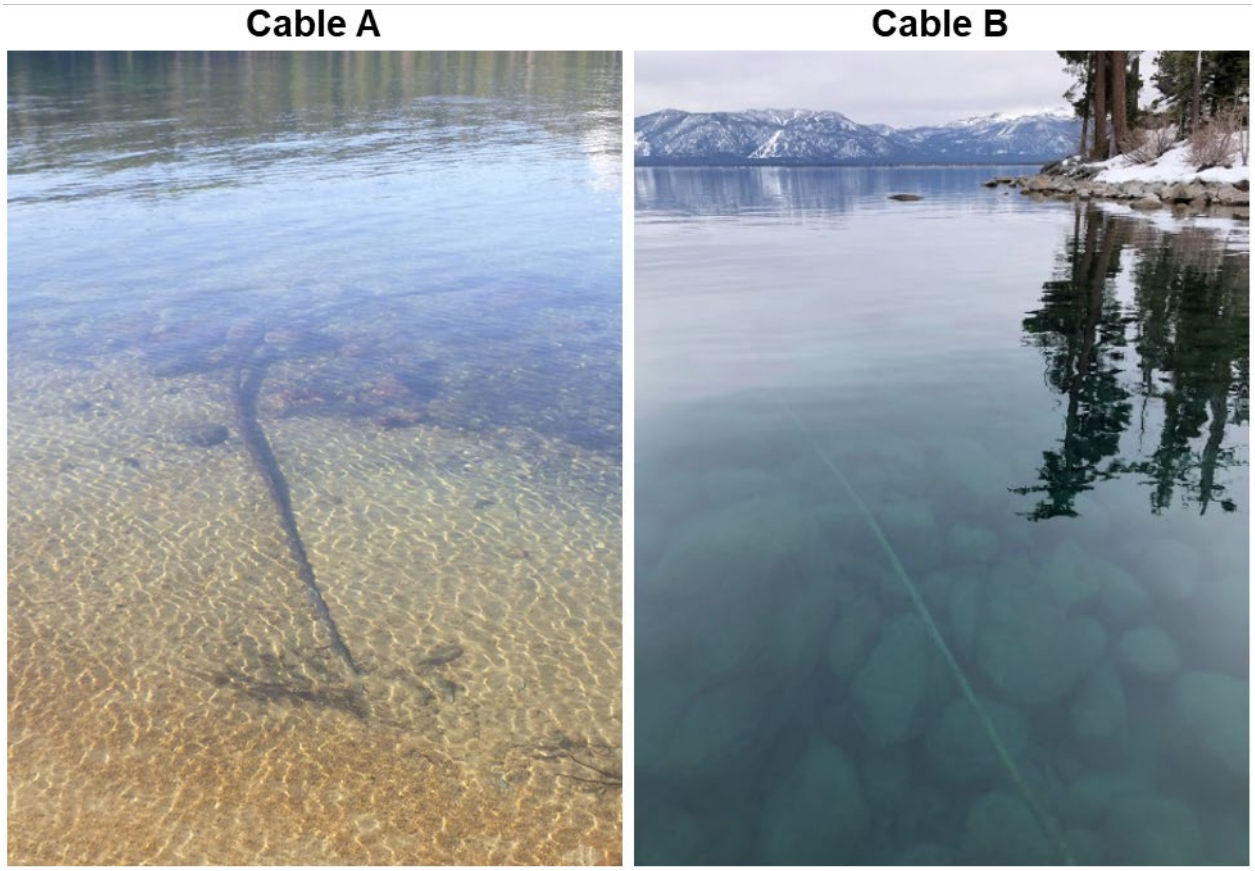

Figure 2. Photographs showing submerged Cables A[22] (Ramboll US Consulting, Inc., photograph) and B[23] (Haley & Aldrich photograph) in Lake Tahoe.

[This space deliberately left blank.]

[22] Ramboll US Consulting, Inc. (August 2023). *Lake Tahoe Water Lead Study*. Figure 3-7.

[23] Haley & Aldrich Inc. (October 2021). *Investigation shows legacy telecommunication cables are not affecting water quality in Lake Tahoe, California*. p. 1.

Cable A

Cable B

Figure 3. Haley & Aldrich photographs showing selected water sampling locations for Cables A and B in Lake Tahoe.[24]

[24] Haley & Aldrich Inc. (October 2021). *Investigation shows legacy telecommunication cables are not affecting water quality in Lake Tahoe, California.* p. 1.

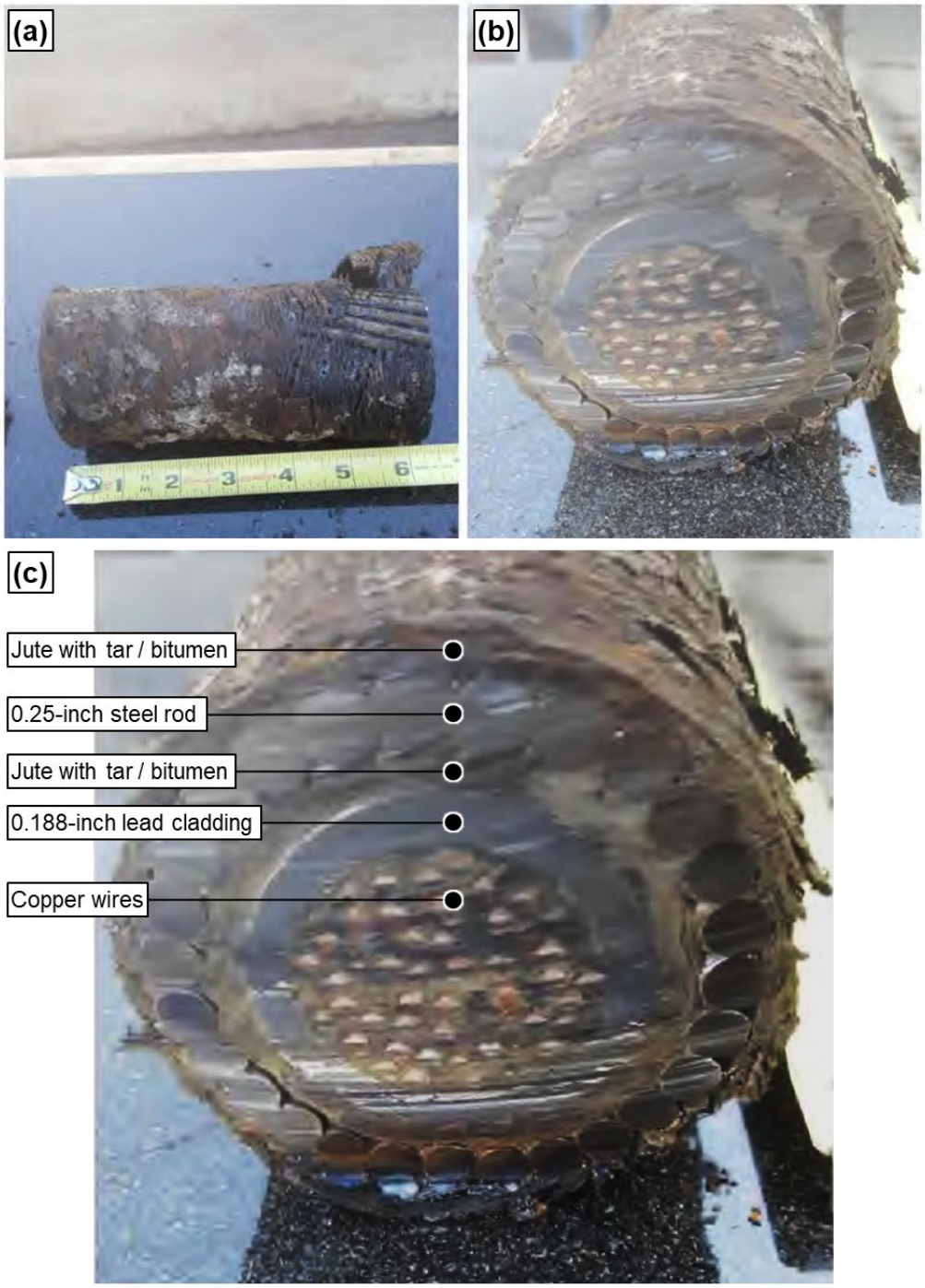

Figure 4. MTS photographs showing (a) a longitudinal view and (b) a transverse cross section through a segment of cable removed from Lake Tahoe,[25] and (c) the same transverse cross section as (b) but labelled by Exponent according to MTS descriptions of each layer in the cable.

[25] BTBMTS0015770.

Bases for Opinion 1

Opinion 1: Lead has been used in many industries and for many applications, including as cladding for telecommunication cables, because it is durable and corrosion resistant.

Introduction to Lead

Lead is a metallic element that has numerous useful properties:[26]

> *The properties of lead that make it useful in a wide variety of applications are density, malleability, lubricity, flexibility, electrical conductivity, and coefficient of thermal expansion, all of which are quite high; and elastic modulus, elastic limit, strength, hardness, and melting point, all of which are quite low. Lead also has good resistance to corrosion under a wide variety of conditions. Lead is easily alloyed with many other metals and casts with little difficulty.*

As described in more detail in Opinions 3 and 4 of this report, lead has been acknowledged as one of the "least corrodible" metals.[27] The American Society for Metals Handbook for nonferrous alloys and special-purpose materials describes that, "[l]ead is highly resistant to corrosion by the atmosphere, by waters, and by a wide range of chemicals in common use."[28] When freshly cut, lead is silvery with a hint of blue; it tarnishes to a dull gray color when exposed to air.[29]

Lead Cladding for Telecommunication and Power Cables

Lead was commonly used in the late 19th and 20th centuries for cladding and protection of power and communication cables due to "its impermeability to water and its excellent resistance to corrosion in a wide variety of soil conditions."[30] See Figure 5.[31] A 1936 review noted that, "while the choice of lead as a cable sheathing material was dictated primarily by

---

[26] Worcester, A. W., & O'Reilly, J. T. (1990). Lead and Lead Alloys. In *Metals Handbook Volume 2: Nonferrous Alloys and Special-Purpose Materials* (10th Edition, p. 545). ASM International.

For a comparison of these properties between lead and several other common metals, see Lyon, S. B. (2010). Corrosion of Lead and its Alloys. In *Shreir's Corrosion* (Vol. 3, pp. 2053-2067). Elsevier.

[27] Burns, R. M. (1936b). Corrosion of Metals—II. Lead and Lead-Alloy Cable Sheathing. *Bell System Technical Journal, 15*(4), p. 605.

[28] Worcester, A. W., & O'Reilly, J. T. (1990). Lead and Lead Alloys. In *Metals Handbook Volume 2: Nonferrous Alloys and Special-Purpose Materials* (10th Edition, p. 547). ASM International.

[29] Van Nostrand, D. (1968). *Van Nostrand's Scientific Encyclopedia*. (4th ed., pp. 998-999). D. Van Nostrand Company, Inc.

[30] Smith, J. F. (1987). Corrosion of Lead and Lead Alloys. In *Metals Handbook, Volume 13: Corrosion* (9th Edition, p. 787). ASM International.

[31] Harn, O. C. (1924). *Lead, the Precious Metal*. Century Company.

physical requirements, notably its adaptability to extrusion, corrosion resistance has been a large factor undoubtedly in its successful use."[32] The same article also indicated that the first lead-clad telephone cables were installed in 1880, and that from 1882 to 1912, the standard clad alloys used for telephone cables were 97% lead and 3% tin. The 1936 review article also described the contemporaneous structure of the lead-clad cable as follows:[33]

> *In certain sections where it is considered economical to bury cables in the ground, a coating has been devised for the protection of the sheathing against corrosion. This consists in wrapping the lead-alloy sheathed cable with asphalt-impregnated paper followed by one or more layers of jute impregnated with a preservative compound, and in some cases steel tape armoring over which there is wrapped a final layer of jute. The structure is flooded with asphalt before and after each serving of paper and each layer of jute. The steel tape is employed where there exists any danger of induction from power lines; it may be omitted in locations where there is little likelihood of trouble from this source.*

Lead-clad cable was historically produced using ram-press equipment such as the example shown in Figure 6.[34] Cable wires were passed through the center of a die while a lead tube was simultaneously formed around them, resulting in a tightly fitting sleeve.[35]

Lead cladding has also been used in paper-insulated lead-clad cable (PILC), which is lead-clad cable used in high-voltage applications. An evaluation of such cables conducted in 1992 indicated that these cables were still extensively in use because of their "excellent long-term reliability and compatibility with the existing distribution infrastructure."[36]

[This space deliberately left blank.]

---

[32] Burns, R. (1936b). Corrosion of Metals—II. Lead and Lead-Alloy Cable Sheathing. *Bell System Technical Journal, **15***(4), pp. 604, 605.

[33] Burns, R. (1936b). Corrosion of Metals—II. Lead and Lead-Alloy Cable Sheathing. *Bell System Technical Journal, **15***(4), p. 607.

[34] Harn, O. C. (1924). *Lead, the Precious Metal*. Century Company.

[35] Harn, O. C. (1924). *Lead, the Precious Metal* (p. 53). Century Company.

[36] Dyba, J., & Goodwin, F. E. (1998). New developments in lead-sheathed cables. *Conference Record of the 1998 IEEE International Symposium on Electrical Insulation (Cat. No.98CH36239)* (p. 587). IEEE.

Figure 5. Lead-clad cable from New York Telephone Company. Top: Lead-clad cable with 2,400 wires. Bottom: Unwinding lead-clad cable.[37]

[37] Harn, O. C. (1924). *Lead, the Precious Metal*. Century Company.

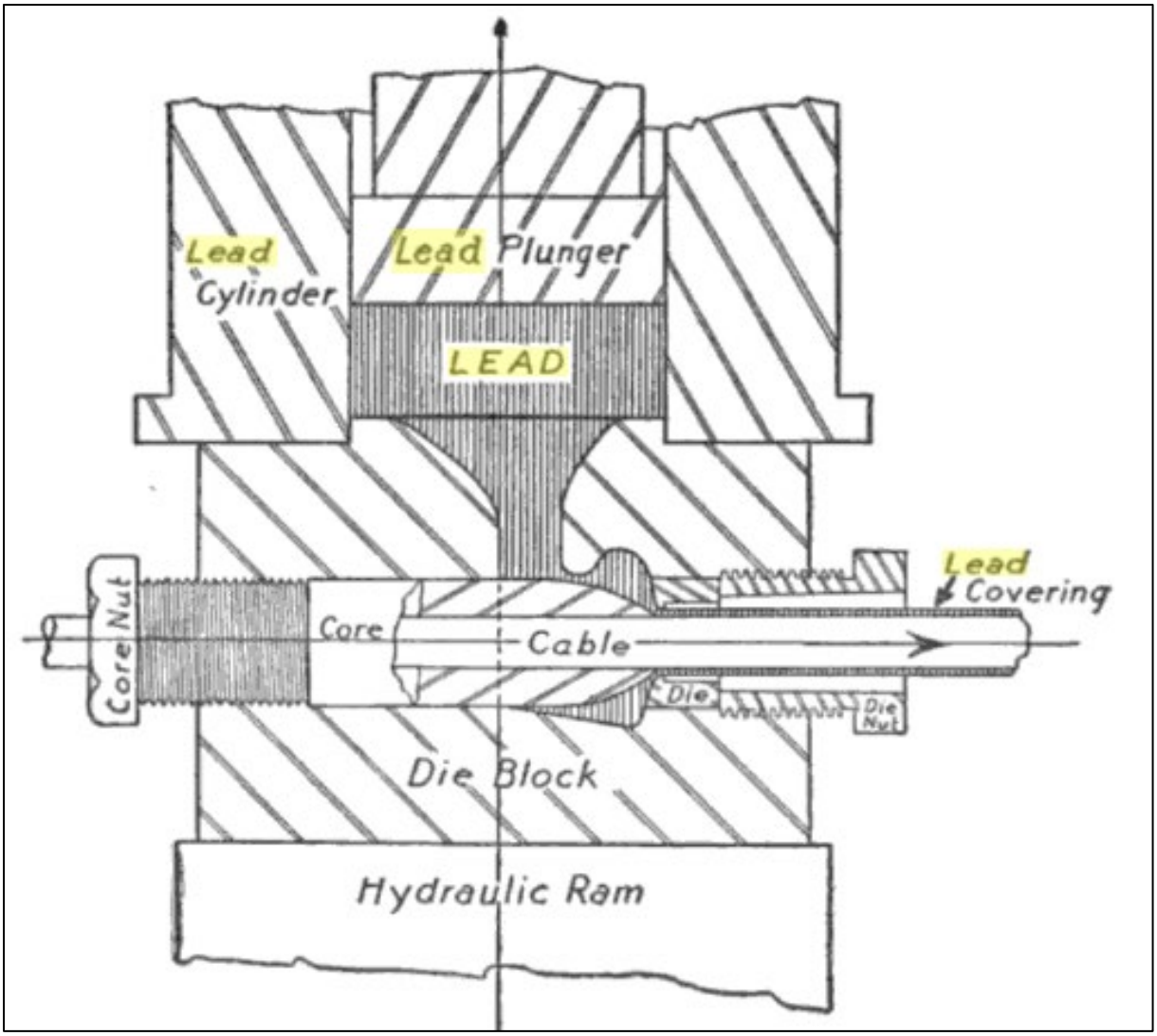

Figure 6. Die block and press for lead cladding wire cable.[38] Highlighted annotations were added by Exponent.

[This space deliberately left blank.]

[38] Harn, O. C. (1924). *Lead, the Precious Metal*. Century Company.

Examples of Lead Use in Other Industries and Applications

Lead has been known and used since prehistoric times and therefore no specific date of discovery or inventor is available.[39] The earliest lead artifacts date to the late sixth millennium BCE[40] or even earlier.[41]

As discussed in Opinion 3 of this report, lead experiences less degradation due to environmental exposure compared to most other materials used for underground, atmospheric, and aqueous applications. Consequently, historical lead artifacts and structures have survived centuries or millennia prior to discovery by archeologists. For example, 1,800-year-old lead pipes were removed from the streets and cellars of Pompeii and Rome in "a perfect state of preservation," as shown in Figure 7.[42] Lead pipes from the Roman period of England were also excavated in good condition almost 1,900 years after their original installation.[43] Additionally, "[m]any magnificent buildings, erected in the 15th and 16th centuries, still stand under their original lead roofs."[43] Also, as reported in 1924, a lead-covered dome built in 1553 in London (Barnard's Inn Hall) still remains and a lead leader-pipe head on Windsor Castle which is inscribed with the year 1589 shows little evidence of corrosion, as shown in Figure 8.[44]

Lead has also been used in a wide variety of other applications that require its unique combination of properties (including corrosion resistance),[45] for example, vessels to contain corrosive chemicals, exterior architectural features, ammunition, and lead fishing weights.

[This space deliberately left blank.]

[39] Rowe, D. J. (2018). The Lead Manufacturing Industry from Ancient Times to the Eighteenth Century. In *Lead manufacturing in Britain: a history* (Vol 16, pp. 1-18). Routledge.

[40] Killick, D., & Fenn, T. (2012). Archaeometallurgy: the study of preindustrial mining and metallurgy. *Annual Review of Anthropology, 41*.

[41] Yahalom-Mack, N., Langgut, D., Dvir, O., Tirosh, O., Eliyahu-Behar, A., Erel, Y., Langford, B., Frumkin, A., Ullman, M., & Davidovich, U. (2015). The earliest lead object in the Levant. *PLoS One, 10*(12).

[42] Harn, O. C. (1924). *Lead, the Precious Metal* (p. 47). Century Company.

[43] Wormser, F. E. (1939). The Lead Industry. In *Metals Handbook* (p. 1512). ASM International.

[44] Harn, O. C. (1924). *Lead, the Precious Metal*. Century Company.

[45] Lyon, S. B. (2010). Corrosion of Lead and its Alloys. In *Shreir's Corrosion* (Vol. 3, pp. 2053-2067). Elsevier.

Figure 7. Left: lead pipes excavated in Roman soil after 1,800 years. The pipes are in sufficiently good condition that the inscriptions (which indicate Roman plumbing firms) are still clearly legible. Right: remains of a Roman home in 67 AD illustrating lead water pipes.[46]

[This space deliberately left blank.]

[46] Harn, O. C. (1924). *Lead, the Precious Metal*. Century Company.

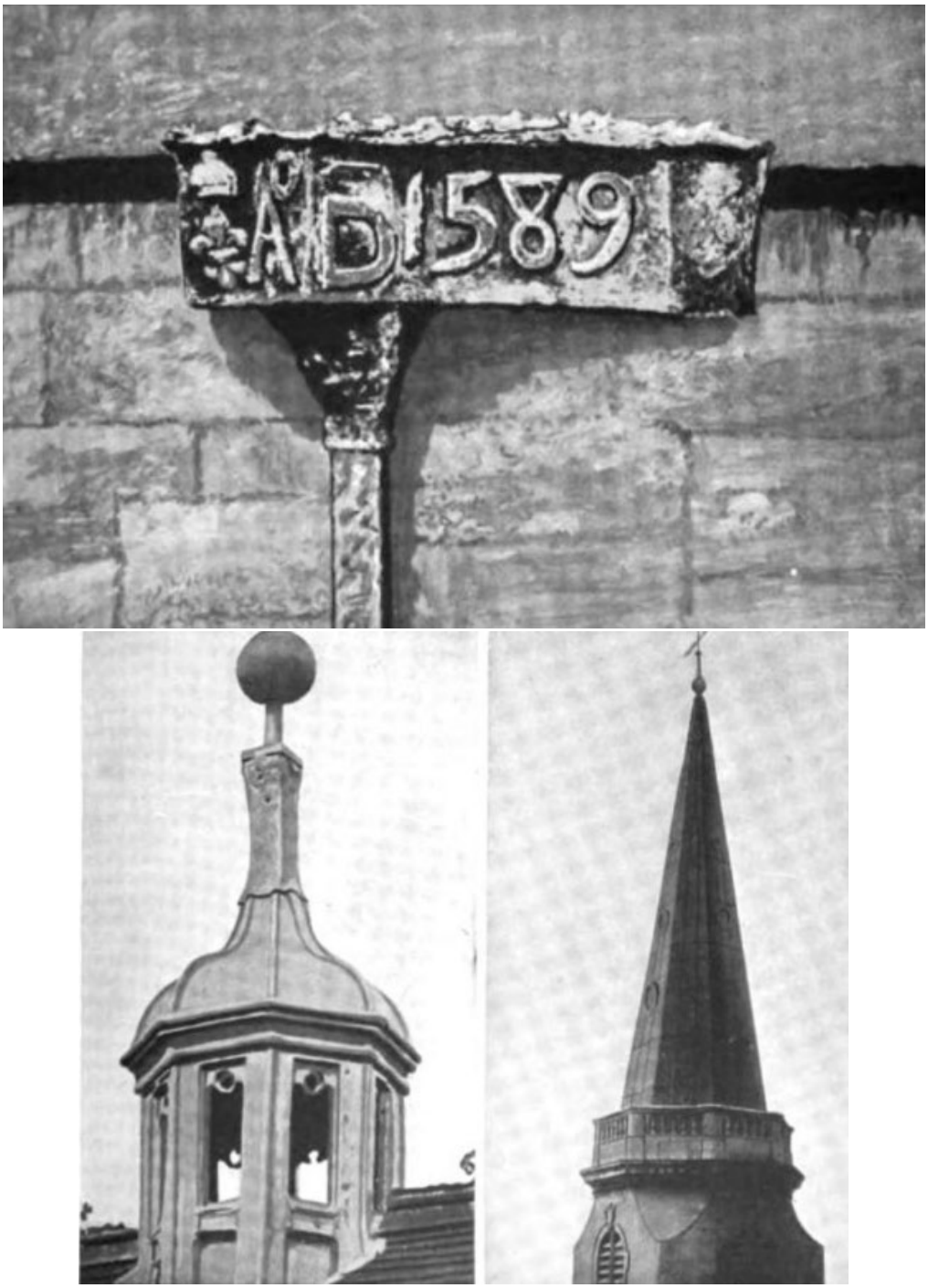

Figure 8: Examples of lead structures: top image illustrates lead leader-pipe head on Windsor Castle from the sixteenth century; bottom images show a lead-covered dome (Barnard's Inn Hall, London) from 1553 AD (left), and a lead-covered spire (St. Swithin's Church, London) from 1682 AD (right).[47]

[47] Harn, O. C. (1924). *Lead, the Precious Metal*. Century Company.

Bases for Opinion 2

Opinion 2: The subject cables in Lake Tahoe have multiple protective layers between the lead cladding and environment (i.e., water and lakebed). I have not seen any evidence of lead release from locations where the external tar-impregnated protective layers and steel rod armor around the lead cladding are intact. Based on photographs and cable survey data, the tar-impregnated protective layers appear to be intact along almost the full length of the subject cables.

Bases for Opinion 2:

As described in the Background section of this report, MTS removed and disassembled a section of cable from Lake Tahoe in or around 2018 and reported that there were several protective layers exterior to the lead cladding (i.e., layers between the lead cladding and the Lake Tahoe water or lakebed):[48]

- An outer layer of petroleum-based tar-impregnated fiber
- An intermediate layer of 27 strands of 0.25-inch solid steel rod
- Three layers of tar-impregnated twine between the lead cladding and the steel rods

All the layers noted above are between the lead cladding and the environment. In other words, the corrosion resistant lead cladding is (1) protected from mechanical damage by the steel rods and (2) protected from corrosion by the two separate layers of tar. The protective layers reduce interaction between environmental moisture and oxygen with the lead cladding, thereby reducing the potential for corrosion.

I am aware of two surveys that evaluated the conditions of the subject cables. The first was a spot survey conducted by Haley & Aldrich, which examined "underwater and unburied portions of Cable A and approximately 1,800 feet of Cable B during the survey."[49] Haley & Aldrich concluded that "[t]he spot surveys revealed that out of 18 locations surveyed along the length of the cables, 16 locations appeared visually competent with the outer jute-bitumen layer intact," and "[o]ur observation of the cables using an underwater drone and video revealed the telecommunication cables along the observed length are predominantly competent with their steel armoring and jute bitumen layer intact."[50]

MTS also conducted a survey of at least Cable B in March 2022. It appears that MTS divers surveyed the entire cable and recorded notes about the condition of the cable at 110

[48] BTBMTS0015770.

[49] Haley & Aldrich Inc. (June 2024). *Supplemental Report on Lake Tahoe Field Sampling and Analysis of Impacts of Legacy Telecommunication Cables on Water Quality, South Lake Tahoe, California*. p. 3.

[50] Haley & Aldrich Inc. (June 2024). *Supplemental Report on Lake Tahoe Field Sampling and Analysis of Impacts of Legacy Telecommunication Cables on Water Quality, South Lake Tahoe, California*. p. 9.

waypoints.[51] These waypoints appear to have been locations of interest rather than a random sample. The descriptive forms for the survey included a "Yes/No" option for the divers to indicate whether lead was visible at each waypoint. Although MTS divers noted that lead was visible at 57 of 110 locations, the written descriptions are often inconsistent with the "Yes" response. For example:

- At Waypoint 9, the divers indicated "Yes" to visible lead, but the written comment for that location was "[d]amage from mooring chains but not through steel."[52] Since the steel rods are external to the lead, and there are three additional layers of tar-impregnated twine between the steel rods and the lead cladding, it is unlikely that the lead would be visible if the steel rods were intact.
- At Waypoint 24, the divers indicated "Yes" to visible lead, but the written comment for that location was "[f]resh anchor damage, not through steel."[53]
- At Waypoint 57, the divers indicated "Yes" to visible lead, but the written comment for that location was "hung on rocks, not through steel."[54]

I reviewed comments for all 57 waypoints at which MTS divers noted that lead was visible. Based on my review, there were comments at 13 waypoints that indicated the lead was likely not visible and the remaining 44 waypoints had comments that were either consistent with lead allegedly being visible (according to the surveyors) or indeterminate.

In locations where the comments are consistent with damage to the cable that potentially exposed the lead cladding, the damage is described as localized (i.e., limited to discrete, isolated, and short sections of cable). For example:

- At Waypoint 14, the description states, "damage, possible lead exposed; sitting on large boulder."[55]
- At Waypoint 23, the description states, "[o]ver boulder, heavy wear and damage, with lead."[56]
- At Waypoint 94, the description states, "hung on rock, heavy damage, cable smashed, 4 ft long; lead visible."[57]

The descriptions listed above indicate that most of the locations where lead was reportedly visible were localized to short sections (e.g., where the cable was in contact with a boulder).

---

[51] See handwritten notes for each waypoint at BTBMTS0044868 – BTBMTS0044928 and a summary spreadsheet at BTBMTS0031728.CSV.

[52] BTBMTS0044915.

[53] BTBMTS0044886.

[54] BTBMTS0044905.

[55] BTBMTS0044881.

[56] BTBMTS0044886.

[57] BTBMTS0044925.

These descriptions are also consistent with photographs produced in this matter. For example, Figure 9 includes six representative photographs produced by Plaintiff that apparently show submerged lead-clad cables (see the references in the figure). I do not see exposed lead cladding in any of these photographs. Several of the photographs show areas where the outer layer of tar-impregnated fiber is absent (for example, see the arrow in the top left photograph), but the solid steel rods and three underlying layers of tar-impregnated twine appear to be intact. The top right photograph appears to show a section of cable that is damaged due to interaction with a large rock, but it does not show if the steel armor and underlying fiber layers are damaged to expose the lead. Moreover, the section of damaged cable in this photograph is very short (not more than a few inches long based on a comparison to the diameter of the cable), discrete, and isolated, as described above. The photographs in Figure 9 are a representative subset of the approximately 200 similar photographs[58] that were provided to me from Plaintiff's production.

Based on photographs and cable survey data described above, at minimum the steel and three layers of tar-impregnated twine between the lead and the environment appear to be intact along almost the entire length of the subject cables.

[This space deliberately left blank.]

[58] Appendix C includes a list of approximately 200 photographs showing submerged or partially submerged cables that I reviewed. I note that some of these photographs may show locations other than Lake Tahoe (i.e., other locations that were investigated as part of the June 2023 report prepared for the EDF – see BTBMTS0016103). I have not seen information about where each photograph was taken. Appendix C includes all the underwater cable photographs that were provided to me except photographs that I could specifically identify were not from Lake Tahoe (e.g., by comparison with annotated photographs from the report referenced above).

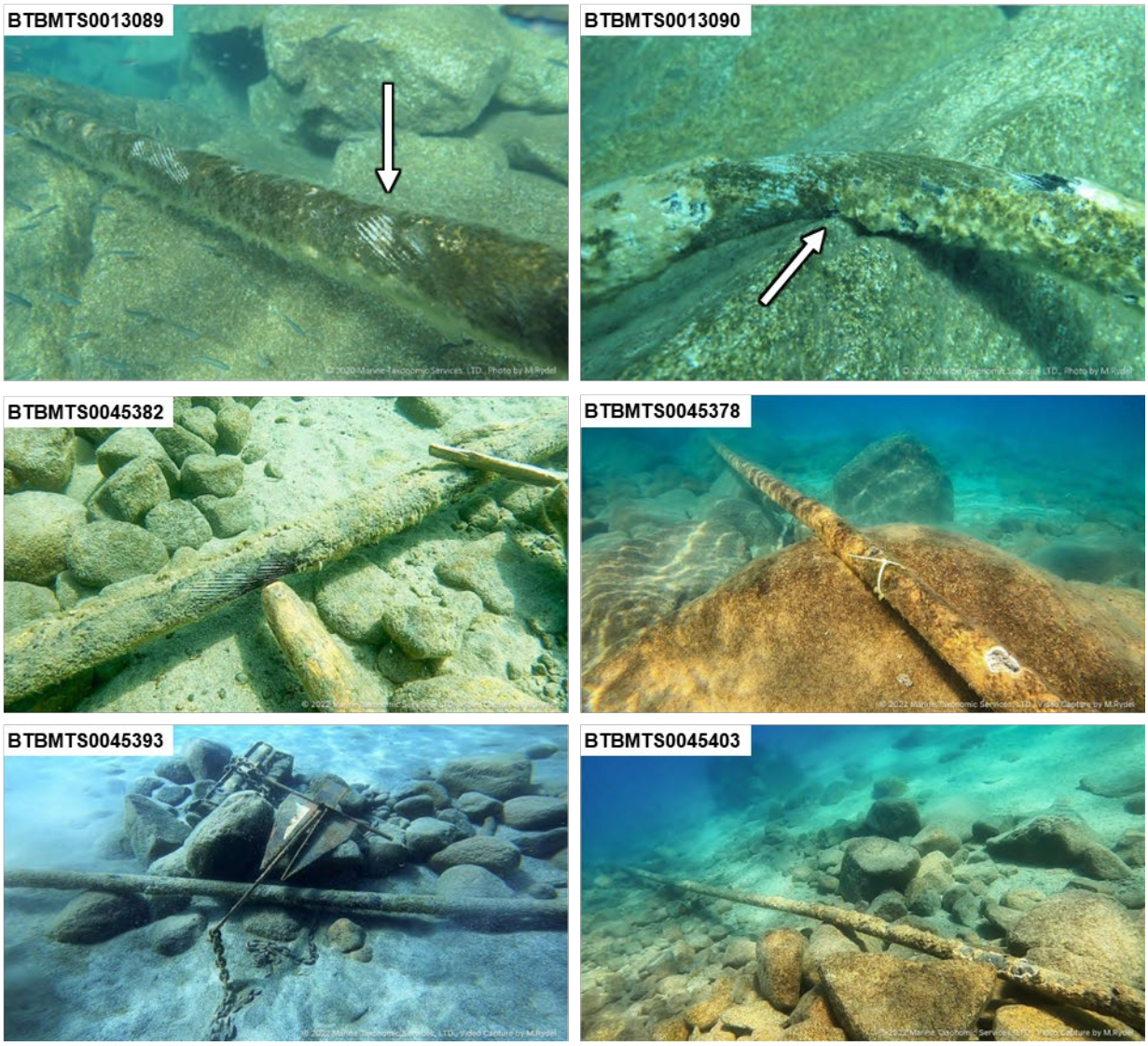

Figure 9. Representative examples of photographs produced by Plaintiff showing submerged lead-clad cables.[59] The arrow in the top left photograph was added by Exponent to illustrate a portion of the cable where the outer layer of tar-impregnated fiber disbonded and exposed the underlying steel rods. The arrow in the top right photograph was added by Exponent to illustrate a location where the cable appears to be damaged and interacting with a large rock. The outer layer of tar-impregnated fiber is absent, and the steel rods may be damaged, but it is unclear if the lead cladding is directly exposed to the water.

[59] BTBMTS0013089, BTBMTS0013090, BTBMTS0045393, BTBMTS0045378, BTBMTS0045403, BTBMTS0045382.

Bases for Opinion 3

Opinion 3: Where the lead cladding from the cables is in direct contact with Lake Tahoe water (e.g., due to cable damage or cut ends), a passivating layer forms that limits the lead corrosion rate (and therefore the rate at which lead can be released to the environment). If the passivating layer is disturbed such that lead again becomes exposed to the environment, the passivating layer re-forms again slowing lead release to the environment.

Bases for Opinion 3

This section of the report discusses corrosion and passivation behavior of lead, and the relationship between those phenomena and lead release to a surrounding environment. I will first provide brief introductory remarks about corrosion and passivation in general.

Introduction to Corrosion

Corrosion is the deterioration of materials when they react with other elements or compounds in the environment such as oxygen, water, sulfur, and carbon dioxide (CO_2). These reactions occur because the reaction products (e.g., metal oxides, sulfides, or carbonates) have lower thermochemical Gibbs free energy (available energy that can be used in a chemical transformation or reaction) than metals in their pure forms.[60,61] Consequently, the stable form (i.e., natural state) of metals is usually as a metal oxide, carbonate, or sulfide ore, and energy input is required to extract pure metals from their ores.

For example, iron is rarely found in nature as a pure metal. Instead, one of the most common sources of iron is a type of iron ore known as hematite, which is an iron oxide compound with the chemical formula Fe_2O_3. Energy (for instance, heat) must be expended to remove oxygen and create metallic iron that can be used for other purposes. However, the pure, metallic iron will not necessarily remain in that state indefinitely. Since metallic iron is not the preferred state (because it has higher Gibbs free energy than iron oxide), it will spontaneously react with oxygen and moisture to return to its natural, lower-energy state. This process is known as corrosion.

Corrosion is an electrochemical process that includes oxidation reactions (in which electrons are lost and valence is increased) and reduction reactions (in which electrons are gained and valence is decreased) on a metal surface. The reactions result in a change of the metal from a metallic state into a non-metallic state. The products of the corrosion reactions can be a dissolved species or a solid corrosion product.

---

[60] Kubaschewski, O., & Alcock, C. B. (1983). *Metallurgical Thermo-Chemistry* (5th edition, pp. 17-26). Pergamon Press.

[61] Marcus, P. (2003). Introduction to Fundamentals of Corrosion Thermodynamics. In *Metals Handbook, Vol. 13A, Corrosion: Fundamentals, Testing, and Protection* (p. 5). ASM International.

For corrosion to occur in an electrochemical system, four components must be present:

1. an anode (the site of an oxidation reaction)
2. a cathode (the site of a reduction reaction)
3. an electrolyte (for ionic transport)
4. an electrical path (for transfer of electrons)

Corrosion processes require a conductive environment such as water (or air with water vapor) must be present to facilitate the movement or transfer of ions.[62]

There are many forms or types of corrosion, but "uniform corrosion" is the most relevant form in the scope of the current matter. Uniform corrosion is a type of corrosion that occurs at approximately the same rate over the entirety of an exposed metal surface (as opposed to other types of corrosion such as pitting that can be localized to specific areas on a metal surface).[63]

Introduction to Passivation

When metals corrode, a protective film or layer of corrosion product can build up on the surface of the metal and act as a barrier between the metal and the environment. This corrosion product is often referred to as a "passivating layer" or "passive film," where passivation is the process defined as "the changing of a chemically active surface of a metal to a much less reactive state."[64] In other words, a metal that passivates becomes less susceptible to further corrosion since the surface changes to become less reactive with the surrounding environment.

In general, passivation reduces the corrosion rate of metals. A passivating layer on a metal surface slows the corrosion process by acting as a protective barrier against corrosive species, such as water and oxygen, and preventing or slowing those species from reacting with the metal. The corrosion inhibition efficiency of this protective layer depends on its characteristics such as density, thickness, adhesiveness, etc.[65] For example, if the passivating layer is thick, adhesive, and dense, then it can reduce the corrosion rate significantly.

The effects of passivating layers are experimentally measurable and have been recognized by corrosion experts for many decades. For example, a 1936 research article illustrated this effect for

---

[62] Jones, D. A. (1992). Thermodynamics and Electrode Potential. In *Principles and Prevention of Corrosion* (2nd Edition, pp. 39-44). Prentice Hall.

[63] Davis, J. R. (Ed.). (2010). Glossary of Metallurgical and Metalworking Terms. In *Metals Handbook, Desk Edition* (2nd Edition, p. 61). ASM International.

[64] Davis, J. R. (Ed.). (2010). Glossary of Metallurgical and Metalworking Terms. In *Metals Handbook, Desk Edition* (2nd Edition, p. 43). ASM International.

[65] Revie, R. W., & Uhlig, H. H. (2008). *Corrosion and Corrosion Control - An Introduction to Corrosion Science and Engineering* (4th Edition, pp. 218-220). John Wiley & Sons.

several metals including lead.[66] Figure 10 shows a plot from this article that depicts decreasing corrosion rates for copper, zinc, and lead with increasing exposure time to atmospheric conditions.[67] In this plot, the extent of corrosion is measured by "Gain in Weight" (shown on the y-axis). Weight gain occurs with corrosion because chemical species from the atmosphere react with the metal and become incorporated in the corrosion product. (Note that much of the academic literature, including other references cited in this report, discuss weight loss during corrosion testing rather than weight gain. This apparent discrepancy results from how corrosion testing is performed and does not reflect a fundamental difference in corrosion mechanisms—see Appendix D for additional details.)

If corrosion occurred at a constant rate, all the curves shown in Figure 10 would be linear (i.e., the slopes of the lines would not change over time). In fact, the slopes of the copper, zinc, and lead curves are initially steep (indicating relatively rapid gain in weight or corrosion) and the slopes decrease over time (indicating a slowing down of gain in weight or corrosion). In this specific instance, the lead curve slows down so much it appears to be horizontal, indicating that corrosion effectively slows to a degree that the rate of corrosion appears to drop to zero (although this is likely just the limit of the weight resolution used in this experiment). The review article explained this result on the basis that the passivating film on lead was "impervious to constituents of the environment."[68] As noted above, the effectiveness of a passivating layer depends on its physical characteristics and properties as well as the specific environment. The next section of this report discusses passivating layers for lead in more detail.

[This space deliberately left blank.]

[66] Burns, R. (1936a). The corrosion of metals—I. Mechanism of corrosion processes. *Bell System Technical Journal, 15*(1), pp. 20-38.

[67] Burns, R. (1936a). The corrosion of metals—I. Mechanism of corrosion processes. *Bell System Technical Journal, 15*(1), p. 24.

[68] Burns, R. (1936a). The corrosion of metals—I. Mechanism of corrosion processes. *Bell System Technical Journal, 15*(1), p. 24.

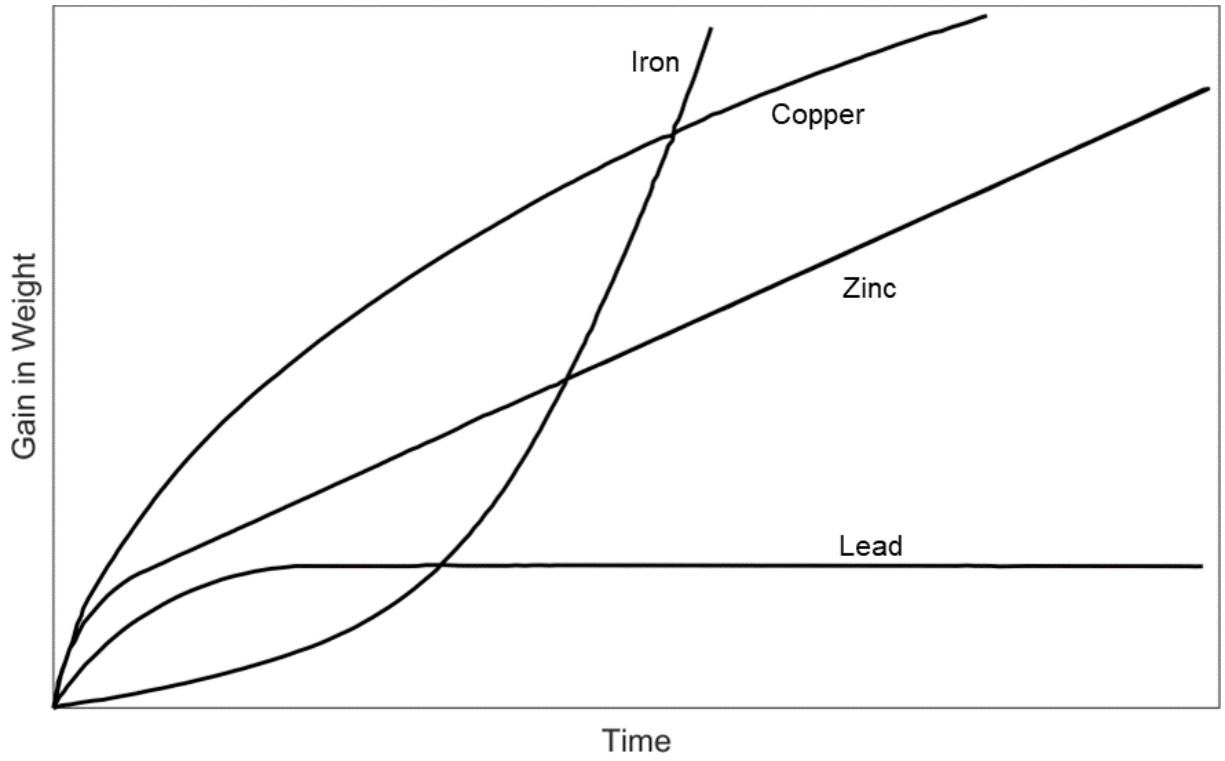

Figure 10. Weight gain versus time for metals exposed to atmospheric conditions. Adapted from original reference.[69]

[This space deliberately left blank.]

[69] Burns, R. (1936a). The corrosion of metals—I. Mechanism of corrosion processes. *Bell System Technical Journal, 15*(1), p. 24.

Corrosion and Passivating Layer Formation in Lead

Lead can form different passivating layers depending on the surrounding environment. Some examples of minerals found in lead passivating layers are listed in Table 2.

Table 2. Examples of some of the minerals found in lead passivating layers

Compound Formula	Compound Name	Reference
$PbCO_3$	Cerussite	Kushnir 2014[70]
$Pb_3(CO_3)_2(OH)_2$	Hydrocerussite	Kushnir 2014[70]
PbO_2	Plattnerite or Scrutinyite	Kushnir 2014[70]
$PbCl_2$	Lead chloride or Cotunnite	Kushnir 2014[70]
PbOHCl	Laurionite (lead oxychloride)	Kushnir 2014[70]
$PbSO_4$	(no name listed in reference)	Kushnir 2014[70]
$Pb_5(PO_4)_3OH$	Hydroxypyromorphite	Tully 2019[71]
$Pb_5(PO_4)_3Cl$	Pyromorphite	Tully 2019[71]
$Pb_5O(OH)_2(CO_3)_3$	Plumbonacrite	Tully 2019[71]
$Pb_3(PO_4)_2$	Tertiary lead orthophosphate	Triantafyllidou 2021[72]
$Pb_9(PO_4)_6$	Lead (II) orthophosphate	Triantafyllidou 2021[72]

In addition to the chemical makeup of the surrounding environment, two additional critical factors that affect corrosion of lead (or any other metal or alloy) are:

1. The pH (degree of acidity or alkalinity) in the surrounding environment, and
2. The oxidizing potential of the surrounding environment. Oxidizing potential refers to the tendency of a solution to acquire electrons in a reaction.

The chemical makeup, pH, and oxidizing potential of an environment are not necessarily independent. For example, the oxidizing potential increases with dissolved oxygen concentration or other oxidizers (i.e., chemical species that accept electrons from lead) that might be present such as chlorine or chloramine, and such species can also affect the chemical makeup of the resulting passivating layer.

The effect of these variables has been investigated for lead in aqueous (water) environments that are similar to Lake Tahoe and the results are often reported using "Pourbaix diagrams."

---

[70] Kushnir, C. S. (2014). *Influence of water chemistry parameters on the dissolution rate of the Lead (II) carbonate hydrocerussite* [Master's thesis, The University of Western Ontario].

[71] Tully, J., DeSantis, M. K., & Schock, M. R. (2019). Water quality–pipe deposit relationships in Midwestern lead pipes. *AWWA Water Science, 1*(2), e1127.

[72] Triantafyllidou, S., & Schock, M. (2021). Lead Corrosion and Release Basics. *18th Annual EPA Drinking Water Workshop: Small System Challenges and Solutions - Corrosion Training Session (Session T1)*. US EPA office of Research and Development (ORD).

Figure 11 shows adaptations of two lead Pourbaix diagrams taken from the scientific literature.[73,74] Pourbaix diagrams can be read like maps to indicate how lead (or other elements) are expected to respond with respect to corrosion in a particular environment. To interpret a Pourbaix diagram, a combination of a particular pH (x-axis) and oxidizing potential (y-axis) are selected and that point is located on the diagram. The point will fall within one of three types of regions that describe the thermodynamically favored reaction of lead. These regions are:

1. The immunity region where there is little or no thermodynamic driving force to oxidize or corrode the lead. For combinations of pH and oxidizing potential in this region, lead is not expected to react with the environment.
2. The passivation region in which a passivating layer forms and protects the lead and significantly slows the rate of corrosion.
3. The corrosion regions where the pH and potentials are such that either no passivating layer forms or the potential is so low that non-protective hydrides form.

It is important to note that passivation is not the complete absence of corrosion. In fact, passivation requires at least a small amount of corrosion because the passivating layer is simply a film of corrosion product on the metal surface. The film of corrosion product is less reactive than the underlying metal and slows the subsequent reaction between the metal and the environment, but it rarely causes the reaction to stop completely. Thus, some corrosion occurs (and in fact, must occur) even if the material passivates, but critically, passivation causes the corrosion rate to decrease over time. In contrast, the corrosion regions of the Pourbaix diagram correspond to dissolution of lead ions into the surrounding environment. Since no passivation occurs under these conditions, corrosion may occur unabated until the metal dissolves. As described below, this is <u>not</u> the case for lead-clad cables in Lake Tahoe.

[This space deliberately left blank.]

[73] Pourbaix, M., Zoubov, N. D., Vanleugenhaghe, C., & Rysselberghe, P. V. (1974). Chapter IV. Section 17.5: Lead. In *Atlas of electrochemical equilibria in aqueous solutions* (p. 490). National Association of Corrosion Engineers.

[74] Triantafyllidou, S., & Schock, M. (2019). Lead (Pb) Corrosion Control Chemistry. *2019 EPA Region 6 and ORD Small System Meeting* (pp. 9, 10).

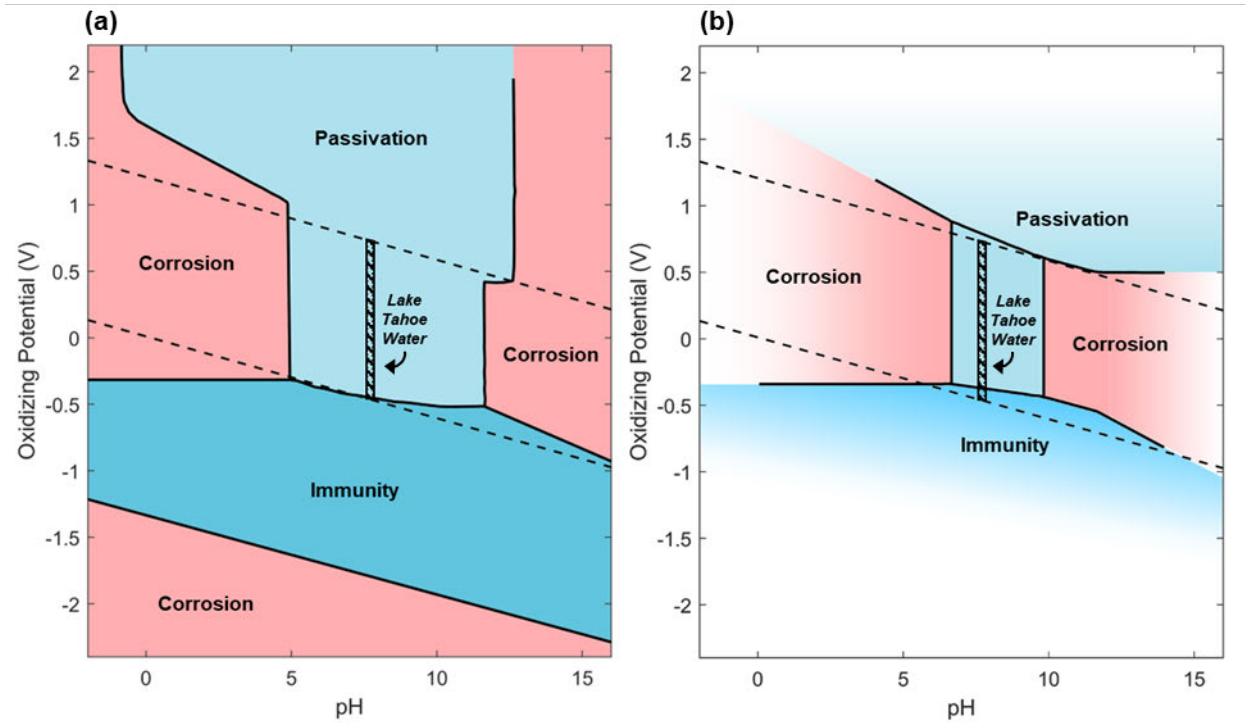

Figure 11. Examples of Pourbaix diagrams for lead. Hashed areas indicate the range of possible conditions in Lake Tahoe water based on measured pH values and physical limitations on water stability. (a) Pourbaix diagram of lead in the presence of solution containing CO_2.[75] (b) Pourbaix diagram for lead in typical drinking water.[76] Plots were adapted by Exponent from their respective sources.

Figure 11 shows Pourbaix diagrams for lead in two different aqueous environments. Figure 11a corresponds to lead in the presence of water with CO_2 at one atmosphere partial pressure and 25°C. Figure 11b corresponds to lead in the presence of typical drinking water. Although I have not seen a Pourbaix diagram specifically developed for lead in the presence of Lake Tahoe water, the pH and oxidizing potential of Lake Tahoe water can be bounded and overlaid on the existing Pourbaix diagrams, as shown by the hashed areas on each plot.

- The lower and upper bounds of pH were measured by Haley & Aldrich to be approximately 7.6 and 7.8, respectively, directly adjacent to Cables A and B.[77] The other pH measurements shown in Table 1 would still place Lake Tahoe water in the passivation region of the Pourbaix diagram.

[75] Pourbaix, M., Zoubov, N. D., Vanleugenhaghe, C., & Rysselberghe, P. V. (1974). Chapter IV. Section 17.5: Lead. In *Atlas of electrochemical equilibria in aqueous solutions* (p. 490). National Association of Corrosion Engineers.

[76] Triantafyllidou, S., & Schock, M. (2019). Lead (Pb) Corrosion Control Chemistry. *2019 EPA Region 6 and ORD Small System Meeting* (pp. 9, 10).

[77] Haley & Aldrich Inc. (June 2024). *Supplemental Report on Lake Tahoe Field Sampling and Analysis of Impacts of Legacy Telecommunication Cables on Water Quality, South Lake Tahoe, California*. Table 2.

- The oxidizing potential of Lake Tahoe water can be bounded by known water stability limits. In general, when the oxidizing potential is sufficiently high, water breaks down to evolve oxygen, and when the oxidizing potential is sufficiently low, water breaks down to evolve hydrogen. The limiting oxidizing potentials change as a function of pH and are shown by the dashed lines in Figure 11. Water is only stable in the range of oxidizing potentials between the two dashed lines. Since Lake Tahoe water does not spontaneously decompose into oxygen or hydrogen, these dashed lines represent upper and lower limits on the possible range of oxidizing potentials. Haley & Aldrich measured oxidizing potential values of 0.4–0.5 V at sampling locations adjacent to and remote from the cables.[78]

When the known pH and oxidizing potential bounds for Lake Tahoe water are plotted on the Pourbaix diagrams in Figure 11, the bounded area is within the passivation or immunity regions. There is no overlap with the corrosion region in which lead ions would be freely released from the metal. This result suggests that in an environment like Lake Tahoe water, lead is expected to develop a passivating layer (or, if oxidizing potentials are low, it may not react at all). As discussed in the next section of this report, as well as Opinion 4, the development of a passivating layer does not necessarily mean that corrosion completely stops. However, the corrosion rate may be significantly slowed.

In general, the following factors affect corrosion and passivating layer formation:[79]

- **Water** is required for corrosion.
- **pH** (i.e., the degree of acidity or alkalinity of the water).
- **Oxidizing potential** of the water. The oxidizing potential in fresh natural water is generally controlled by the dissolved oxygen content in the water. The water in Lake Tahoe is reportedly highly oxygenated.[80] Other additions to water such as chlorine or chloramine can also increase the oxidizing potential, but such additions are unlikely to be present in significant quantities in Lake Tahoe.
- **Temperature** of the water. Temperature may affect the thermodynamic stability of different passivating layers (i.e., boundaries of pH and potential where the passive material is stable; in other words, the size and shape of the domains on the Pourbaix diagram). The Pourbaix diagrams shown in Figure 11 were reportedly generated at 25°C. Based on my experience with Pourbaix diagrams, I

---

[78] Haley & Aldrich Inc. (June 2024). *Supplemental Report on Lake Tahoe Field Sampling and Analysis of Impacts of Legacy Telecommunication Cables on Water Quality, South Lake Tahoe, California*. Table 2.

[79] Pourbaix, M. (1974). *Atlas of electrochemical equilibria in aqueous solutions*. National Association of Corrosion Engineers.

[80] Rowe, T. G., Saleh, D. K., Watkins, S. A., & Kratzer, C. R. (2002). *Streamflow and water-quality data for selected watersheds in the Lake Tahoe basin, California and Nevada, through September 1998* (Water-Resources Investigations Report No. 02-4030, p. 1). U.S. Geological Survey.

expect lower temperatures in Lake Tahoe (e.g., 4–6°C in March 2021[81]) to negligibly affect the size and shape (range of pH and temperature) of the passivation regions. I also note that, separately from any effect on the Pourbaix diagrams, temperature will also affect the rate of corrosion (i.e., the reaction kinetics). Lowering the temperature generally slows the corrosion rate.

- **Dissolved inorganic carbon** (DIC) is a measure of the dissolved CO_2, bicarbonate, and carbonate.
- **Other aqueous species** such as phosphates, chlorides, sulfate, etc., can affect the variables described above and influence the chemical makeup (and resulting physical properties) of the passivating layer.

[This space deliberately left blank.]

[81] Haley & Aldrich Inc. (June 2024). *Supplemental Report on Lake Tahoe Field Sampling and Analysis of Impacts of Legacy Telecommunication Cables on Water Quality, South Lake Tahoe, California*. Table 2.

Relationship Between Lead Corrosion, Passivation, and Environmental Release

The Pourbaix diagrams shown in the previous section indicate that in aqueous environments like Lake Tahoe, lead will react with the environment and passivate. This section of the report describes how that reaction changes with time of exposure and how it relates to lead release into the surrounding environment.

When metallic lead is placed into an aqueous environment, there are two pathways by which lead can infiltrate the water:

1. Lead atoms are oxidized, and the resulting lead ions enter the water. This reaction can occur if the bare metallic lead is in contact with the water, or it can occur after a passivating layer has developed (in which case the lead ions must first diffuse through the passivating layer to reach the water, which may substantially slow the reaction rate). See Appendix E for more detailed descriptions of this chemical reaction with and without the presence of a passivating layer.
2. The passivating layer dissolves in the water and releases lead.

Figure 12 shows a simplified schematic representation of how the total lead release rate and the contributions of these pathways change with time. This figure assumes that lead is placed in an aqueous environment that causes passivation. The top image in Figure 12 is a schematic plot showing lead release rate with time. The schematic diagrams below the plot provide simplified representations of the reactions occurring at the metal surface assuming that no external protective layers are present:

- Time Point 0 represents the condition prior to environmental exposure, so the release rate is zero. In other words, the lead has not yet been placed in the water. The schematic shows metallic lead without any corrosion or passivating layer. (In reality, even exposure to humid air would likely promote the development of a passivating layer, so it is unlikely that the lead-clad cable was placed in Lake Tahoe as completely bare metal.)
- Time Point 1 represents the instantaneous moment when metallic lead is placed in water. Since there is no barrier at the lead-water interface (because the passivating layer has not had time to form), lead ions can migrate directly into the water across the entire exposed surface. Consequently, Time Point 1 on the plot has the highest lead release rate to the environment.
- Time Point 2 represents an intermediate state in which a thin passivating layer has formed. This passivating layer is simply a film of corrosion product. Since the passivating layer is still thin, it takes relatively little time for anionic species to diffuse in from the environment and react with lead ions, so the passivating layer continues growing relatively quickly. Lead ions can also still diffuse

through the passivating layer to directly reach the water (the first pathway described at the beginning of this section), but the rate is slower than at Time Point 1 because of the extra time needed to diffuse through the passivating layer. Additionally, the passivating layer that is now present can dissolve into the water and release lead (the second pathway described at the beginning of this section). Since the anionic species and lead ions do not need to diffuse very far to meet and react, the passivating layer can still grow faster than it dissolves. Overall, the rate of lead release at Time Point 2 is slower than the rate of lead release at Time Point 1.

- Time Point 3 represents the condition of the system after the passivating layer has grown thicker. Because the layer is thicker, it takes longer for the anionic species and lead ions to diffuse towards each other and react. Consequently, the growth of the passivating layer is relatively slow. Eventually, the growth rate approximately equals the rate at which the passivating layer dissolves into the water, so the thickness approaches a steady state condition. The passivating layer is also thick enough that lead ions from the metal surface take a relatively long time to diffuse through it, so the lead release to the environment predominantly comes from the slow dissolution of the passivating layer. Overall, the rate of lead release at Time Point 3 is slower than the rate of lead release at Time Points 1 and 2.

After Time Point 3, the lead release rate is effectively controlled by the dissolution rate of the passivating layer (i.e., the contribution from lead ions diffusing through the passivating layer into the environment is negligible). The dissolution rate of the passivating layer and the corrosion rate are equal.

[This space deliberately left blank.]

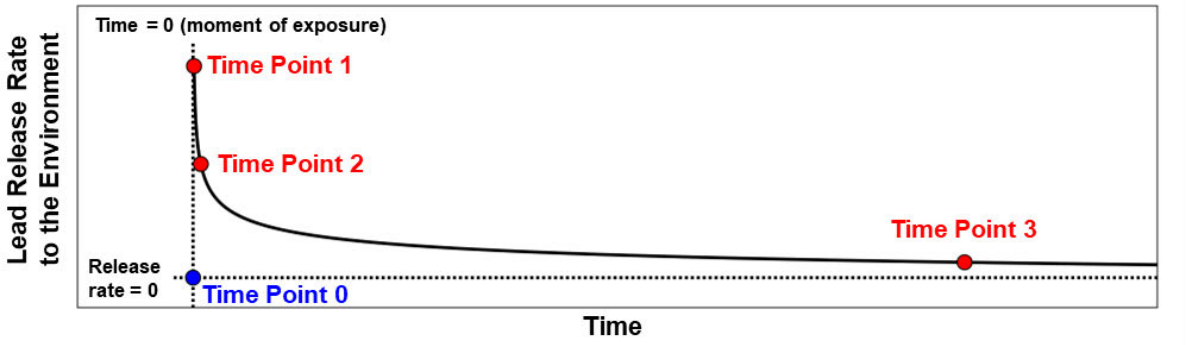

Time Point 0: Bare metallic lead before environmental exposure; no corrosion / passivating layer

Time Point 1: Instantaneous moment of initial exposure; no passivating layer formed yet

Time Point 2: Passivating layer forms and metal release rate slows

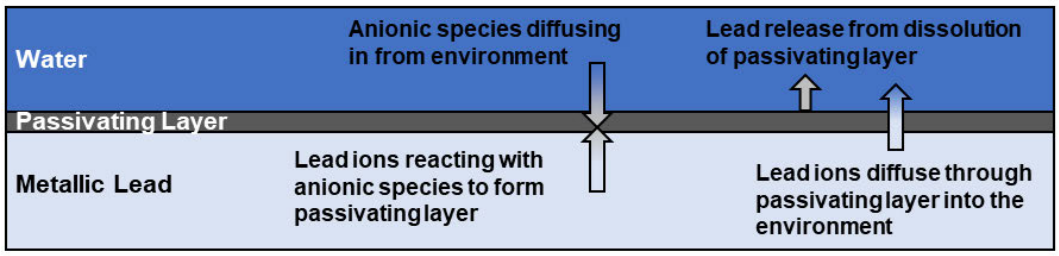

Time Point 3: Passivating layer thickness and metal release rate approach steady state

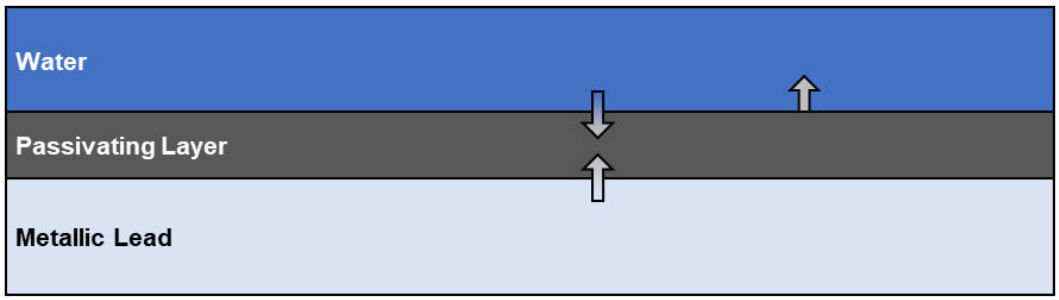

Figure 12. Simplified schematic representation of how lead release rates change with time (created by Exponent). See text for descriptions of each time point.

The conceptual model described above and shown in Figure 12 is consistent with corrosion science and engineering and indicates that corrosion rates drop to very low levels at steady state for materials that form passivating films such as lead. To accurately determine corrosion rates and the metal release to the environment at these levels, it is necessary to use more sensitive methods than traditional techniques such as those described in ASTM G1.[82] The United States Environmental Protection Agency and various academic researchers have extensively studied the amounts, mechanisms, and pathways by which lead gets into drinking water.[83,84,85,86,87,88,89] These researchers show that lead release rates to the environment can be accurately measured based on the dissolution rate of hydrocerussite or other mineral passivating layers. This method has a distinct advantage over the commonly used methods for reporting corrosion rates that are based on weight loss measurements which overestimate the amount of lead release to the surrounding environment, since the weight of the protective film is also included in this rate. Appendix D includes a more detailed discussion of this topic.

[This space deliberately left blank.]

[82] ASTM G1 (2003). Standard Practice for Preparing, Cleaning, and Evaluating Corrosion Test Specimens. ASTM International.

[83] Noel, J. D., & Giammar, D. E. (2008). The Influence of Water Chemistry on Dissolution Rates of Lead (II) Carbonate Solids Found in Water Distribution Systems. *Water Quality Technology Conference*.

[84] Giammar, D. E., Nelson, K. S., Noel, J. D., & Xie, Y. (2010). Water chemistry effects on dissolution rates of lead corrosion products [Project #4064]. *Water Research Foundation.*

[85] Xie, Y., Wang, Y., Singhal, V., & Giammar, D. E.(2010). Effects of pH and carbonate concentration on dissolution rates of the lead corrosion product PbO2. *Environmental Science & Technology, 44*(3).

[86] Xie, Y., & Giammar, D. E. (2011). Effects of flow and water chemistry on lead release rates from pipe scales. *Water Research, 45*(19).

[87] Noel, J. D., Wang, Y. and Giammar, D. E. (2014). Effect of water chemistry on the dissolution rate of the lead corrosion product hydrocerussite. *Water Research, 54.*

[88] Harmon, S. M., Tully, J., DeSantis, M. K., Schock, M. R., Triantafyllidou, S., & Lytle, D. A. (2022). A holistic approach to lead pipe scale analysis: Importance, methodology, and limitations. *AWWA Water Science*, *4*(2), e1278.

[89] Schock, M. R. (1989). Understanding corrosion control strategies for lead. *Journal AWWA*, 81(7), 88-100.

Typical Lead Corrosion Rates in Aqueous Environments

Corrosion rate data are available in scientific and engineering handbooks and literature for lead in aqueous (water-containing) environments including natural freshwater environments like Lake Tahoe. Because the corrosion rates are so low, they are typically reported in mils/year, where 1 mil is equal to 0.001 inches. For example:

- The American Society of Metals corrosion handbook lists a freshwater corrosion rate of 0.08 mils/year for lead in Gatun Lake, Panama.[90] The same reference reports steady state corrosion rates in seawater that range from 0.11 to 0.60 mils/year. Due to the presence of chlorides, seawater is generally a more corrosive environment than freshwater like Lake Tahoe.
- In another study, the corrosion rates of 16 metals and alloys, including lead, were determined over 30 months for total immersion in seawater at Port Hueneme, California. The highest reported lead corrosion rate was 0.2 mils/year.[91] Lead also exhibited the slowest corrosion rate out of the 16 metals, which included other corrosion-resistant metals like copper and stainless steel.
- Another study of metals in seawater environments reported a lead corrosion rate of 0.6 mils/year.[92]
- Another study evaluated lead for use as a corrosion-resistant barrier for high-level nuclear waste packaging, which is required to isolate nuclear waste for 1,000 years. This study found that the maximum initial corrosion rate of lead in brine was 0.04 mils/year (measured after approximately 200 days) and decreased to less than 0.01 mils/year after about 800 days of exposure. (The decrease in corrosion rate was likely associated with the formation of a passivating layer.)[93]

Critically, these rates are only applicable to exposed lead and therefore are not applicable to most of the Cable length where the external protective layers are intact. Additionally, as noted in the previous section, these corrosion rate measurements likely overestimate the lead release rate to the environment, as discussed in Appendix D of this report.

---

[90] Alhassan, S. J. (2005). Corrosion of lead and lead alloys. In *Metals Handbook, Volume 13B, Corrosion: Materials (*p. 196). ASM International.

[91] Brouillette, C. V. (1958). Corrosion Rates in Port Hueneme Harbor. *Corrosion, 14*(8).

[92] Beavers, J. A., Koch, G. H., & Berry, W. E. (1986). *Chapter 13: Lead, Zinc, Cadmium, Tin. In Corrosion of Metals in Marine Environments - A state-of-the-Art Report* (No. AD-A-171167/0/XAB; MCIC-86-50). Battelle Columbus Labs., OH (USA). Metals and Ceramics Information Center.

[93] Xiong, Y., Wang, Y., Roselle, G., & Kim, S. (2021). Lead/lead-alloy as a corrosion-resistant outer layer packaging material for high level nuclear waste disposal. *Nuclear Engineering and Design, 380*, 111294.

Bases for Opinion 4

Opinion 4: Based on the available measurements, there is no statistically significant difference between lead concentrations a few inches away from the cable and in control locations far from the cable.

Bases for Opinion 4

I am aware of the following reports that provide measurements of lead concentrations in Lake Tahoe:

- A 2019 scientific article by Chien et al., evaluated how atmospherically deposited particles, ground water, and river water inputs contribute to the trace metal content in Lake Tahoe.[94] Lead content was measured in lake water and various sources.
- A 2021 Haley & Aldrich report[95] included measurements of lead concentrations in Lake Tahoe water near and remote from Cables A and B.
- An April 2023 Pace Analytical Services report measured lead concentrations in Lake Tahoe water and sediment near to and remote from Cables A and B.[96]
- A May 2023 Pace Analytical Services report measured lead concentrations in Lake Tahoe water and sediment near to and remote from Cables A and B.[97]
- A 2023 Ramboll US Consulting, Inc. (Ramboll), report[98] measured lead concentrations in Lake Tahoe water near and remote from Cables A and B.
- A 2023 Ramboll report[99] measured lead concentrations in Lake Tahoe sediment near and remote from Cables A and B.
- Two June 2023 Cranmer Engineering, Inc., reports[100] measured lead concentrations at Eagle Point campground adjacent to Lake Tahoe and Emerald Bay.
- A 2024 Haley & Aldrich report supplementing its 2021 report noted above.[101]

---

94 Chien, C. T., Allen, B., Dimova, N. T., Yang, J., Reuter, J., Schladow, G., & Paytan, A. (2019). Evaluation of atmospheric dry deposition as a source of nutrients and trace metals to Lake Tahoe. *Chemical Geology, 511*.

95 Haley & Aldrich Inc. (October 2021). *Investigation shows legacy telecommunication cables are not affecting water quality in Lake Tahoe, California*.

96 BTBMTS0034679.

97 BTBMTS0034706.

98 Ramboll US Consulting, Inc. (August 2023). *Lake Tahoe Water Lead Study*.

99 Ramboll US Consulting, Inc. (August 2023). *Lake Tahoe Sediment Lead Study*.

100 "Lead Testing – Distribution – 6-23 (1)" and "Lead Testing – Intake – 6-23".

101 Haley & Aldrich Inc. (June 2024). *Supplemental Report on Lake Tahoe Field Sampling and Analysis of Impacts of Legacy Telecommunication Cables on Water Quality, South Lake Tahoe, California*.

I reviewed these reports to evaluate whether there was evidence of a measurable corrosion-based release of lead into Lake Tahoe water. I did not evaluate lead measurements in sediment because I understand that another expert in this matter, Dr. Andrew Nicholson, is addressing that topic.

The scientific article by Chien et al., provides baseline measurements of lead in Lake Tahoe water far from the cables (approximately 0.003 to 0.058 ppb) and other sources of lead to Lake Tahoe. However, since this article was not specifically related to the subject cables, there are no measurements of lead concentrations near the cables. Therefore, this article is useful for general context, but it is excluded from the analysis described below.

The two reports from Pace Analytical Services include measurements of lead from water and sediment collected by MTS in 2023.[102] I understand that Dr. Brian Drollette, an environmental expert engaged in this matter, has opined that these data are not reliable. Moreover, some of the lead concentration measurements in these documents exceed the equilibrium solubility of lead in Lake Tahoe water (i.e., approximately 60–100 ppb[103]). To reach the concentrations that are documented in the Pace Analytical Services reports, these water samples must have contained disturbed corrosion product, sediment, or other solid contamination that is not representative of water near an undisturbed cable. Therefore, the two reports from Pace Analytical Services are excluded from the analysis described below.

The two reports from Cranmer Engineering include measurements of lead from water near or at Eagle Point campground. One sample was collected near the Eagle Point water intake from a test tap on land connected to the intake line. The second sample was collected from campground drinking water. These reports are also excluded from the analysis described below because (1) I have not seen any information about how these samples were collected or processed, (2) I have not seen any information about the systems from which they were collected, and (3) these reports do not include corresponding measurements near and far from the subject cables.

Overview of Lead Measurements by Ramboll and Haley & Aldrich

Measurements of Lake Tahoe water by Ramboll showed that at all locations sampled, the concentration of lead was similar to background levels in Lake Tahoe.[104] In most cases, lead was not detected even when using the most sensitive method for lead detection (i.e., a lower detection limit than used in prior studies of Lake Tahoe water). The method detection limit

---

[102] BTBMTS0034679, BTBMTS0034706.

[103] This estimate is based on solubility measurements of hydrocerrusite in water with a DIC level of 10 mg C/L and a pH of 7.6 (see Table 1 for Lake Tahoe DIC and pH measurements). The June 2024 Haley & Aldrich report measured a pH of 7.6 directly adjacent to the Cables. The solubility estimate is based on values reported in Noel, J. D., Wang, Y. and Giammar, D. E. (2014). Effect of water chemistry on the dissolution rate of the lead corrosion product hydrocerussite. *Water Research, 54.*

[104] Ramboll US Consulting, Inc. (August 2023). *Lake Tahoe Water Lead Study*.

(MDL) was 0.006 ppb and the method reporting limit (MRL) was 0.02 ppb. Only one sample location out of six near a cable (conducted in duplicate) had a detectable concentration of lead—one of which was 0.049 ppb dissolved, 0.044 ppb total. The corresponding duplicate test was 0.027 ppb dissolved, 0.064 ppb total.

The Haley & Aldrich report showed similar lead levels as those measured by Ramboll.[105] The Haley & Aldrich report had a higher MDL of 0.043 ppb whereas the Ramboll report had an MDL of 0.006 ppb. The Haley & Aldrich report stated that "the lake's water quality is not adversely impacted by the two legacy telecommunication cables" based on samples collected nearest the cables (within approximately 4 inches) in most of which lead was not detected.

Statistical Analyses of Data from Ramboll and Haley & Aldrich Studies

Statistical analyses of data from the Ramboll and Haley & Aldrich studies confirm that the concentration of lead in water samples collected near the cables is not significantly higher, on average, than the concentration in samples collected farther from the cables.

The Ramboll study was conducted in June 2023 and involved the collection of seven water samples (including one field duplicate) from six monitoring stations, each near one of two lead-clad cables in Lake Tahoe, as well as eight water samples (including one field duplicate) from seven reference or offshore locations. Statistical comparisons of the data from monitoring and reference locations were performed using a lognormal regression model and treating water samples with non-detectable concentrations of lead as left-censored observations. Field duplicates and samples taken at different depths at the same location were assumed to yield independent and identically distributed measurements. For both dissolved lead (p-value=0.103) and total lead (p-value=0.109), the estimated median concentration at monitoring locations did not differ significantly from the estimated median concentration at reference locations.

Similar comparisons were performed using data from the Haley & Aldrich study, which was conducted in March 2021 and involved the collection of ten water samples (including two field duplicates) from two monitoring stations, each near one of two lead-clad cables in Lake Tahoe, as well as six water samples (including one field duplicate) from three reference (control) locations. Using the same model, methods, and assumptions as in analysis of the Ramboll study data, the estimated median concentration of total lead at monitoring locations did not differ significantly (p-value=0.779) from the estimated median concentration at reference locations. Because no control sample contained a detectable concentration of dissolved lead, the statistical comparison was based on the number of samples with detectable concentrations, and no statistically significant difference was found between the monitoring and control locations (p-value=0.5).

[105] Haley & Aldrich Inc. (June 2024). *Supplemental Report on Lake Tahoe Field Sampling and Analysis of Impacts of Legacy Telecommunication Cables on Water Quality, South Lake Tahoe, California.*

Bases for Opinion 5

Opinion 5: The cable segment testing conducted in a "plastic container" described in Plaintiff's Complaint is not representative of the conditions in Lake Tahoe.

Bases for Opinion 5

Plaintiff's Complaint described testing that, according to Plaintiff, demonstrates "that lead in the cables is being disseminated into the aquatic environment of Lake Tahoe":[106]

> *A piece of the Cable approximately 40 centimeters in length was submerged in a plastic container of Lake Tahoe water. A sample was taken of the water after one day and analysis of that sample showed that enough lead had dissolved from the Cable into the water to cause the water to have a concentration of 650 micrograms of lead per liter of water. A second sample of the water was taken after seven days and analysis of that sample showed that enough lead had continued to be dissolved from the Cable to raise the concentration of lead in the water to 1,500 micrograms per liter.*

Plaintiff produced the July 2020 Enthalpy Analytical laboratory report associated with this testing,[107] but I have not seen any other information about how the test was conducted. Such details are critical for interpreting the test results. For example:

- If the cut ends of the sample were not encapsulated, the results would only be applicable to a freshly cut lead surface and not a cable that had built up a passivating layer for years. The results would overestimate lead release rates from continuous sections of cable that had intact outer protective layers.

- Plaintiff also omitted details about the sample geometry and surface area to volume ratio, which are important parameters to report when doing corrosion and metal release rate testing.[108,109] Notably, the length of the cable described in the Complaint (40 cm) appears to be different from the length of the cable described in contemporaneous documentation from 2020 (30 cm).[110]

- Plaintiff did not describe the condition of the outer protective layers external to the lead cladding on the test article (i.e., the three layers of tar-impregnated twine

[106] Second Amended Complaint (August 20, 2021) ¶7.

[107] CSPA000002. Enthalpy Analytical Report (July 2020). Job Number 429751.

[108] ASTM G31 (2012). Standard Guide for Laboratory Immersion Corrosion Testing of Metals. ASTM International.

[109] ASTM F3306 (2019). Standard Test Method for Ion Release Evaluation of Medical Implants. ASTM International.

[110] BTBMTS0024692.

between the lead cladding and the steel rods, the steel rods, or the outer layer of tar-impregnated fiber) or if those layers had been disturbed or removed.

- Plaintiff also omitted details about the exact volume of water used for the testing and how control measurements were made.

Aside from the considerations noted above, Plaintiff's experiment likely overestimated the release rate because cutting and removing the test article from Lake Tahoe would have disturbed the passivating layer. The passivating layer generally acts to slow the corrosion rate, so disturbing the passivating layer during removal and handling of the test article is likely to produce an artificially high corrosion rate (compared to the corrosion rate that would have occurred had the test article been left in its original environment).

This issue is well known to corrosion scientists studying metal release rates from components that were previously exposed to an environment of interest. For example, old lead pipes, cautiously removed from buildings or underground and placed into standardized rack systems, initially exhibited inconsistent outcomes due to disturbances on the pipe surfaces, which disturbed the passivating layers within the pipes.[111] As stated by Schock et al., "[w]ith months of continuous flushing, restabilization took place, and the systems could be used for plumbosolvency evaluation. Even minor adjustments to the pipe racks or the addition of replicate loops or other equipment could disturb the surface films and necessitate restabilization."[112] Devine et al., have also noted that lead removed from its natural environment can take months for the passivating film to stabilize.[113]

It also appears that additional lead release testing from the Cable was performed but not discussed in the Complaint. For example, Enthalpy Analytical issued an additional report for a sample identified as "TAHOE – CAPPED" in September 2020[114] and another report with five additional samples in October 2020.[115]

---

[111] Schock, M. R., Wagner, I., & Oliphant, R. J. (1996). Corrosion and Solubility of Lead in Drinking Water. In *Internal Corrosion of Water Distribution Systems* (2nd Edition, pp. 131-230). American Water Works Association Research Foundation & DVGW-Technologiezentrum Wasser.

[112] Schock, M. R., Wagner, I., & Oliphant, R. J. (1996). Corrosion and Solubility of Lead in Drinking Water. In *Internal Corrosion of Water Distribution Systems* (2nd Edition, p. 139). American Water Works Association Research Foundation & DVGW-Technologiezentrum Wasser.

[113] Devine, C., & Triantafyllidou, S. (2023). A literature review of bench top and pilot lead corrosion assessment studies. *AWWA Water Science*, *5*(2), e1324.

[114] 2020.09.02 432773_level2.pdf. Enthalpy Analytical Report. (September 2020). Job Number 432773.

[115] 2020.10.19 434413_level2.pdf. Enthalpy Analytical Report. (October 2020). Job Number 434413.

Calculation of Corrosion Rate Based on Plaintiff's Testing

Based on the limited information provided by Plaintiff, the corrosion rate from Plaintiff's testing can be estimated. The corrosion rate can be expressed as a function of three variables:

$$Corrosion\ Rate\ \left(\frac{cm}{year}\right) = \frac{Mass\ Loss\ (\frac{g}{year})}{Surface\ Area\ (cm^2) \cdot Density\ (\frac{g}{cm^3})}$$

These variables are described below:

- Mass loss (grams/year): This is the total mass of lead that was lost from the Cable during testing. This quantity can be determined from the lead concentrations that were measured by Plaintiff. Specifically, Plaintiff reported a mass loss of 650 µg/L in one day and 1500 µg/L in one week.[116] Since the volume of water in the container was approximately 4 L,[117] the total mass loss after one day was approximately 2600 µg and the total mass loss after seven days was approximately 6000 µg. These values can be converted to mass loss per year:

Time Point	Total Mass Loss (µg)	Extrapolated Mass Loss per Year (g/year)
One day	2600	0.95
Seven days	6000	0.31

- Surface area (cm^2): This is the exposed surface area of lead that was in contact with the water in the plastic container. I assume for this calculation that the cut ends of the cable were directly exposed to the water, but the rest of the protective layers around the outside of the cable were intact. (If Plaintiff removed the outer protective layers for this testing, the corrosion rate I calculate in this section of the report would be significantly lower.) Therefore, the surface area is simply the area of lead on the ends of the cable. The lead cladding has an outer diameter of approximately 1.36 inches[118] and a reported thickness of 0.188 inches.[119] The calculated inner diameter is therefore 0.980 inches.

---

[116] Second Amended Complaint (August 20, 2021). ¶7.

CSPA000002. Enthalpy Analytical Report (July 2020). Job Number 429751.

[117] BTBMTS0024692–BTBMTS0024693.

[118] I have not seen any measurements of the outer diameter of the lead cladding, nor have I had the opportunity to directly measure the cable that Plaintiff tested. I approximated the outer diameter from the weight per foot measurements and lead cladding thickness measurements reported in BTBMTS0015770.

[119] BTBMTS0015770.

The surface area is:

$$= Area\ of\ circle\ with\ outer\ diameter - Area\ of\ circle\ with\ inner\ diameter$$

$$= \pi(\frac{D_{outer}}{2})^2 - \pi(\frac{D_{inner}}{2})^2$$

$$= 0.690\ \text{in}^2$$

Therefore, the surface area from both ends is twice this value, 1.38 in^2 or 8.90 cm^2.

- Density: This is the density of lead, 11.34 g/cm^3.[120]

Therefore, using the equation described at the beginning of this section, the corrosion rate from Plaintiff's testing was approximately:

Based on Measured Lead Concentration After...	Corrosion Rate (mils/year)
One day	3.7
Seven days	1.2

These estimated values support my opinion that Plaintiff's testing was not representative of conditions in Lake Tahoe. Notably, the apparent corrosion rate markedly decreased between sampling on the first and seventh days. This change is a result of passivation that began to occur during this interval. If Plaintiff continued taking measurements, the corrosion rate would have continued decreasing as the passivating layer continued to thicken and stabilize. In contrast, the Cable submerged in Lake Tahoe has likely been present for decades, so the passivating layer has had many years to develop. Even where lead is directly exposed to the water, which only occurs along a small fraction of the cables, the corrosion and release rates are expected to be significantly lower than the corrosion rates reported above due to the presence of a well-developed passivating layer.

[This space deliberately left blank.]

[120] Anderson, H. L. (1981). *AIP 50th anniversary: Physics vade mecum* (p. 46). American Institute of Physics.

Limitations

At the request of Paul Hastings, Exponent investigated specific issues relevant to the use of lead-clad cable. The scope of services performed during this investigation may not adequately address the needs of other users of this report, and any reuse of this report or its findings, conclusions, or recommendations is at the sole risk of the user. The opinions and comments formulated during this investigation are based on observations and information available at the time of the investigation. Exponent reserves the right to supplement or modify the findings expressed in this report, to add to the basis of and reasons for any conclusions reached, and to supplement or modify this presentation because of its ongoing investigation. No guarantee or warranty as to future life or performance of any reviewed condition is expressed or implied.

The findings presented herein are made to a reasonable degree of engineering certainty. I have endeavored to be accurate and complete in our assignment. If new data becomes available or there are perceived omissions or misstatements in this report, I ask that they be brought to my attention as soon as possible so that I can address them.

Nothing in this report should be construed as design services, and no material procurement or construction should proceed based on the information in this report.

Materials Relied Upon

Pleadings

- California Sportfishing Protection Alliance, Plaintiff, v. Pacific Bell Telephone Company, Defendant. Second Amended Complaint for Declaratory and Injunctive Relief and Civil Penalties. Filed August 20, 2021.

Produced Documents

- BTBMTS0015770.
- BTBMTS0016103
- BTBMTS0024692
- BTBMTS0031728.
- BTBMTS0034679.
- BTBMTS0034706.
- BTBMTS0044868 – BTBMTS0044928.
- CSPA000002.
- Lead Testing – Distribution – 6-23 (1)
- Lead Testing – Intake – 6-23
- 2020.09.02 432773_level2
- 2020.10.19 434413_level2
- See additional list of photographs in Appendix C.

Expert Reports

- Haley & Aldrich Inc. (June 2024). *Supplemental Report on Lake Tahoe Field Sampling and Analysis of Impacts of Legacy Telecommunication Cables on Water Quality, South Lake Tahoe, California*.
- Haley & Aldrich Inc. (October 2021). *Investigation shows legacy telecommunication cables are not affecting water quality in Lake Tahoe, California*.
- Ramboll US Consulting, Inc. (August 2023). *Lake Tahoe Sediment Lead Study*.
- Ramboll US Consulting, Inc. (August 2023). *Lake Tahoe Water Lead Study*.
- Expert Report of Dr. Tiffany Thomas.

Scientific Literature and Standards

- Alhassan, S. J. (2005). Corrosion of lead and lead alloys. In *Metals Handbook, Volume 13B, Corrosion: Materials* (p. 196). ASM International.
- Anderson, H. L. (1981). *AIP 50th anniversary: Physics vade mecum*. American Institute of Physics.
- ASTM G31 (2012). Standard Guide for Laboratory Immersion Corrosion Testing of Metals. ASTM International.
- ASTM F3306 (2019). Standard Test Method for Ion Release Evaluation of Medical Implants. ASTM International.
- ASTM G1 (2003). Standard Practice for Preparing, Cleaning, and Evaluating Corrosion Test Specimens. ASTM International.
- Beavers, J. A., Koch, G. H., & Berry, W. E.(1986). *Chapter 13: Lead, Zinc, Cadmium, Tin. In Corrosion of Metals in Marine Environments - A state-of-the-Art Report* (No. AD-A-171167/0/XAB; MCIC-86-50). Battelle Columbus Labs., OH (USA). Metals and Ceramics Information Center.
- Brouillette, C. V. (1958). Corrosion Rates in Port Hueneme Harbor. *Corrosion, 14*(8).
- Burns, R. (1936a). The corrosion of metals—I. Mechanism of corrosion processes. *Bell System Technical Journal, 15*(1).
- Burns, R. M. (1936b). Corrosion of Metals—II. Lead and Lead-Alloy Cable Sheathing. *Bell System Technical Journal, 15*(4).
- California State Water Resources Control Board. *Lahontan Regional Board - Water Quality Monitoring Dashboard.* Retrieved July 2, 2024, from Lahontan Regional Board - Water Quality Dashboard (ca.gov)
- Chien, C. T., Allen, B., Dimova, N. T., Yang, J., Reuter, J., Schladow, G., & Paytan, A. (2019). Evaluation of atmospheric dry deposition as a source of nutrients and trace metals to Lake Tahoe. *Chemical Geology, 511*.
- Davis, J. R. (Ed.). (2010). Glossary of Metallurgical and Metalworking Terms. In *Metals Handbook, Desk Edition* (2nd Edition). ASM International.
- Devine, C., & Triantafyllidou, S. (2023). A literature review of bench top and pilot lead corrosion assessment studies. *AWWA Water Science*, *5*(2), e1324.
- Dyba, J., & Goodwin, F. E. (1998). New developments in lead-sheathed cables. *Conference Record of the 1998 IEEE International Symposium on Electrical Insulation (Cat. No.98CH36239)*. IEEE.
- Giammar, D. E., Nelson, K. S., Noel, J. D., & Xie, Y. (2010). Water chemistry effects on dissolution rates of lead corrosion products [Project #4064]. *Water Research Foundation.*
- Harmon, S. M., Tully, J., DeSantis, M. K., Schock, M. R., Triantafyllidou, S., & Lytle, D. A. (2022). A holistic approach to lead pipe scale analysis: Importance, methodology, and limitations. *AWWA water science, 4*(2), e1278.

- Harn, O. C. (1924). *Lead, the Precious Metal*. Century Company.
- Heyvaert, A. C., Reuter, J. E., Chandra, S., Susfalk, R. B., Schladow, S. G., & Hackley, S. (2013). *Lake Tahoe nearshore evaluation and monitoring framework*. Final Report prepared for the USDA Forest Service Pacific Southwest Research Station. Lake_Tahoe_Nearshore_Evaluation_and_Monitoring_Framework.pdf (sacriver.org)
- Imboden, D. M., Weiss, R. F., Craig, H., Michel, R. L., & Goldman, C. R. (1977). Lake Tahoe geochemical study. 1. Lake chemistry and tritium mixing study. *Limnology and Oceanography*, *22*(6).
- Jones, D. A. (1992). Thermodynamics and Electrode Potential. In *Principles and Prevention of Corrosion* (2nd Edition). Prentice Hall.
- Killick, D., & Fenn, T. (2012). Archaeometallurgy: the study of preindustrial mining and metallurgy. *Annual Review of Anthropology, 41*.
- Křivý, V. (2012). Design of corrosion allowances on structures from weathering steel. *Procedia Engineering, 40.*
- Kubaschewski, O., & Alcock, C. B. (1983). *Metallurgical Thermo-Chemistry* (5th edition). Pergamon Press.
- Kushnir, C. S. (2014). *Influence of water chemistry parameters on the dissolution rate of the Lead (II) carbonate hydrocerussite* [Master's thesis, The University of Western Ontario].
- Lyon, S. B. (2010). Corrosion of Lead and its Alloys. In *Shreir's Corrosion* (Vol. 3). Elsevier.
- Marcus, P. (2003). Introduction to Fundamentals of Corrosion Thermodynamics. In *Metals Handbook, Vol. 13A, Corrosion: Fundamentals, Testing, and Protection*. ASM International.
- Nathenson, M. (1989). *Chemistry of Lake Tahoe, California-Nevada, and nearby springs* (Open File Report 88-641). Department of the Interior, US Geological Survey.
- Noel, J. D., & Giammar, D. E. (2008). The Influence of Water Chemistry on Dissolution Rates of Lead (II) Carbonate Solids Found in Water Distribution Systems. *Water Quality Technology Conference*.
- Noel, J. D., Wang, Y. and Giammar, D. E. (2014). Effect of water chemistry on the dissolution rate of the lead corrosion product hydrocerussite. *Water Research, 54.*
- Pourbaix, M. (1974). *Atlas of electrochemical equilibria in aqueous solutions*. National Association of Corrosion Engineers.
- Revie, R. W., & Uhlig, H. H. (2008). *Corrosion and Corrosion Control - An Introduction to Corrosion Science and Engineering* (4th Edition). John Wiley & Sons.
- Rowe, D. J. (2018). The Lead Manufacturing Industry from Ancient Times to the Eighteenth Century. In *Lead manufacturing in Britain: a history* (Vol 16). Routledge.
- Rowe, T. G., Saleh, D. K., Watkins, S. A., & Kratzer, C. R. (2002). *Streamflow and water-quality data for selected watersheds in the Lake Tahoe basin, California and Nevada, through*

September 1998 (Water-Resources Investigations Report No. 02-4030). U.S. Geological Survey.

- Schock, M. R., Wagner, I., & Oliphant, R. J. (1996). Corrosion and Solubility of Lead in Drinking Water. In *Internal Corrosion of Water Distribution Systems* (2nd Edition). American Water Works Association Research Foundation & DVGW-Technologiezentrum Wasser.
- Schock, M. R. (1989). Understanding corrosion control strategies for lead. *Journal AWWA*, 81(7), 88-100.
- Smith, J. F. (1987). Corrosion of Lead and Lead Alloys. In *Metals Handbook, Volume 13: Corrosion* (9th Edition). ASM International.
- Tracy, B. (2011). *Carbon Fluxes and Carbon Loading at Lake Tahoe, California-Nevada* [Master's thesis, University of California, Davis].
- Triantafyllidou, S., & Schock, M. (2021). Lead Corrosion and Release Basics. *18th Annual EPA Drinking Water Workshop: Small System Challenges and Solutions - Corrosion Training Session (Session T1)*. US EPA office of Research and Development (ORD).
- Triantafyllidou, S., & Schock, M. (2019). Lead (Pb) Corrosion Control Chemistry. *2019 EPA Region 6 and ORD Small System Meeting*.
- Tully, J., DeSantis, M. K., & Schock, M. R. (2019). Water quality–pipe deposit relationships in Midwestern lead pipes. *AWWA Water Science, 1*(2), e1127.
- Van Nostrand, D. (1968). *Van Nostrand's Scientific Encyclopedia*. (4th ed.). D. Van Nostrand Company, Inc.
- Worcester, A. W., & O'Reilly, J. T. (1990). Lead and Lead Alloys. In *Metals Handbook Volume 2: Nonferrous Alloys and Special-Purpose Materials* (10th Edition). ASM International.
- Wormser, F. E. (1939). The Lead Industry. In *Metals Handbook*. ASM International.
- Xie, Y., & Giammar, D. E. (2011). Effects of flow and water chemistry on lead release rates from pipe scales. *Water Research, 45*(19).
- Xie, Y., Wang, Y., Singhal, V., & Giammar, D. E.(2010). Effects of pH and carbonate concentration on dissolution rates of the lead corrosion product PbO2. *Environmental Science & Technology, 44*(3).
- Xiong, Y., Wang, Y., Roselle, G., & Kim, S. (2021). Lead/lead-alloy as a corrosion-resistant outer layer packaging material for high level nuclear waste disposal. *Nuclear Engineering and Design, 380*, 111294.
- Yahalom-Mack, N., Langgut, D., Dvir, O., Tirosh, O., Eliyahu-Behar, A., Erel, Y., Langford, B., Frumkin, A., Ullman, M., & Davidovich, U. (2015). The earliest lead object in the Levant. *PLoS One, 10*(12).

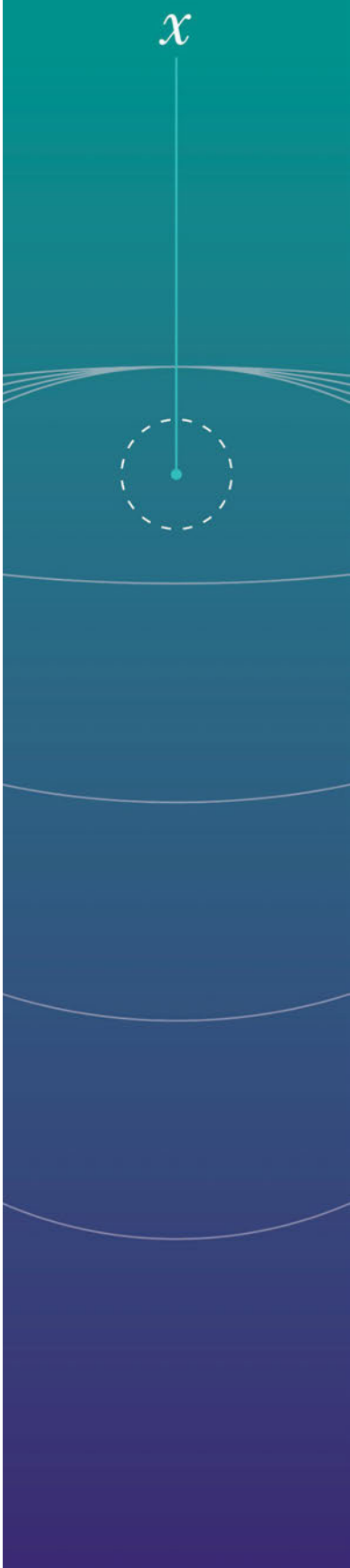

Appendix A

Résumé of L. E. Eiselstein, Ph.D., P.E.

Exponent®
Engineering & Scientific Consulting

Larry Eiselstein, Ph.D., P.E.
Principal Engineer | Materials and Corrosion Engineering
Menlo Park
+1-650-688-7084 tel | eisel@exponent.com

Professional Profile

Dr. Eiselstein specializes in failure analysis, accident reconstruction, risk analysis, and materials science (corrosion, metallurgy, composites, polymers, ceramics, and glass) as applied to product design, manufacture, intellectual property issues, and materials testing and evaluation. He has more than 30 years of experience assisting clients in the areas of design and failure analysis of a wide range of commercial and civil structures.

Dr. Eiselstein's research includes the mechanical behavior of materials (strength, fracture, fatigue, and creep), armor development, corrosion science, and testing as applied to material selection, coating evaluation, breakdown potential, repassivation, polarization, galvanic, stress corrosion cracking (SCC), hydrogen embrittlement issues and indentation hardness and fracture toughness of ceramics and single crystals.

Dr. Eiselstein's medical device consulting includes aerosol delivery devices, anastomosis devices, catheters, cochlear implants, delivery systems, electrosurgical tools, feeding tubes, fertility control devices, guidewires, heart valves, heart valve repair devices, aneurysm repair devices, orthopedic devices, hypodermic needles, batteries, intra-aortic balloon pumps, pacemakers, stents and stent grafts, syringe, trocars, as well as other medical devices. His consulting includes design analysis and testing for FDA approval of implantable devices manufactured from plastics, ceramics, stainless steel, superelastic nitinol (NiTi), Elgiloy, and MP35N; support for 510K and PMA submissions to FDA as well as failure modes and effect analysis (FMEA) for medical devices; failure analysis of implantable medical devices; and intellectual property issues.

Dr. Eiselstein has applied his materials and corrosion science skills to investigate and prevent accidents involving chemical releases, fires, and explosions. He has extensive experience dealing with fatigue, deformation and fracture of materials, fractography, electronic and microelectronic failure analysis, and all aspects of corrosion (including corrosion fatigue, environmentally assisted cracking, and hydrogen embrittlement) as applied to bridges, chemical and power plant components, construction industry, condensers, boilers, consumer products, electrical and electronic products, fire and explosion investigations, oil and gas pipelines, plumbing and piping, pressure vessels, reactor vessels, steam turbines, solder joints, thermal interface, underground storage tanks, and welds and brazing.

Prior to joining Exponent, Dr. Eiselstein was a metallurgist with SRI International, worked as a Research Associate at Stanford University, was a consultant for EPRI, and worked at Huntington Alloys, an INCO company.

Academic Credentials & Professional Honors

Ph.D., Materials Science, Stanford University, 1983

M.S., Materials Science, Stanford University, 1976

B.S., Metallurgical Engineering, Virginia Polytechnic Institute and State Univ, 1974

International Nickel Company Scholarship, Virginia Tech

Townsend Fellowship, Stanford University

Wire Foundation Competition Prize

A.O. Smith-Inland Company 4th Annual Ferrous Powder Metallurgy Competition prize winner

Licenses and Certifications

Professional Engineer Metallurgical, California, #1779

Professional Engineer Corrosion, California, #1067

Professional Affiliations

Surface Mount Technology Association—SMTA

American Water Works Association (member)

American Society for Testing and Materials, Committee on Medical and Surgical Materials and Devices (member)

American Society for Metals (member)

American Institute of Mining and Metallurgical Engineers (member)

National Association of Corrosion Engineers (member)

Publications

Spece H, Underwood RJ, Baykal D, Eiselstein LE, Torelli DA, Klein GR, Lee GC, and Kurtz SM. Is there material loss at the conical junctions of modular components for total knee arthroplasty? The Journal of Arthroplasty, 2019.

Huet R, Eiselstein LE. Lessons learned from explosion in ammonium nitrate neutralizer. Symposium on Chemistry, Process Design, and Safety in the Nitration Industry, Spring ACS Meeting, San Diego, CA, March 25-29, 2012.

Caligiuri RD, Eiselstein LE, Eastep LN. Proper design, and fabrication of socket welds for use in sour service. Materials Science Forum/Advanced Materials Research, 2010; 638-642: 3649-3654.

Eiselstein LE, Caligiuri RD. Metal Ion leaching from implantable medical devices. Materials Science Forum/Advanced Materials Research, 2010; 638-642: 754-759.

Fasching A, Kuş E, James B, Bhargava Y, Eiselstein L. The effects of heat treatment, surface condition and strain on nickel-leaching rates and corrosion performance in nitinol wires. Materials and Processes

for Medical Devices, ASM International, Minneapolis, MN, August 2009.

Eiselstein LE, et al. Acceptance criteria for corrosion resistance of medical devices: statistical analysis of nitinol pitting in in vivo environments. J Mater Eng Perform, 2009; 18(5-6):768-780.

Guyer EP, Eiselstein LE, Verghese P. Accelerated testing of active implantable medical devices. Paper No. 09464, Corrosion 2009, NACE International, 2009.

Sjong A, Eiselstein LE. Marine atmospheric SCC of unsensitized stainless-steel rock-climbing protection. J Failure Analy Prev, 2008; 8(5).

Caligiuri RD, Eiselstein LE, Schmidt CG, Giovanola JH. Stable deformation at very high strain rates in UHCS. Int J Microstructure Mat Properties, 2008; 3(5).

Eiselstein LE, Steffey D, Nissan A, Corlett N. Toward an acceptance criterion for the corrosion resistance of medical devices: a statistical study of the pitting susceptibility of nitinol. Proceedings, SMST-2007 the International Conference on Shape Memory and Superelastic Technologies, ASM International, Tsukuba City, Japan, December 2-4, 2007.

Nissan A, Corlett N, Eiselstein LE, Steffey D. Effect of long-term immersion on the pitting corrosion resistance of nitinol. Proceedings, SMST-2007 ASM International Conference on Shape Memory and Superelastic Technologies, Tsukuba City, Japan, December 2-4, 2007.

Eiselstein LE, Proctor DM, Flowers TC. Trivalent and hexavalent chromium issues in medical implants. Materials Science Forum 2007; 539-543:698-703.

Eiselstein LE, James BA. Medical device failures. 2nd International Conference on Engineering Failure Analysis, Toronto, Canada, September 12-15, 2006.

Beaudet RA, Berkowitz JB, Doherty RM, Eiselstein LE, Gekler WC, Gollin M. Review and assessment of the proposals for design and operation of designated chemical agent destruction pilot plants (DCAPP-Blue Grass II). National Research Council of the National Academies, July 2006.

Caligiuri RD, Eiselstein LE, Schmidt CG, Giovanola JH. Stable deformation at very high strain rates in UHCS. THERMEC'2006, International Conference on Processing and Manufacturing of Advanced Materials, Chandra T (ed), Trans Tech Publications, July 2006.

Eiselstein LE, Proctor DM, Flowers TC. Trivalent and hexavalent chromium issues in medical implants. THERMEC'2006, International Conference on Processing and Manufacturing of Advanced Materials, Chandra T (ed), Trans Tech Publications, July 2006.

James B, Wood L, Murray S, Eiselstein LE, Foulds J. Compressive damage-induced cracking in nitinol. Proceedings, International Conference on Shape Memory and Superelastic Technologies, Baden-Baden, Germany, October 3-7, 2004; ASM International, pp. 117-124, 2006.

Eiselstein LE, Sire RA, James BA. Review of fatigue and fracture behavior in NiTi. Proceedings, Materials and Processes for Medical Devices Conference, Boston, MA, November 14-16, 2005; ASM International, pp. 135-147, 2006.

James BA, Foulds J, Eiselstein LE. Failure analysis of NiTi wires used in medical applications. Journal of Failure Analysis and Prevention 2005; 82-87.

Beaudet RA, Barton C, Berkowitz JB, Doherty RM, Eiselstein LE, Forsen HK, Gekler WC, Gill CF, Roy CM, Smith KA, Stenstrom MK, Webler T. Interim design assessment for the blue grass chemical agent destruction pilot plant. Committee to Assess Designs for Pueblo and Blue Grass Chemical Agent Destruction Pilot Plants, Board of Army Science and Technology, National Research Council of the

National Academies, The National Academies Press, Washington, DC, 2005.

James BA, Foulds J, Eiselstein LE. Failure analysis of NiTi wires used in medical applications. Proceedings from the Materials & Processes for Medical Devices Conference, St. Paul, MN, August 25-27, 2004; ASM International, pp. 44-49, 2005.

Beaudet RA, Barton C, Berkowitz JB, Cooper AT, Doherty RM, Eiselstein LE, Forsen HK, Gekler WC, Gill CF, Jenkins-Smith HC, Merson JA, Roy CM, Smith KA, Stenstrom MK, Webler T. Interim design assessment for the Pueblo chemical agent destruction pilot plant. R.A. Beaudet, Chair, Committee to Assess Designs for Pueblo and Blue Grass Chemical Agent Destruction Pilot Plants, Board of Army Science and Technology, National Research Council of the National Academies, The National Academies Press, Washington, DC, 2005.

Eiselstein LE, James BA. Medical device failures — Can we learn from our mistakes? Keynote paper and address, Proceedings from the Materials and Processes for Medical Devices Conference, St. Paul, MN, August 25-27, 2004; ASM International, pp. 3-11, 2005.

Eiselstein LE, Caligiuri RD. Particulate composite of white cast iron. Materials Science Forum, Trans Tech Publications, Switzerland, Vol. 426-432, pp. 895-900, 2003.

Caligiuri RD, Eiselstein LE. Superplastic densification of ultrahigh carbon steel powder compacts. Materials Science Forum, Trans Tech Publications, Switzerland, Vol. 426-432, pp. 877-882, 2003.

Andrew SP, Caligiuri RD, Eiselstein LE, Parnell TK. Evaluation of a failure in a chlorine production facility. Proceedings IMECE2001, ASME International Mechanical Engineering Congress and Exposition, New York, NY, November 2001.

Moncarz PD, Eiselstein LE, Saraf V. Prestressing wire failures in prestressed concrete pipeline. Proceedings, Awarie Budowlane, 20th Engineering Conference on Construction Failures, Szczecin-Miedzyzdroje, Poland, May 2001. (In Polish).

Caligiuri RD, Eiselstein LE. Superplasticity at ultrahigh strain rates — Can it occur? Deformation, Processing and Properties of Structural Materials, Taleff EM, Syn CK, and Lesuer DR (eds), The Minerals, Metal and Materials Society, Warrendale, PA, March 2000.

Moncarz PD, Eiselstein LE. Loss of composite system reliability due to long term environmental alteration. Proceedings, International Federation for Information Processing (IFIP), 9th Working Conference on Reliability and Optimization of Structural Systems, pp. 167-174, Ann Arbor, MI, September 2000.

Eiselstein LE, Harris DO, Scoonover TM, Rau CA. Probabilistic fracture mechanics evaluation of local brittle zones in HSLA-80 steel weldments. Fracture Mechanics, 23rd Symposium, ASTM STP 1189, Chona R (ed), American Society for Testing Materials, pp. 808-825, Philadelphia, PA, 1993.

Rau CA, Eiselstein LE, Rau SA, Harris DO, Sire R, Dedhia D, McMinn A. Probabilistic assessment of crack initiation and growth in shrunk-on disks. Proceedings, Life Prediction of Corrodible Structures International Conference, National Association of Corrosion Engineers International, p. 51/1, Cambridge, UK, September 1991.

Andrew SP, Caligiuri RD, Eiselstein LE. A review of penetration mechanisms and dynamic properties of tungsten and depleted uranium penetrators. Proceedings, Tungsten and Tungsten Alloys - Recent Advances Symposium, The Metallurgical Society, Chen E (ed), 1991.

Rau CA, Eiselstein LE, Harris DO, Sire R, Dedhia D, McMinn A. Probabilistic assessment of crack initiation and growth in shrunk-on disks. Proceedings, Fossil Steam Turbine Disc Cracking Workshop, Charlotte, NC, October 10-11, 1990; EPRI GS-7250, pp. 9-2 to 9 7, April 1991.

Caligiuri RD, Eiselstein LE. Powder metallurgy near net shape processing of heavy metal chemical energy warhead liners. Proceedings, 11th International Symposium on Ballistics, Brussels, Belgium, May 1989.

Eiselstein LE, Caligiuri RD. Application of laminated metallic armors to heavy hybrid armor systems. Proceedings, 4th TACOM Armor Coordinating Conference for Light Combat Vehicles, Monterey, CA, March 1988.

Eiselstein LE, Caligiuri RD. Atmosphere corrosion of the suspension cables on the Williamsburg Bridge. Degradation of Metals in the Atmosphere, ASTM STP 965, American Society for Testing and Materials, pp. 78-95, Philadelphia, PA, 1988.

Eiselstein LE, Caligiuri. Development of advanced, all-metallic laminated armor systems for lightweight applications (U). Proceedings, 3rd TACOM Armor Coordinating Conference, Naval Post-Graduate School, Monterey, CA, February 1987; Metals and Ceramics Information Center, Battelle, Columbus, OH, 1987 (SECRET).

Caligiuri RD, Eiselstein LE, Sherby OD. Properties and applications of ultrahigh carbon steel laminates. Proceedings, 34th Sagamore Army Materials Technology Conference: Innovations in Ultrahigh Strength Steel Technology, pp. 499-525, Lake George, NY, September 1987.

Schmidt CG, Caligiuri RD, Eiselstein LE, Wing S, Cubicciotti. Low temperature sensitization of Type 304 stainless steel pipe weld heat affected zone. Metallurgical Transactions A 1987; 18A:1483-1493.

Eiselstein LE, Caligiuri RD, Schmidt CG. Stress corrosion cracking of steam turbine disc alloys in dilute environments. Proceedings, 2nd International Symposium on Environmental Degradation of Materials in Nuclear Power Systems — Light Water Reactors, Monterey, CA, September 1985; American Nuclear Society, pp. 311-318, La Grange Park, IL, 1986.

Caligiuri RD, Eiselstein LE, Schmidt CG. Development of advanced all-metallic laminated armor systems for lightweight applications (U). Proceedings, Symposium on Composite Materials in Armament Applications, U.S. Army Armament Research and Development Center, Picatinny Arsenal, Dover, NJ, August 1985 (SECRET).

Schmidt CG, Caligiuri RD, Eiselstein LE. Stress corrosion cracking susceptibility of alternative alloys for BWR piping. Paper 99, presented at Corrosion/85, Annual Meeting of the National Association of Corrosion Engineers, pp. 99/1-99/11, Boston, MA, March 1985.

Caligiuri RD, Eiselstein LE, Schmidt CG. Use of constant extension rate tests to characterize low temperature sensitization in Type-304 stainless steel weld-heat-affected zone. Proceedings, 2nd Seminar on Countermeasures for Pipe Cracking in BWRs, Palo Alto, CA, November 1983; EPRI NP-3684-SR, Electric Power Research Institute, p. 10-1, Palo Alto, CA, September 1984.

Schmidt CG, Caligiuri RD, Eiselstein LE. Intergranular stress corrosion cracking of low temperature sensitized Type 304 stainless steel pipe welds. Proceedings, International Symposium on Environmental Degradation of Materials in Nuclear Power Systems — Light Water Reactors, Myrtle Beach, SC, August 1983; National Association of Corrosion Engineers, pp. 423-437, Houston, TX, 1984.

Caligiuri RD, Eiselstein LE, Curran DR. Microkinetics of stress corrosion cracking in steam turbine disk alloys. Proceedings, International Symposium on Environmental Degradation of Materials in Nuclear Power Systems — Light Water Reactors, Myrtle Beach, SC, August 1983; National Association of Corrosion Engineers, pp. 824-836, Houston, TX, 1983.

Caligiuri RD, Eiselstein LE, Fox MJ. Low temperature sensitization of Type 304 stainless steel pipe weld heat affected zones. Proceedings, Specialists Meeting on Subcritical Crack Growth, Freiburg, West Germany, May 1981; NUREG/CP-0044, US Nuclear Regulatory Commission, pp. 199-228, May 1983.

Eiselstein LE, Syrett BC, Wing SS, Caligiuri RD. The accelerated corrosion of Cu-Ni alloys in sulphide-polluted seawater: Mechanism No. 2. Corrosion Science 1983; 23(3):223-239.

Eiselstein LE, Ruano OA, Sherby OD. Room temperature strength and ductility of rapidly solidified white cast irons. Powder Metallurgy 1983; 26(3):155-159.

Eiselstein LE, Ruano OA, Sherby OD. Structural characterization of rapidly solidified white cast iron powders. Journal of Materials Science 1983; 483-492.

Eiselstein LE, Ruano OA, Sherby OD, Wadsworth J. Microstructural and mechanical properties of rapidly solidified white cast iron powders. Proceedings, 3rd Conference on Rapid Solidification Processing, National Bureau of Standards, Mehrabian R (ed), Gaithersburg, MD, pp. 246-251, December 1983.

Eiselstein LE, Syrett BC, Wing SS, Caligiuri RD. The accelerated corrosion of copper-nickel alloys in sulfide polluted seawater. Paper No. 59, Corrosion/82, Annual Meeting of the National Association of Corrosion Engineers, Houston, TX, March 1982.

Ruano OA, Eiselstein LE, Sherby OD. Superplasticity in rapidly solidified white cast iron. Metallurgical Transactions 1982; 13A:1785-1792.

Wadsworth J, Eiselstein LE, Sherby OD. The development of ultrafine superplastic structures in white cast irons. Materials Engineering Application 1979; 1(3):143-153.

Sherby OD, Wadsworth J, Caligiuri RD, Eiselstein LE, Snyder BC, Whalen RT. Superplastic bonding of ferrous laminates. Scripta Metallurgica 1979; 13:941-946.

Book Chapters

Eiselstein LE, Huet R. Chapter 1: Corrosion Failure Analysis with Case Histories. In: Uhlig's Corrosion Handbook, Third Edition, Editor: R. Winston Revie, The Electrochemical Society, Inc., John Wiley & Sons, Inc., 2011.

Eiselstein LE. Chapter 38: Corrosion of Shape Memory Alloys. In: Uhlig's Corrosion Handbook, Third Edition, Editor: R. Winston Revie, The Electrochemical Society, Inc., John Wiley & Sons, Inc., 2011.

Corlett N, Eiselstein LE, Budiansky N. Chapter 29. Types of Corrosion in Liquids: Crevice Corrosion in Shreir's Corrosion. Vol. 2, Editor: T. Richardson, Elsevier, 2010, pp. 753-771.

Presentations

Lemberg J, Guyer E, Eiselstein L. Possible microbiologically induced corrosion (MIC) of stainless-steel weld used in domestic water risers. MS&T 2014, Pittsburgh, PA, October 12-16, 2014.

Lemberg J, Gibbs J, Birringer R, James B, Eiselstein L. Fire cracking of leaded and lead-free brasses for use in water, oil, and gas applications. MS&T 2014, Pittsburgh, PA, October 12-16, 2014.

Huet R, Eiselstein LE. Lessons learned from explosion in ammonium nitrate neutralizer. Symposium on Chemistry, Process Design, and Safety in the Nitration Industry, Spring ACS Meeting, San Diego, CA, March 25-29, 2012.

FDA, Cardiovascular metallic implants: Corrosion, surface characterization, and nickel leaching, March 8, Erica Takai: Moderator, CDRH, FDA: FDA White Oak Conference Center, Silver Spring, Maryland, 2012.

Guyer E, Eiselstein LE. Getting it right the first time: Accelerated testing of active implantable medical devices. Exponent Webinar, October 16, 2008.

Eiselstein LE, Steffey D, Nissan A, Corlett N, Dugnani R, Kus E, Stewart S. Acceptance criterion for the corrosion resistance of medical devices: A statistical study of the pitting susceptibility of Nitinol, accounting for the in-vivo environment. International Conference on Shape Memory and Superelastic Technologies, Stresa, Italy, 2008.

Corlett N, Eiselstein LE, Steffey D, Nissan A, Dugnani R, Kus E, Stewart S. Effect of long-term immersion on the localized corrosion resistance of Nitinol wire under aerated conditions. ASM International Conference on Shape Memory and Superelastic Technologies. International Conference on Shape Memory and Superelastic Technologies, Stresa, Italy, 2008.

Eiselstein LE. Material degradation issues in the implantable medical industry. Meeting of the San Francisco Bay Area Section of the Electrochemical Society, Menlo Park, CA, February 25, 2008.

Eiselstein LE, Steffey D, Nissan A, Corlett N. Toward an acceptance criterion for the corrosion resistance of medical devices: A statistical study of the pitting susceptibility of Nitinol. Proceedings, ASM International Conference on Shape Memory and Superelastic Technologies, Tsukuba City, Japan, 2007.

Nissan A, Corlett N, Eiselstein LE, Steffey D. Effect of long-term immersion on the pitting corrosion resistance of Nitinol. Proceedings, ASM International Conference on Shape Memory and Superelastic Technologies. Tsukuba City, Japan, 2007.

Eiselstein LE, James B. Medical device failure analysis. Keynote Session VI - Failure Analysis (Fracture, Fatigue, Corrosion, and Materials Degradation), Materials, Medicine, and Nanotechnology Summit, ASM International, Cleveland, OH, October 20-25, 2006.

Eiselstein, LE, James B. Keynote lecture - medical device failures. 2nd International Congress on Engineering Failure Analysis, Toronto, Canada, September 12-15, 2006.

Eiselstein, LE. Medical device failures. Medical Device Seminar: Leaders and Visionaries, Stanford University, Stanford, CA, October 25, 1999.

Eiselstein, LE. Material considerations for biomedical devices. Golden Gate Materials and Welding Technologies Conference, San Francisco, CA, February 26-28, 1997.

Caligiuri RD, Eiselstein LE. Development of metallic laminate composites for heavy armor. Defense Advanced Research Projects Agency/Army/Marine Corps Armor/Anti-Armor Joint Program Office Information Exchange, Los Alamos National Laboratory, Los Alamos, NM, March 1990.

Caligiuri RD, Andrew SP, Eiselstein LE. A review of high strain rate properties and penetration mechanisms of depleted uranium and tungsten alloys. Army Research Development and Engineering Command/Army Research Office Workshop on Metallurgical Aspects of Deformation/Failure Mechanisms in "The Terminal Ballistics of Heavy Metal Kinetic Energy Penetrators," Picatinny Arsenal, Dover, NJ, April 1990.

Reports

Eiselstein LE. Declaration of Lawrence Eiselstein in Support of Motion for Summary Judgment. Fireman's Fund Insurance Company, Plaintiff, v Columbia Mechanical Contractors, Inc., Defendants, Exponent Report to William B. Waterman, October 2005 (Rule 26B Report).

Eiselstein L, Belanger J, Buehler C, Reza A, Ogle R, Adan M. Investigation of the explosion at Ultem Monomer production plant. Exponent Failure Analysis Associates, December 2003.

Eiselstein LE. Support of Plaintiff Microlife Intellectual Property GmbH's Opposition to Defendant Actherm, Inc.'s Motion for Summary Judgment of Non-Infringement of U.S. Patent No. 6,419,388, Microlife Intellectual Property GmbH Plaintiff and Counter defendant, v Actherm Inc. Defendant and Counterclaimant. Civil Action No. C 03-1117 (SBA) in U.S. District Court for Northern District of California, Oakland Division, September 2003 (Rule 26B Report).

Eiselstein LE. Supplemental Declaration of Lawrence E. Eiselstein, Marchon Eyewear, Inc. and Rothandberg, Inc., Plaintiffs, v Global Optical Resources, Inc., Defendant, Exponent Report to Frommer Lawrence & Haug LLP, June 2003 (Rule 26B Report).

Eiselstein LE. Stern tube corrosion and cathodic protection. Exponent Report to United States Coast Guard, Lockport, LA, May 2003.

Eiselstein LE. "Declaration of Lawrence E. Eiselstein, Marchon Eyewear, Inc. and Rothandberg, Inc., Plaintiffs, v Global Optical Resources, Inc., Defendant, Exponent Report to Frommer Lawrence & Haug LLP, January 2003 (Rule 26B Report).

Eiselstein LE. Stern tube corrosion on 87-foot cutters. Exponent Report to United States Coast Guard, Alameda, CA, October 2002.

Eiselstein LE, Giddings V, Kennedy R, Mahnovski S, Medhekar S. Zelickson Patent Valuation. Enteric Medical Technologies and Boston Scientific, Exponent Report, August 2002.

Eiselstein LE. Valley Transit Authority (VTA) Rail Fracture. Exponent Report, June 2002.

Eiselstein LE. Equilon/Texaco Pipe Release. Expert Report to McCutchen, Doyle, Brown & Enerson, March 2002 (Rule 26B Report).

Eiselstein LE. Declaration of Lawrence E. Eiselstein, regarding underground corrosion of ARCO station piping, Report to O'Melveny & Myers LLP, September 2001 (Rule 26B Report).

Eiselstein LE. FSI International v Particle Measuring Systems, Exponent Report to Robins, Kaplan, Miller & Ciresi, August 2001 (Rule 26B Report).

Eiselstein LE. Rebuttal Expert Report, Varian Associates, Inc. v General Electric. Exponent Report to Farella Brawn & Martel, March 2001 (Rule 26B Report).

Eiselstein LE. Trident Weld Consumables Rebuttal Report. Exponent Report to Castro and Worthge, LLP, March 2001 (Rule 26B Report).

Eiselstein LE. Stress Corrosion Cracking of CAP Wire. Exponent Report to Rogers, Joseph, O'Donnell & Quinn, July 2000.

Eiselstein LE. Support of COM/Energy's Memorandum of Law on Harvard's Purported Damages in President and Fellows of Harvard College, Plaintiff v COM/Energy Steam Company. Report to Riemer & Braunstein, April 2000 (Rule 26B Report).

Eiselstein LE and Moncarz P. Hayden-Rhodes Aqueduct Siphon Rebuttal Report. Exponent Report to Rogers, Joseph, O'Donnell & Quinn, March 2000.

Paduano D and Eiselstein LE. CS Integrated v. Vilter Manufacturing Exponent report to McCutchen, Doyle, Brown & Enersen, May 2000 (Rule 26B Report).

Eiselstein LE. Rebuttal Report (Subject to Protective Order). Cordis Corporation, Plaintiff v Advanced Cardiovascular Systems, Inc., Medtronic AVE, Inc., Boston Scientific Corporation, and Scimed Life Systems, Inc. Defendants and Medtronic AVE, Inc. Plaintiff, v Cordis Corporation, Johnson & Johnson,

and Expandable Grafts Partnership, Defendants. United States District Court for the District of Delaware, February 2000 (Rule 26B Report).

Eiselstein LE. Report (Subject to Protective Order). Cordis Corporation, Plaintiff v Advanced Cardiovascular Systems, Inc., Medtronic AVE, Inc., Boston Scientific Corporation, and Scimed Life Systems, Inc. Defendants and Medtronic AVE, Inc. Plaintiff, v Cordis Corporation, Johnson & Johnson, and Expandable Grafts Partnership, Defendants, U.S. District Court of Delaware, January 2000 (Rule 26B Report).

Moncarz P and Eiselstein LE. Summary of Hayden-Rhodes Siphon Distress Study by Exponent Failure Analysis Associates. Volume I, Exponent Report to Rogers, Joseph, O'Donnell & Quinn, January 2000.

Eiselstein LE and Moncarz P. Summary of Hayden-Rhodes Siphon Distress Study by Exponent Failure Analysis Associates. Volume II, Exponent Report to Rogers, Joseph, O'Donnell & Quinn, January 2000.

Eiselstein LE and Haussmann G. Investigation of the October 23, 1995, Chemical Release at Gaylord Chemical, Bogalusa, Louisiana. Exponent Report, September 1998.

Reza A, Eiselstein LE, Huet R, Belanger J. Investigation of the April 1994 Halliburton perforation gun explosion in Kenai, Alaska. Failure Analysis Associates Report to DeLisio Moran Geraghty & Zobel and Lane Powell Spears Lubersky, January 1998.

Eiselstein LE, Wachob HF, Mimmack GF. Failure Analysis Report of Limit Switch. Failure Analysis Associates Report to Puget Sound Naval Shipyard, Bremerton WA, November 1997.

Caligiuri RD, Parnell TK, Eiselstein LE, Wu M, Huet R. Analysis of Drill Pipe Joint Failures and Recommendations for Service. Exponent Failure Analysis Associates Report, November 1997.

Eiselstein LE and Wachob HF. Report for Failure Modes and Effects Analysis of the NiCl800 Needle Disposal System. Failure Analysis Associates Report for NIC Limited and Wilson Sonsini Goodrich & Rosati, July 1997.

Eiselstein LE and Wachob HF. Test Report for Efficacy and Use Life Validation for the NiCl800 Needle Disposal System Using Clinically Destroyed Needles. Failure Analysis Associates Report for NIC Limited and Wilson Sonsini Goodrich & Rosati, August 1997.

James B and Eiselstein LE. Investigation of Sensitization and Cracking of an Incoloy 800H Silane-Production Reactor Vessel. Failure Analysis Associates Report to Bullivant, Houser, Bailey, April 1997.

Ross B, Haussmann G, Eiselstein LE, Huet R, James B. Evaluation of Fan Failure and Boiler Explosion, Unit #3, Dave Johnson Power Plant, Glenrock WY. Failure Analysis Associates Report, March 1996.

Eiselstein LE, Huet R, and Nell J. Materials Evaluation of the Broken Porcelain Bus Bar Spacer-Insulator at Diablo Canyon. Failure Analysis Associates Report, September 1994.

Eiselstein LE and Kokarakis J. Analysis of the Broken Blowdown Valve Bolts on the USNS San Diego. Failure Analysis Associates Report to Military Sealift Command, August 1994.

Petersen JF and Eiselstein LE. The Role of Copper Azides in Detonator Explosion Phillip E. Beckner v. Owen Tools, Inc., et al. Failure Analysis Associates Report, July 1994.

Eiselstein LE and Caligiuri RD. Examination and Corrosion Testing of Leaking Celulosa Del Pacifico Recovery Boiler Superheater Heater Tubes. Failure Analysis Associates Report, April 1994.

Rao VB, Rao GL, Eiselstein LE, Caligiuri RD. Report on Failure Modes and Effects Analysis for Carbon-Dioxide Powered Syringe. Failure Analysis Associates Report, May 1994.

Eiselstein LE, Wagner A, Reza A, Rao GL, Caligiuri RD. Experiments on the Effect of Suction-Side Leaks on Refrigerator Performance. Failure Analysis Associates Report, April 1994.

Eiselstein LE, Rao GL, Caligiuri RD, Wagner A. Experiments on Gas Dispersion from Sealed System Leaks. Failure Analysis Associates Report, April 1994.

Eiselstein LE, Rao GL, Caligiuri RD. Internal Isobutane-Air Ignition Experiments. Failure Analysis Associates Report, April 1994.

Eiselstein LE, Analysis of the Hull Perforation on U.S. Coast Guard Cutter. Failure Analysis Associates Report, March 1994.

Appiarius JC, Boukarim GE, Owen EL, Mayer CB, Murdoch A, Taylor TM, Eiselstein LE, Foulds JR, Harris DO. Bus Transfer Criteria for Plant Electric Auxiliary Systems. Electric Power Research Institute, Final Report, Project 2626-01, EPRI TR-103185, October 1993.

Eiselstein LE. Failure Analysis of Powerheads Used to Install Morgrip Bolts. Final Report to LaQue Center for Corrosion Technology, Inc., May 1993.

Eiselstein LE, Andrew SP, Caligiuri RD. Recommended Practices for Materials Compatibility. Failure Analysis Associates Report, November 1992.

Andrew SP, Caligiuri RD, Parnell TK, Eiselstein LE. Computational Modeling of Dynamic Failure in Armor/Anti-Armor Materials. Failure Analysis Associates Final Report to U.S. Army Research Office, Contract DAA-L03-88-C-0029, May 1992.

Eiselstein LE, Wachob HF, Caligiuri RD. Improved Corrosion Resistance of Magnesium Alloys through Mechanical Alloying. Failure Analysis Associates Final SBIR Phase I Report to Wright-Patterson Air Force Base, 1989.

Eiselstein LE, Harris DO, Rau CA, Dedhia DD, Sire RA. Probabilistic Fracture Mechanics Evaluation of Local Brittle Zones in HSLA-80 Steel Weldments. Failure Analysis Associates Report to Department of Navy, Contract N6153389-M1103, Report No. DTRC/SME-CR-05-90, David Taylor Research Center, Annapolis, MD, December 1989.

Rau CA, Eiselstein LE, Harris, Sire RA, DO, Dedhia DD, McMinn A. Probabilistic Risk Assessment of Low-Pressure Disks on Oak Creek Unit No. 1. Failure Analysis Associates Report, 1988.

Shockey DA, Caligiuri RD, Eiselstein LE, Marchand AH, Klopp RW, Florence AL. Technical Support for the Honeywell Blue Team Heavy Armor Program. SRI Final Report to Honeywell Underseas Systems Division, SRI Project PYD-3345, December 1988.

Eiselstein LE, Caligiuri RD. Rapid Solidification Processing of Wire for Tire Reinforcement. SRI International Report, SRI Project PYC 3497, January 1988.

Eiselstein LE, Caligiuri RD. Explosive Compaction of Rapidly Solidified Nd-Fe-B Ferromagnetic Powders. SRI International Final Report, December 1987.

Eiselstein LE and Caligiuri RD. Development of Advanced, All-Metallic Laminate Armor Systems for Lightweight Applications (U). SRI International Final Report to the DARPA and the Army Research Office, Contract DAAG-29-84-K-0206, July 1987 (SECRET).

Eiselstein LE and Caligiuri RD. Stress Corrosion Cracking of A-471 Steam Turbine Disk Alloys. SRI International Final Report to Electric Power Research Institute, EPRI NP-5182, Contract 1398-12, June 1987.

Eiselstein LE, Caligiuri RD, Werner AT. Corrosion Behavior of Materials Used in Sour-Gas-Rich Oil Fields. SRI International Report, May 1987.

Schmidt CG, Caligiuri RD, Eiselstein LE. Stress Corrosion Cracking Susceptibility of Type 316 Nuclear-Grade Stainless Steel and XM 19 Alloy in Simulated BWR Water. SRI International Final Report to Electric Power Research Institute, EPRINP-05177-LD, Project T305-2, April 1987.

Eiselstein LE, McKubre MCH, Caligiuri RD. Prediction of Crack Growth in Aqueous Environments. SRI International Final Report to the Office of Naval Research, Contract N00014-82-K-0343, July 1986.

Eiselstein LE, McKubre MCH. The Suitability of Stainless Steel as a Replacement for Zinc Plated Mild Steel as a Structural Frame Material for Computer Applications. SRI International Report, May 1986.

Eiselstein LE, Peppers NA, Schaefer LF, Schmidt CG, Young JR. Automated Printed-Circuit-Board Inspection. SRI Report to SRI Multi-Client Project on Automated Printed-Circuit-Board Inspection, SRI Project 6869, March 1986.

Eiselstein LE, Caligiuri RD. Corrosion Damage to the Williamsburg Bridge Main Suspension Cables. SRI International Report, May 1985.

Eiselstein LE, McKubre MCH, Caligiuri RD. Prediction of Crack Growth in Aqueous Environments. SRI International Second Annual Report to the Office of Naval Research, Contract N0014-82-K-0343, March 1984.

Eiselstein LE and Caligiuri RD. Microkinetics of Stress Corrosion Cracking in Steam Turbine Disk Alloys. SRI International Final Report to Electric Power Research Institute, Contract RP1398-12, November 1984.

Schmidt CG, Caligiuri RD, Eiselstein LE. Low-Temperature Sensitization of Type-304 Stainless Steel Weld-Heat-Affected-Zone. SRI International Final Report to Electric Power Research Institute, EPRI NP-3368, Contract T110 1, November.

McKubre MCH, Leach SC, Eiselstein LE. Crevice Corrosion of Lattice-Support Alloys in Secondary Environments of Nuclear Steam Generators. SRI International Final Report to Electric Power Research Institute, EPRI NP-3045, Contract RPS204-1, July 1983.

Caligiuri RD, Eiselstein LE, Curran DR, Shockey DA. Microkinetics of Stress Corrosion Cracking in Steam Turbine Disk Alloys. SRI International Interim Report to Electric Power Research Institute, Contract RP 1929-8, April 1983.

Caligiuri RD, Eiselstein LE. Investigation of Water-Based Corrosion in Radiant Heating Systems. SRI International Report, January 1983.

Eiselstein LE. Friction Measurements of Steel on Refractory Bricks. SRI International Final Report to Electric Power Research Institute, EPRI NP 1987, Contract 1704-17, August 1981.

Eiselstein LE and Lamoreaux RH. Assessment of Mechanical Property Degradation of Steels Exposed to PLBR Liquid Sodium. SRI International Final Report to Electric Power Research Institute, EPRI NP-1985, Contract 1704-15, August 1981.

Eiselstein LE, Caligiuri RD, Wing S, Syrett BC. Mechanisms of Corrosion of Copper-Nickel Alloys in Sulphide-Polluted Seawater. SRI International Final Report to the Office of Naval Research, Contract 00014-177-C-0046, WR036-116, December 1980.

Eiselstein LE, Fatigue Testing of Betalloy Couplings. SRI International Report, July 1980.

Wadsworth J, Eiselstein LE, Sherby OD. The Development of Ultrafine, Superplastic Structures in White Cast Irons. Stanford University Department of Materials Science and Engineering Technical Report to the Office of Naval Research, Contract N-00014-75-C-0662, November 1978.

Project Experience

General Failure Analysis and Prevention

Power Plant Steam Explosion—Investigated a steam explosion at a fossil-fueled power plant that killed four plant personnel. One of the plant's main steam lines had been severed after the failure of a large primary air draft fan that had been used to blow crushed coal into the boiler. Fractography, fracture mechanics, material testing, and metallurgy were used to help investigate the cause of this accident. Pieces of the fan were put back together to identify the origin. The failure was traced to a weld crack. These results were presented to the plant personnel concerned about plant safety.

Railroad—Determined the cause of a freight train rail car axle failure that resulted in a train derailment. A combination of corrosion, fatigue, and inadequate nondestructive examination (NDE) and repair was found to be the cause.

Structural Fasteners—Analysis of the metallurgy, corrosion, pull-out strength, and fracture of steel shot pins used to fasten framing of single-family homes to their foundation. Power-actuated fasteners (PAFs) are nail-like pins used to attach materials to concrete, masonry, or steel base materials by a system that uses either explosive powder, gas combustion, or compressed air to embed the fastener in structural elements. The general term is "shot pin." Measured and analyzed pull-out strength, and analyzed how it may have been affected by atmospheric corrosion.

Automotive—Examined fatigue and corrosion induced cracks in automotive stabilization bars.

Brake Assembly—Evaluated corrosion of the internal component of the brake assembly, including possible galvanic coupling between a zinc piston and a steel spring. Determined that this is not an issue if the Department of Transportation (DOT) rated brake fluid is replaced in accordance with the manufacturer's specifications. This replacement limits water accumulation, prevents acidification, and replenishes corrosion inhibitors.

Power Steam Turbine Experience—Investigated the corrosion mechanisms associated with stress corrosion cracking (SCC) of steam rotor materials for EPRI (Electric Power Research Institute). This research included measurements of initiation and growth of SCC cracking in low-pressure (LP) steam turbine disks. Another project involved performing a probabilistic-based risk analysis of LP steam turbine disk cracking for many units operating at a power plant in the Midwest.

New York City Williamsburg Suspension Bridge—Investigated the atmospheric corrosion damage that had occurred over the 80-year life (now over 100 years old) to the Williamsburg Suspension Bridge main suspension cables. This bridge was opened to traffic in 1903, and the four main support cables are composed of 7,696 high-carbon patented steel wire. These wires were not galvanized but were given a protective organic coating when installed. Wire samples were removed from the cables and evaluated for corrosion damage and mechanical properties. Mechanical properties had been degraded. Accelerated corrosion tests were used to estimate the current rate of corrosion.

Atmospheric Corrosion of Copper Coated Stainless-Steel Architectural Material—Investigated the nature of corrosion failures that was occurring on copper-coated stainless steel sheet that was being used as roofing, gutters, and siding on homes and businesses. In some cases, the atmospheric corrosion of the electroplated stainless steel sheet had corroded sufficiently to expose the underlying stainless steel. In other cases, the stainless steel sheet had undergone pitting to such an extent to allow water to leak

through. Atmospheric corrosion rates that can be expected for copper in various environments such as marine or coastal, urban, and rural areas were reviewed. The potential for galvanically assisted pitting of the stainless steel was also investigated. The acidic condensation from chimneys and flues was found to rapidly strip off the copper plating.

Geothermal Power Plant—Operation of a geothermal power plant located in a marine environment was interrupted by a volcanic eruption. Provided help evaluating atmospheric corrosion damage claims to the surface of equipment (air-cooled condensers, switchgear, transformers, motors, generators, turbines, pumps, etc.) as the result of volcanic gases and marine atmospheric exposure during the plant forced shutdown. Performed site inspections and analyzed other site inspection reports, plant status reports, repair invoices, vendor reports on damage repairs, and maintenance records to qualitatively rank the amount of damage that likely resulted from the eruption.

LM2500 Gas Turbine Failure—Investigated the reason for the failure of an LM2500 turbine. Turbine bolting manufactured from Inconel 718 that had been plated with silver for anti-galling (low friction) had failed while the unit was at full power. Issues were turbine operating temperature, creep-fatigue, and hot corrosion (sulfur and chloride).

Steam Turbine Rotor Straightening—Investigated the reasons for the warpage (bowing) of HP/IP rotors manufactured from Ni-Cr-Mo-V steel. The effect of turning gear failure, creep during time at temperature while stationary, the effect of thermal gradient induced thermal stresses (from rubbing or loss of turning gear) on plastic and creep deformation, and the resulting residual stresses induced by these permanent deformations were considered along with the effectiveness of proposed straightening methods.

Failure of Forged Alloy 718 Disks—Forged Inconel 718 (Alloy 718) disks had been ordered from a forging supplier. These forgings were machined into disks for testing a new design for a turboshaft jet engine. The disks failed during testing, destroying the test stand placing the development program behind schedule. The root cause of the failure was that, although the disk had been ordered in an age-hardened condition, it had not received this heat treatment.

Fertilizer Plant Explosion—Investigated massive explosions that leveled portions of a Port Neal, Iowa, ammonium nitrate plant owned by Terra Industries. Four plant workers were killed, 18 others suffered serious injury, and damage to the plant and surrounding community was estimated in the hundreds of millions of dollars. Reviewed and analyzed the plant's process data for reliability, and conducted extensive research regarding ammonium nitrate properties and decomposition mechanisms. Also completed analytical modeling and experimental testing to resolve the conflicting accident theories, and inspected and performed metallurgical analysis of various artifacts from the explosion site. Plant operators allowed the ammonium nitrate in the neutralizer vessel to become contaminated and highly acidic. When superheated steam was injected into the neutralizer vessel, a runaway chemical reaction occurred.

Inconel 718 Fuel Nozzle Cracking—A commercial airliner experienced an in-flight engine fire and shutdown in Paris that was linked to the failure of the superalloy Inconel 718 forged fuel spray nozzle used in certain Rolls Royce engines installed on Airbus and Boeing aircraft. This led to the worldwide replacement of thousands of fuel spray nozzles on hundreds of aircraft. Investigated the nature of the aircraft fuel nozzle cracking, the forging procedures (forgeability limits, forging temperature), ingot size, and inspection and manufacturing techniques used to make these nozzles.

Ammonium Perchlorate Plant Explosion—Investigated the cause of a series of explosions that destroyed a solid rocket oxidizer plant (ammonium perchlorate manufacturing facility) in Henderson, Nevada. The largest of five individual explosions at PEPCON was equivalent to 1.5 million pounds of TNT, and another explosion was equivalent to 500,000 pounds of TNT. Assessed the role that ERW weld defects in a 16-inch-diameter high-pressure natural gas pipeline that traversed the plant and was damaged by the explosions may have played in the incident.

Materials Study for Generator—Provided recommendations for appropriate accelerated corrosion and wear testing for materials to be used in a portable combustion powered electrical generator. Tribology, high-temperature oxidation, acid dewpoint corrosion, metal dusting/carburization, and other effects were considered. Materials considered included precipitation hardenable stainless steels (17-4PH and 17-7PH), Nitronic 60, Duplex 2507, and graphite.

Natural Gas Fitting Failure and Explosion—Investigated a natural gas explosion that occurred in a mobile clinic. Examined a broken copper natural gas fitting on the clinic's heater to determine the cause of failure. The failure was found to be a result of fatigue and not stress corrosion cracking.

Refrigerator Compressor Failures—Excessive field failures were observed a few years after introduction of a new type of refrigerator compressors. The investigation included engineering analysis of wear in the compressor parts as well as statistical analysis to determine the factors associated with field failures.

Membrane Permeation Cartridges—Investigated the performance of vapor-permeating membranes for ethanol purification (dehydration) for fuel grade ethanol. This included a thorough review of plant operating conditions as well as establishing a mathematical model of the cartridges to deduce the membrane permeability from the cartridge operating parameters. The membrane had a high tolerance to high water contents; the distillation stage did not need to go up to the azeotrope (92%), which enables the process to be more energy efficient when compared to other dehydration methods. In addition, the dehydration process is continuous rather than a batch one, as there is with zeolite-based fuel grade ethanol dehydration processes.

High-Efficiency Home Furnace—Examined the corrosion damage to the enameled steel heat exchanger used in a condensing home furnace. X-ray photoelectron spectroscopy (XPS, also known as ESCA) was used to characterize the pitting damage.

Furnace Fuel Filter Issues—Several environmental remediation matters regarding leaking fuel filters used in home heating furnaces. The fuel was generally supplied from an aboveground fuel oil tank with a line out the bottom that generally fed the fuel into the furnace in the basement after going through a fuel filter. Fuel filters that are not changed out as frequently as recommended can collect moisture in the bottom of the filter; given enough time, this can result in through-wall corrosion leading to fuel oil leaking into the basement. Investigated issues of galvanization, coating, compliance with manufacturer's recommendations, and the rate of microbiologically influenced corrosion (MIC).

Oxidation and Carburization—Evaluated the rate of oxidation and carburization (metal dusting) at high temperatures for various high-temperature alloys subjected to extended exposure times and thermal cycling. Looked at the effects of spallation, chromia evaporation, and penetration depths to develop degradation rate model.

Armor/Anti-Armor—Worked on various armor and anti-armor projects. Designed, manufactured, and ballistically tested these armor systems (metallic laminates and ceramics) against a variety of threats from small caliber to shaped charges and kinetic energy penetrators. Manufacturing techniques included roll bonding, superplastic solid-state pressure-induced diffusion bonding, electron beam welding, and hot isostatic pressing (hipping). Hardness, metallography, and grain size analysis of tantalum shape charge liner materials.

Shaving Cream Can Corrosion—Investigated "rust-free" exploding shaving cream cans. This incident resulted in a product recall. The pressurized "rust-free" (i.e., aluminum, not steel) shaving cream cans were filled with shaving cream foam with an isobutene propellant. The pH of one of the two shaving cream formulations was of a sufficiently high pH to result in corrosion penetration of the uncoated aluminum can inner surface.

Wastewater Treatment—A major regional county sanitation district experienced a leak in its sulfur dioxide evaporator within 72 hours after placing a 90-ton rail car on-line. The wastewater processed at the plant

goes through a series of treatment steps before it is released to the environment. Steps include primary and secondary treatment, chlorination, and de-chlorination. Sulfur dioxide (SO_2) is used to neutralize residual chlorine (de-chlorination). The corrosion induced SO_2 release was attributed to the much higher than specified moisture of the SO_2 in the rail car.

Sanitation District Methane Gas Storage—Investigated corrosion on the inside of methane gas storage spheres. The corrosion investigation looked at issues of atmospheric corrosion and the effect of the presence of condensation and carbon dioxide in the methane.

Dechlorination Facility Corrosion—Investigated through-wall penetration of the steel carbon dioxide line (CO_2) used for dichlorination/dechloramination prior to filling a lake reservoir with excess treated water. The effect of soil chemistry and stray current were investigated as potential causes for the leak.

Anaerobic Digester—Investigated corrosion control issues in an anaerobic digester. This “dry” fermentation anaerobic digestion was used to produce biogas consisting of up to 65% methane and compost. The biogas is utilized to produce compressed natural gas (CNG). Ammonia and volatile organic compounds (VOCs) and odor-producing compounds are removed from the air, and thermophilic anaerobic conditions are established after the aerobic microbes consume the available oxygen. During the anaerobic digestion, gases such as methane, CO_2, hydrogen sulfide (H_2S), or ammonia are produced. Microbially induced corrosion (MIC) conditions were considered such as the numerous acid-forming bacteria associated with methane-forming bacteria. For instance, acetate-forming (acetogenic) bacteria grow in a symbiotic relationship with methane-forming bacteria as well as the effects of sulfate-reducing bacteria (SRBs), which can produce hydrogen sulfate that can be further oxidized to sulfuric acid. The fermentation of volatile organic acid (RCOOH) resulting in the production of methane and the reduction of carbon dioxide to produce methane was also considered.

Digester Facility Coating—Steel tanks used for anaerobic digestion of waste had been painted, and the coating was failing at and above the water line. The issue was to determine if the coating failed because of thermo-chemical degradation or because of having been improperly applied.

Power Plant Structure—Steel roofing and siding panel coating on new construction at a power plant was blistering, peeling, and cracking, and the steel underneath was exposed after a short time in service. Investigated the root cause of the coating failure.

Boiler Steam Explosion—Soon after commissioning a boiler at a smelter plant, severe corrosion was discovered in the bottom section. To reduce the corrosion/erosion rates of the SA-192 steel tubes, it was decided to weld overlaid these tubes with Inconel 625. About two years later, there was a steam explosion in the boiler. Laser ablation–inductively coupled plasma–mass spectroscopy (LA-ICP-MS) was used to identify the weld and tube chemistry.

Corrosion Study—Performed life assessment for solder pile. Considered the underground corrosion rate for the steel members, considering the variation in corrosion rate, presence, or absence of coating and cathodic protection (impressed current or sacrificial anodes), galvanization, and drainage conditions.

Oil and Gas

There have been various projects in the oil and gas industry, including various aspects from upstream (hydraulic fracturing and perforation guns) to downstream (piping, refinery, underground storage tanks, and gasoline fuel tanks in automobiles). The following are a few examples of this project experience.

Oil Well Perforation Gun Explosion—Investigated a perforation gun explosion at the Halliburton Industries assembly plant in Kenai, Alaska, that killed one employee and seriously injured five others. Perforation guns are used in oil well completion to perforate the oil well casings to allow oil to flow into the well. A perforation gun consists of numerous explosive shaped charges aligned within a pipe. The explosion occurred and workers were injured during the shop assembly of the perforation gun. Exponent’s forensic

investigation involved detailed examination of the remaining fragments, combined with mapping of the fragment locations after the explosion, to determine the sequence of events that led to the explosion. The evidence indicated that an employee accidentally ignited the shaped charges or the detonation cord within the gun.

Drill String Failures—Investigated the cause of several drill string failures. These failures involved complete separation of the string at the threaded coupling, rather than the more commonly observed washout failures that occur in the main pipe segment. These failures occurred at various depths and total drilling hours. Testing and finite element analysis was performed to determine if these failures were a result of stress corrosion cracking (SCC) or from fatigue from stresses in the shoulder of the coupling.

Galvanization of Steel Structural Steel Beam Cracking—Investigated reported incidents of cracked galvanized structural beams found in buildings. Although cracking of steel beams in galvanizing baths is not a new phenomenon, there was a concern that the rate of cracking, although still small, had increased. The cracking was from liquid metal assisted cracking (LMAC), a form of liquid metal embrittlement (LME). Predicting how and when LMAC will occur is challenging. Selecting appropriate nondestructive testing (NDT) for inspection requires careful consideration as the cracks can be filled or covered with the zinc (Zn) galvanizing alloy making visual and dye penetrant testing impossible. Modified magnetic particle, ultrasonic testing (UT), eddy-current testing (ECT) techniques were suggested to detect such cracks.

Refinery Pipe Rupture and Fire—Performed a metallurgical evaluation into the cause of the rupture of an elevated temperature steel pipe in a petrochemical refinery. The pipe had been in crude oil distillation service for many years. The pipe was found to have thinned and ruptured because of sulfidation corrosion (also known as sulfidic) corrosion. Rates of sulfidation corrosion as a function of various variables were reviewed, including McConomy and modified McConomy curves.

Refinery Ducting—Determined the degree of graphitization on samples of carbon steel and condition of stainless steels taken from steel ducting from a refinery that had been in high temperature service (790°F) for 30 years. The Grade 70 carbon steel sample exhibited a ferrite/pearlite microstructure with a small amount of transformed graphite, consistent with the extended exposure at elevated temperature. No internal cracking or significant deviation from the expected microstructure was observed. The 304 stainless steel exhibited sensitized microstructure with carbide precipitates at the grain boundaries. Minor grain boundary attack was observed on the stainless steel inlets.

Casing and Coupling Gas Well—Investigated issues regarding the design, manufacture, and assembly oil country tubular goods for use in oil and gas wells in Texas. Five-and-a-half-inch P110 steel connectors were bucked onto the casings (about 45,000 feet of seamless casing) and were in several wells in Texas. The production strings were subjected to high-pressure hydraulic fracturing (“fracking”). During the early stages of the hydraulic fracturing of the wells, some of the connections failed (cracked) at pressures below design specification, resulting in a loss of the wells. Reviewed evidence regarding the allegations that the coupling/connectors were improperly designed, manufactured from substandard steel, improperly heat treated, were subjected to excessive torque, were coated improperly leading to hydrogen charging, subjected to an acidic environment during the hydraulic fracture from the fracking fluid, and exposure to “sour” environment (hydrogen sulfide) resulting hydrogen cracking or sulfide stress cracking.

Inconel 625 Piping and Fittings—Six-inch-diameter Inconel 625 (N06625 or Alloy 625) seamless pipes and fittings were supplied to a Middle East project for an oil extraction and conditioning facility. The crude was sour and contained very high concentrations of hydrogen sulfide (H2S). The piping was to be supplied in the cold-worked and annealed condition in accordance with ASTM B444. Through mechanical testing, metallography, and NDE ultrasonic testing, it was determined that most of the piping and fittings did not comply with the technical specifications.

Corrosion Behavior of Steel Tubulars Used in Sour-Gas-Rich Oil Fields—Measured the corrosion rate of steel (A387 and A516) in highly saline (salt saturated) hot brines (100°C) that were in equilibrium with very high pressure hydrogen sulfide (20 atmospheres) and carbon dioxide (5 atmospheres), as a function of flow velocity up to 10 m/s. This work helps to understand the life of steel tubing used in deep oil and

gas wells that are subjected to these corrosive conditions, i.e., high temperatures, high flow rates, high salt concentration brines, and corrosive dissolved gases such as H2S and CO2.

Oil Rig Accident in Texas—A worker fell through the grate hatch door into a mud pit and sustained burns. Exponent's analysis indicated that there had been post-manufacturing modifications to the mud pit latches and grating that insufficiently supported the grating and resulted in the grating and the employee falling into the mud pit.

Food and Beverage

Pear Can Corrosion—Approximately 8 million cans of cooked fruit were produced over a two- to three-month period; 5.8 million cans were produced on one production line. Three months later, when cans were being removed from the pallets for labeling and shipping to customers, noticeable and extensive rusting was noted. Investigated the cause of the rusting and determined whether the rusting would continue and eventually cause leakage. Several factors that may have contributed to the rusting included:

• Stray current from the cooker resulting in rapid corrosion of the cans;
• Too much chlorine added to the water used to wash and cool the cans; or
• The cans may have been too wet (or too cool) when they came out of the cooler, and therefore did not dry immediately, thereby allowing corrosion to occur.

Carbonated Beverage Can Corrosion—Several cargo shipping containers containing carbonated beverage (soda) cans were found to have leaked during oversea transport to market. Most of these soda cans were found to be empty because of corrosion-induced leaks. Typically, there is no protective coating on the outer surface of the cans. When one can leaked, it resulted in a chain reaction of leaking cans as the first leaking can wetted the cardboard containers with low pH carbonated cola. The unprotected can bottoms then rapidly corroded and leaked, wetting more cardboard, and thereby causing more cans to leak.

Food Contamination—Investigated a claim of mercury contamination in a frozen food product and identified the source: metallic objects found in fruit juice.

Coating Defects in Cans—Analyzed the extent and degree of coating defects in cans used for jalapeños, green chiles, and enchilada sauce

Leaking Beverage Cans—Performed a root cause analysis to understand why sparkling beverage cans from three products were leaking. Analysis included optical microscopy, scanning electron microscopy (SEM), energy-dispersive spectroscopy (EDS), and Fourier transform infrared spectroscopy (FTIR). Electrochemical analysis of the coating was also used. Both electrochemical impedance spectroscopy (EIS) and linear polarization resistance (LPR) were used in this analysis.

Welds and Welded Connections

Steel Moment Frame Weldment Failures—Investigated the causes of failed steel moment frame welds after the Northridge earthquake in Los Angeles, California. Investigation included metallurgical examinations of failed welds removed from buildings, chemical analysis of weld material, and analysis of the potential for hydrogen-induced weldment cracking.

Engineering Significance of Local Brittle Zones (LBZs) in U.S. Navy Ships—The Navy's certification of HSLA-80 (ASTM A710) for use in ship hull construction occurred in 1984. It provided shipbuilders with their first new steel since the mid-1950s. This steel has been used in the construction of Navy ships, beginning with cruisers of the Ticonderoga class. The low-carbon content of HSLA-80 makes it much less sensitive to hydrogen-assisted heat-affected zone (HAZ) cracking, and therefore it can be welded without the expensive preheat and process controls required for HY-80. The Navy conducted an intensive testing

program to characterize HSLA-80 base plate and weldment properties and found the presence of LBZs in the multi-pass weldments and wanted to better understand how this may affect the weldment when subjected to large strains such as those that occur during explosive bulge testing. This was evaluated using probabilistic fracture mechanics. The model calculated the failure probability of weldments as they are strained, simulating the growth of preexisting crack-like weld defects. The model incorporates the variation of the toughness for the base metal, weld metal, and LBZs to model the tearing resistance along the fracture path. This modeling indicated that the distribution and toughness of LBZs only have a small effect. The calculated failure probabilities agree with a limited number of actual explosive bulge tests.

Stainless Steel Piping Welds—Investigated the corrosion damage to stainless steel piping and welds in a semiconductor equipment manufacturing facility that had a hydrochloric acid (HCl) spill. The heat-affected zone of the welded stainless steel piping was inspected for pitting and stress corrosion cracking. Evaluated methods for cleaning and passivating the stainless steel piping in place.

Residual Stress in Space Satellite Fuel System—Investigated the effect of residual stress in an electron beam (EB) welded component used in a satellite fuel system. The failures appeared to be the result of low-cycle fatigue.

ERW Weld Corrosion Attack—The electrical resistance weld (ERW) in steel piping used to pipe water to and from the cooling tower in an HVAC system was analyzed to determine if it was defective.

Ceramic-to-Metal Seal Braze—An exploding bridge wire detonator used in the aerospace industry was analyzed for reliability. The thermal stresses resulting from the difference in thermal expansion coefficient between the low expansion alloys used (Kovar and Invar), alumina, and the brazing alloy were analyzed.

Failure Analysis of EB and Laser-Welded Inconel 718 (Alloy 718) Nickel-Hydrogen Battery—Some batteries used for an aerospace application developed a leak while in service after various charge/discharge cycles that cyclically pressurize and depressurize the battery. The manufacturing methods and materials used to manufacture nickel hydrogen battery were reviewed. Micro-fissuring grain boundaries during welding, niobium enrichment, delta phase precipitation, deep drawing and heat treatment variations, hydrogen-assisted crack growth, caustic SCC, and other factors were considered as a potential cause for leaks.

Cracking of Nickel 200 Spot Welds on Cathodes in a Clorox Chlor-Alkali Plant—Examined some Nickel 200 spot welds that were found cracked in the cathode portion of chlor-alkali production cells at a chlorine production facility and determined the nature of this cracking. The nickel was exposed to 32-wt% caustic at 90°C. These cracks occurred in the heat-affected zone (HAZ) of the welds and therefore were not associated with defects in the weld metal, such as solidification porosity or hot tearing. The cracking was intergranular with little, if any, indication of ductile rupture. The location of the intergranular cracking in the HAZ of the spot welds may indicate that this cracking is associated with precipitation of a carbon film (or graphite), or segregation of sulfur, antimony, tin, or some other known embrittling trace element in the Nickel 200, at the grain boundaries during cooling. It is also at or near the maximum stress location. This cracking is most consistent with hydrogen embrittlement cracking driven by hydrogen charging at the cathode, potentially exacerbated by mechanical embrittlement from graphite precipitation or metalloid segregation in the grain boundaries.

Post-Tensioning Strands—Investigated the failure of post-tensioning strands used in several different projects. For example, Exponent performed a metallurgical failure analysis investigation on two post-tensioning strands that failed in service on a bridge tendon in Tampa, Florida. The failed strands were identified during the bridge's first annual inspection. The investigation included optical microscopy, scanning electron microscopy (SEM), metallographic examination, microhardness, and chemical analysis. The investigation determined that the strands fractured due to environmentally assisted cracking (EAC) because of water ingress into the tendon combined with a lack of protective wax coating on areas of the strands that failed. The EAC fractured strands exhibited microstructures, microhardness, and chemical composition consistent with high-strength steel wire typical of post-tensioning wires. There was no evidence of gross corrosion that would have reduced the wire cross-sectional area to the point that wires

would break under normal post-tensioning loads. Corrosion product in some of the environmentally assisted cracks indicated that the EAC had occurred months earlier prior to discovery.

Underground Storage Tanks (USTs), Pipelines, Piping, and Plumbing

Leaking Underground Fuel Storage Tanks—There were several projects regarding this issue. Investigations included corrosion analysis to determine the likely time that the leaks started, analysis of the risk of corrosion thinning and weld defects being underestimated from various inspection methods, and the effect of cathodic protection and coatings on increasing useful life.

Hot Water Recirculation Systems—Investigated the reasons for copper plumbing (piping) leaks in a housing development. The failure investigation indicated the reason was too high a flow rate of the water in the hot water recirculation system that caused erosion-corrosion of the copper piping, which consisted of both hard and soft copper lines.

Pitting of Copper Tubing in Computer Room Air Handlers (HVAC) System—Investigated the cause of through-wall pitting of aluminum finned copper tubing used in the chilled water system of a large data center's air handler (i.e., computer room air handler, or CRAH). This system, containing both steel and copper piping in the computer room, had originally been run with a nitrite-based water chemistry with the addition of tolyl-triazole (TT) as the copper corrosion inhibitor. These units had been in operation for about five months when the first leaks were reported. The copper coils leaked because of internal pitting corrosion from microbiologically influenced corrosion (MIC) of the copper. Some algae were found in the chilled water. In addition, the presence of MIC was supported by the corrosion morphology (isolated pits under deposits), and DNA/RNA testing indicating the presence of denitrifying and nitrifying bacteria. The use of nitrite in an open loop system that can allow oxygen ingress that will convert the nitrite to nitrate may have provided a food source for the nitrifying-denitrifying bacteria. In addition, the lack of a biocide would allow MIC to occur. The very thin wall of the copper tubes makes them very susceptible to corrosion-induced leaks.

Internal Corrosion of Copper Piping Used to Supply Potable Water—Several projects dealt with this issue, including the "Blue Water Problem" that occurred in the early 1990s in the Danville and San Ramon Valley area of California. Issues considered includes stray current, solder flux, water flow rates, time of stagnation, soft versus hard, copper piping and the inner surface condition (Campbell carbon film theory), MIC, water chemistry including scaling index, dissolved oxygen, and residual chlorine effects. Projects also included several cases of pitting-induced leaks in potable copper piping. In one instance, after some 30 years of few water leak reports, there was a sudden onset and frequency of pinhole leaks. It was expected that the localized corrosion on the inner surface of the copper piping was a result of a recent change in the water chemistry of the supplied water as there was no indication of erosion-corrosion, defective piping, or solder flux induced corrosion.

Crude Oil Pipeline Release—Investigated and performed a failure analysis, and provided testimony regarding the adequacy of the corrosion protection (coating and cathodic protection) of a 20-inch-diameter crude oil line that leaked. The leak was found to have occurred on the bottom side of the pipe elbow. The corrosion that caused the crude oil release was a result of anaerobic MIC. This type of corrosion can be very rapid and can occur even if the pipe is being appropriately cathodically protected—i.e., maintained at a pipe-to-soil potential below –850 mV versus Cu/CuSO4. There was no evidence that this line was improperly cathodically protected or that the leak was a result of stray current from either high-voltage electrical transmission lines overhead, the railroad nearby, or other potential sources. Exponent performed an experiment that allowed the amount of oil released to be calculated given certain assumptions regarding the temperature and pressure history at the elbow, oil viscosities, and time at which the elbow was penetrated.

Corrosion Investigation of Piping, Tanks, and Joints at Gasoline Stations—Investigated the condition of metal product (gasoline) piping (primarily galvanized pipe), joints, and unions at gas stations, and evaluated the corrosion, if any, that was observed.

Natural Gas Pipeline Rupture and Explosion—Investigated the cause of a 36-inch natural gas transmission pipeline rupture that occurred in Carlsbad, New Mexico. This investigation included evaluation of the effects of internal corrosion and assessment of the extent to which water ingress into the transmission line from third-party producers and the pipeline configuration may have contributed to the observed internal corrosion.

Natural Gas Pipeline Permit to Increase Operating Pressure—Performed a technical evaluation of a petition to modify an existing special PHMSA permit to allow a gas transmission company to increase the maximum allowable operating pressure (MAOP) in this section of its pipeline. This modification would allow the company to undertake fewer excavations and repairs at areas where surveys indicate damage to the pipeline coating. Analysis of alternating-current voltage gradient (ACVG) indications of coating damage could have been a result of either third-party excavations at various locations along the pipeline or corrosion. Factors such as external SCC and denting or gouging—as determined by in-line inspection (ILI) and external corrosion direct assessment (ECDA)—were considered.

Painted Steel Pipe Aqueduct—Investigated the condition of 10 miles of painted aboveground steel piping with approximately half-inch-thick wall that had become submerged because of a flooding event. Pipe diameter varied from 65 inches to 87 inches. Some flood-induced abrasion damage to the paint was noted on some of the pipelines. Biological growth was also observed on the paint on the undersides of the pipelines. There was little to no significant corrosion damage to the steel pipeline. Various alternatives were considered regarding how to bring the pipeline coatings to pre-flood conditions.

Evaluation of Corrosion on Stainless Steel—Carbon steel and stainless steel piping and fittings were submerged for several days in flood waters. These pipes and fittings were to be used in the construction of a liquefied natural gas (LNG) facility. These components were inspected and subjected to wipe sampling for the presence of chlorides and sulfates and swab sampling for the presence of microbes that could cause MIC. The microbiological testing was performed using a DNA method that does not involve culturing. Samples, including positive and negative test controls, were analyzed for slime formers. As some slime formers are associated with MIC of carbon steel and stainless steel, but the primary microbial groups associated with MIC are the iron-depositing bacteria (IDB), sulfate-reducing bacteria (SRB), sulfuric-acid-producing bacteria (APB), and nitrifying bacteria.

Underground Corrosion of Cast Iron Water Main—Investigated and testified on the reasons for a cast iron water main failure. The reasons were graphitic corrosion and lack of cathodic protection (CP).

City Water Main Failures—Investigated several instances of water main failures. In one instance, as described in the following, the reasons for repeated water main failures in a municipal water distribution system was investigated. The system consisted of a network of 6-inch-, 8-inch-, and 10-inch-diameter cast iron pipes. A section of 10-inch-diameter pipe ruptured several times and the Department of Public Works (DPW) took the section of water main out of service until repairs or replacement could be completed. The DPW reported that this water main system had been repaired five times during the past two decades. Our investigation was to identify the cause of recent breaks and to help the city identify portions of the water main within the area that could remain in service without significant risk of imminent rupture. Those pipe sections were gray cast iron with a mortar coating on the interior surface and no coating on the exterior surface. There was no CP on this pipeline as determined by the pipe-to-soil potential measurements. The most recent pipe rupture showed signs of extensive graphitic corrosion.

External Underground Corrosion of Copper Laterals—Investigated the reasons for through-wall corrosion of copper laterals in a new housing development. CP was recommended.

External Underground Corrosion of HVAC Supply/Return Water Piping—Investigated the reasons for through-wall corrosion of steel HVAC supply and return underground water piping to an office building. Stray current effects were evaluated. Isolation and cathodic protection were suggested as a remediation method.

PEX Plumbing System Failures—Leaks in many homes utilizing cross-linked polyethylene (PEX) plumbing. Most leaks occurred on the hot water supply line. The PEX plumbing joint is composed of PEX piping, a brass elbow or tee, and stainless steel crimp bands. The stainless steel bands are used to clamp PEX tubing to brass fittings. Some of these clamps had failed, resulting in a leaking joint. Scale or deposits were found on the inside and outside of the incident brass fittings. Analysis of the corrosion deposits was done with energy-dispersive spectroscopy (EDS) in a scanning electron microscope (SEM). The deposits were composed mainly of zinc, oxygen, and aluminum with traces of carbon, lead, iron, and nickel. SEM examination of the fractured stainless steel crimp bands indicated it failed from intergranular stress corrosion cracking (SCC). EDS analysis revealed chlorine present on the band near the fracture surface. The SCC of the stainless steel clamp appears to be the result of moisture and contaminants leaking through the wall of the dezincified brass.

Brass Valves and Fittings—There were many projects involving SCC, intergranular attack (IGA), fire cracking, and dezincification (dealloying) of brass valves and fittings manufactured from brass for water, oil, and gas plumbing service (WOG). Analyzed red brass, yellow brass, and low lead (Pb) or lead-free brass components. Issues included water chemistry effects, alloy chemistry, microstructure, hardness, residual stress, and installation stresses, temperature of operation. ISO and NSF dezincification standards as well as ammonia vapor testing for SCC resistance per ASTM B858 testing.

Polybutylene Potable Water Pipe Failure—A landslide occurred on a steep hillside. A leak in polybutylene (PB) potable water fitting on supply main may have been the reason the landslide occurred after a long dry spell. PB pipe has a high susceptibility to chemical degradation, and a low resistance to cracking. The rate at which antioxidants are leached from the pipe interior water chemistry, stress in the PB pipe at the rigid coupling, and other factors in environmental stress cracking (ESC) were considered. Fractography of the PB pipe fracture surface was performed to determine if the pipe failed because of ESC and thereby was a cause of the landslide, or because of ductile overload and thereby was a result of the landslide.

Ethylene Steam Pyrolysis Furnace—Investigated two ethylene plant incidents. Both incidents resulted in damage to the high temperature tubes that are used to convert the ethane to ethylene. Both incidents resulted from a sudden and unplanned shutdown of an ethylene steam cracker plant from a loss of electrical power. This rapid shutdown caused immediate and potentially latent damage to the expensive nickel-chromium-iron (Ni-Cr-Fe) centrifugal case furnace tubes (cast HP or HK alloys or Incoloy 800H.). Ethylene is produced by reacting hydrocarbons (e.g., ethane) and steam inside tubes heated in a furnace The tube temperature is about 1000°C (1800°F). At these temperatures the tube metal experiences several damage mechanisms that eventually result in tube failure and replacement. The various damage modes and operating conditions leading to tube failures were investigated and include:

- Carburization during normal operation.
- Deposits that increase tube temperature, accelerating carburization.
- Oxidation and wear of the inside surface during decoking cycles.
- Overheating and melting of the tubes if the coke deposits are too thick or if a tube becomes partially or completely plugged.
- Sulfidation: Hydrocarbon mixtures frequently contain some level of sulfur. Iron- and nickel-based alloys are susceptible to accelerated high-temperature degradation when exposed to sulfur compounds, because of the low melting temperature of various metal sulfides. For example, nickel sulfide (Ni_3S_2) melts at 635°C.
- Creep, which is a phenomenon in which metal under stress at high temperature will slowly deform and eventually crack.
- Thermal fatigue, due to cyclic stresses.
- Metal embrittlement due to formation of intermetallic phases or sigma phases.

Central Arizona Project (CAP) Pipe Failure—Investigated the reason for prestressing wire failures that occurred on the pipe used in the CAP. CAP is a waterway that transports water from the Colorado River to central and southern Arizona. At the time of construction, it was the longest single water transportation project authorized in the United States. Where CAP crosses seven major riverbeds and washes, 6.4 m

(21 foot) diameter inverted siphons are used. Six of these seven siphons, ranging in length from one quarter mile to almost two miles in length, were constructed from what was at the time the largest precast prestressed concrete pipe (PCP) ever manufactured—i.e., pipe with an internal diameter of 6.4 m (252 inches), a wall thickness of 0.54 m (21 inches), and a length of 6.9 m (22.6 feet). Individual PCP sections weighed as much as 225 tons. The prestressing wire was high-strength patented steel wire (ASTM A648 Class III), and up to 35 km (22 miles) of wire was used to prestress each pipe segment. The pipe sections were not coated or cathodically protected. Wire fractures and splits were the main symptoms of wire distress in the CAP pipes. While the mortar initially contained low concentrations of chloride, evaporation led to a chloride concentration build-up to levels supporting SCC. Chloride levels in the wet/dry transition zone of the siphons were high enough to cause SCC without any significant carbonation of the mortar or the core.

Water Transmission Pipeline Leaks—Horizontal directional drilling (HDD) was used in the construction of a water transmission pipeline project. An 1,800-foot length of 31-inch-diameter, half-inch-thick spiral-welded steel pipe was pulled through the 1,800-foot-long HDD drilled hole at a river crossing. No leaks were found after installation. However, after about four years of service, this pipeline was found to be leaking. Investigated issues regarding the pipe coating, weld defects in the spiral welds, the corrosion rates, the pipe bend radius during the HDD operation, and resulting strains at the pipe welds.

Brass Plumbing Failure—Several brass elbows from two different commercial installations had failed. The cracking on the female end was examined with optical microscopy, and the fracture surfaces were examined with SEM/EDS. Ion chromatography of debris, corrosion product, and solder flux found on piping and fittings was examined for contaminates that may be responsible for SCC. The evidence pointed to fitting failures from overtightening.

Copper Plumbing Leaks—Leaks in copper piping were a result of pitting corrosion on the inner surface of the pipe caused by the supplied water chemistry. There was no indication of general corrosion, erosion-corrosion (also known as flow-induced corrosion), mechanical damage, defective piping, or solder flux induced corrosion.

Connector Hose Leaks—Investigated the reasons for leaks in plumbing in both stainless steel and copper corrugated flexible connector hoses where the connectors were attached to the elbow joint. The leaks were initiated on the inside surface where the corrugated tube was attached to the elbow joint. There was no evidence of obvious signs of corrosion, pitting, SCC, or fatigue. X-ray imaging and metallography was used to locate and target the leak locations. Significant porosity inside the solder/braze joints, from the time of manufacture, appeared to have interconnected over years of operational service. This interconnection of porosity was likely a combination of fatigue and corrosion that slowly opened a leak path between the porosity.

Flexible PVC Hose Leak—Investigated a leaking flexible hose manufactured from PVC tube with rigid PVC helix. It was used in a data center and was operating with a propylene glycol and water mixture at 28 psi at 136°F at the time of the leak. It had been operating within its pressure and temperature limits for a couple of hours prior to failure. There was no evidence of embrittlement or environmental stress cracking of the PVC or stiffening helix. Three short cracks were found only at the rigid PVC stiffening helix component at one location in the hose and all were aligned co-linear along the tube's longitudinal axis. The leak was caused by local deformation on one side of the tube, perhaps damaged by another tube laying on the hose that fractured the rigid helix stiffening ring but not compromising the hose pressure integrity. When placed into elevated temperature and pressure service, creep rupture resulted in crack propagation through this cracked and weakened region.

Powder Metallurgy

There have been many projects involving powder metallurgy. These projects included developing unique microstructures and properties using various methods of consolidation such is high-temperature high-pressure (HT-HP) sintering, hot isostatic pressing (HIP), and other processing techniques to make monolithic and composite structures. The following are a few examples of this project experience.

• Superplastic densification of ultrahigh carbon steel powder compacts
• Near net shape processing of heavy metal chemical energy warhead liners
• Development of very high strength and ductile white cast iron by stabilizing the carbides against transforming to graphite and heat treating
• Characterization of superplasticity in white cast iron
• Explosive compaction of Nd-Fe-B ferromagnetic powders

Intellectual Property (IP) Litigation

There have been various projects in the IP area involving patent infringement and validity, trade secrets, and inter partes review (IPR). The following are a few examples of this project experience.

Nitinol Patent Infringement—Provided expert testimony in an IP litigation involving whether multiple companies were infringing a patent involving superelasticity and shape memory properties of nitinol (NiTi). This effort included reviewing the patent, reviewing the court rulings, and testing exemplar materials to determine their shape memory and superelastic properties.

Stent Patent—Testified in an IP dispute regarding whether a stent being manufactured and sold infringed on a stent patent. The issues involved both manufacturing methods as well as design issues.

Wafer Cleaning Patent Infringement—Reviewed a new wafer cleaning apparatus to determine if there might be infringement of existing patents. The apparatus used the Maragoni effect (mass transfer along an interface between two phases due to a gradient of the surface tension) as part of the cleaning process.

Mitral Valve Repair Patent—Reviewed a patent and a venture capital funded company's proposed mitral valve repair device to see if there would be infringement.

Gastroesophageal Reflux Disease (GERD) Patent—Developed a probabilistic economic model to estimate the present value of a GERD patent.

Digital Thermometer Patent—Performed inspections using microfocus X-ray radiography that demonstrated infringement on a patent.

Lead Alloys for Anodes—Trade secret litigation regarding improper use, disclosure of confidential information, and trade secrets regarding lead (Pb) alloys used for anodes in the electrowinning/ electroplating of copper and lead recycling.

Use of Coiled Steel Tubing—Patent regarding manufacturing coiled steel tubing use in the oil and gas industry. Specific issues included the microstructure of the base material, heat-affected zone (HAZ), and weld metal and the various techniques that can be used to evaluate them. Of particular interest were martensite, tempered martensite, and bainite microstructures.

Hydraulic Fracturing Method—Patent regarding a method of hydraulic fracturing involving, among other things, a well service pump, fluid end body, salinity (salt concentration) of hydraulic fluid, corrosion-resistant steel, a minimum fatigue limit, maximum working pressure, and tensile stress. Addressed both validity and infringement.

Hazardous Chemical Releases

Ammonia Release—An injury resulted when a worker was overcome by ammonia that had been released from failed tubing that was part of the refrigeration system at a large frozen foods warehouse facility. This effort involved a microscopic examination of the failed part with scanning electron microscopy (SEM) and energy-dispersive spectroscopy (EDS) and a comparison with exemplar products. Issues considered

were silver brazing, joint strength, vibration-induced fatigue, and whether a manufacturing defect was present.

Chlorine Release from Rail Car—Two trains collided, and a pressure tank car loaded with liquefied chlorine was punctured, releasing a vaporized cloud of chlorine gas about 700 feet in radius prior to drifting away from the site. Three people died in this incident. Exponent was asked to investigate the extent of corrosion or other environmentally induced damage, if any, done to property that was being transported on one of the two trains. This investigation included a thorough visual inspection and wipe sampling of all the consumer product products being transported.

Chlorine Release from Chlor-Alkali Plant—Investigated the root cause failure of a large chlorine release that occurred at a liquid chlorine production facility located in Henderson, Nevada. This release required the evacuation of areas surrounding the plant. This investigation reviewed the various plant processes, including the primary chlorine liquefier. Efforts included detailed metallurgical examination of corroded components, use of computational fluid dynamics to model the flow of liquid chlorine, and corrosion experiments in brine contaminated chlorine. Experiments and computational fluid mechanics were used to evaluate the erosion-corrosion in which chilled brine entered the liquid chlorine stream at a hole that had developed in the primary liquefier. The corrosion rate of steel in liquid chlorine/brine mixtures at high-flow velocities was measured to determine how fast this mixture would corrode through the rundown elbow, causing the chlorine release.

Toxic Effects of Tungsten Alloys—Tungsten-based alloys have been gaining in usage as munitions since they are considered an environmentally friendlier alternative for lead and depleted uranium-based materials. For larger caliber munitions (>30 mm), a two-phase material called tungsten heavy alloy (WHA), is used. WHA consists of pure tungsten bound together with a lower melting temperature metal alloy binder. The alloy binder is typically composed of nickel and either iron or cobalt (sometimes both). For smaller caliber munitions, tungsten carbide (WC) particles are bound together or "cemented" by a ductile binder phase of cobalt or other alloys. These materials are variously known as hard metals, cemented carbide, or cermets, and are used in armor-piercing rounds. When WHA and hard metal munitions are used, there is the possibility that fragments (shrapnel) may be present in vivo for long periods of time. Recently, an unexpected adverse toxicological response to some of these was discovered during laboratory animal testing. Preliminary work suggested that galvanic interactions between the tungsten particles and the surrounding metal matrix binder phase in these materials may be responsible for this behavior. To develop a better understanding of the corrosion behavior of these materials in vivo, a set of in vitro laboratory experiments was conducted to assess corrosion in these materials in three ways: through galvanic testing of selected material pairs, through long-term immersion metallic ion release testing of WHA and other materials, and through characterization of these materials using ASTM F 2129—a standardized testing procedure for assessing localized corrosion in medical implants (ASTM F 2129-08 2008). All the experiments were conducted in a simulated physiological environment—i.e., pH 7.4 phosphate-buffered saline (PBS) solution at 37°C.

Chlorine Release from Train Collision—A train collided with a stationary train that carried a liquefied chlorine rail car, which was punctured in the collision. The resulting chlorine cloud killed several people and resulted in corrosion damage to the factory that was located at the site. The extent of corrosion damage to various plant equipment, structures, and electronics was evaluated using wipe sampling, SEM/EDS, and atmospheric corrosion coupons.

Iodine Release from Drug Manufacturing Laboratory—A glass container stored in a laboratory refrigerator that contained an organic iodine compound came into contact with the plastic lining of the refrigerator, and then leaked onto the floor. It is likely that this compound decomposed into iodine and hydrogen iodine, which caused extensive atmospheric corrosion damage to stainless steel and other equipment and facilities throughout the lab.

Corrosion-Induced Nitrogen Tetroxide (N_2O_4) Release from Rail Car—Investigated the circumstances leading up to the failure of a carbon steel rail car that was transporting approximately 110,000 pounds of N_2O_4. Upon receipt, the contents were found to be contaminated with water. The contents were diluted

with water until the tank rupture occurred. The jacket head was blown 350 feet from the rail car, the inner tank liner was ruptured, and the rail car was propelled 35 feet and derailed. A large reddish-brown cloud was released as a result of this rupture. The interior and exterior of the rail car was inspected along with components removed from the rail car. A series of laboratory tests were conducted in Exponent's corrosion/chemistry laboratory to recreate conditions inside the rail car prior to its rupture. A chemical corrosion reaction between nitric acid and carbon steel inside the rail car caused a dramatic and localized reduction in the wall thickness. This substantially decreased the pressure required for rupture. Nitric acid corrosion of the carbon steel rail car shell resulted in continued wall thinning, very rapid gas generation, rapidly increasing the pressure inside the tank car, ultimately causing the tank car end to fail.

Silane Release—Investigated the cause of cracking and leakage of a silane-producing chemical reactor vessel after 13 years of service. This reactor vessel processes superheated hydrogen and silicon tetrachloride in a fluidized bed of metallurgical grade silicon operating at 1,000°F and 300 psi. This produces an effluent of approximately 80% silicon tetrachloride and 20% trichlorosilane. Metallographic, corrosion, and mechanical property testing were performed on the Incoloy 800H hydrogenation reactor vessel material. ASTM G28 sensitization was performed on the vessel material. Cracks were in both the weld and the heat-affected zones (HAZ). Intergranular carbides were present in both the base and the HAZ material. The failure was likely the result of sensitization-induced intergranular stress corrosion cracking (SCC).

Sodium Hydroxide Release—Investigated the SCC that occurred to steel and Nickel 200 used in a multiple-effect evaporator for sodium hydroxide. Both the first-effect and second-effect vessels had experienced some levels of cracking.

Hydrogen Sulfide Release—Assessed the occurrence and cause of sulfide-induced SCC in small bore process piping welds that led to releases of hydrogen sulfide (H2S) gas into the environment at an upstream oil and gas processing facility.

Thorium-Containing Dust Particles—Evaluated issues surrounding a glioblastoma brain tumor cluster alleged to have been the result of either exposure to X-ray radiation or small levels of dust containing thorium. Provided critical review of the characterization of the few very small dust particles that were found to contain thorium and their likely source.

Electronic and Electrical Equipment and Consumer Goods

Ball Grid Array (BGA) Fatigue Failure—Investigated the reasons for the failure of an electronic consumer product. This investigation involved thermal management, BGA solder joints, low cycle fatigue, and underfill issues. Accelerated life testing, statistical analysis of field failure data, modeling of creep-fatigue and intermetallic compound formation, and finite element analysis (FEA) were used to help understand the reason for the BGA cracking.

Lead Free Solder—Examined the effect of various board finishes, such as organic solder preservative (OSP), hot air solder leveling (HASL), electroless-nickel immersion gold (ENIG), and Immersion Silver (ImAg) on the reliability of lead-free (SAC) solder BGA-mounted devices.

Oxidation Rates—Evaluated liquid metal oxidation rates for gallium-indium-tin solders (Ga/In/Sn) and the effect of relative humidity.

Backup Alarm on Earthmoving Equipment—A fatality occurred when a grader backed up over an employee at a construction site. The backup alarm on the grader was not operating when inspected after the accident, because one of the wires had been cut. The cut wire was examined to determine the nature and timing of the cut. This investigation determined it was not cut with wire cutters. Examination of the cut wire with SEM/EDS could not reliably determine whether the cut had been made near the time of the accident or several years earlier.

Limit Switch Failure—Investigated a limit switch that reportedly failed to turn off and disengage the control circuit for an electric motor on a hoist on board a U.S. Navy ship, resulting in a serious injury. The accident limit switch and exemplar switches were examined and tested electrically and mechanically. Scanning electron microscopy (SEM) and energy-dispersive spectroscopy (EDS) were used to investigate the atmospheric marine corrosion that had developed on the various materials of construction, 6000 series aluminum, copper, and steel. The primary cause of failure was that the wrong type of limit switch was specified and installed. However, even if the appropriate limit switch had been used, the accident still may have occurred since the tab was incorrectly placed on the lever and the accumulation of debris from the marine atmospheric corrosion may have prevented correct operation.

Bus Transfer Criteria for Power Generating Stations—Computer simulation and mechanical analysis was used to see the effect of the ANSI C50.41-1982 criteria for bus transfer on electrical power generating equipment damage. Some methods of bus transfer result in all external sources of power being removed from auxiliary buses for a short period of time. Electric motor-driven equipment will decelerate when all external power sources are removed. The rates of deceleration depend on the inertia of the drives and the synchronizing power. Data on motor-driven equipment, including pumps, fans, compressors, and pulverizers, and, where possible, their motors, were collected from various manufacturers. Single machine simulations showed that high-inertia fan drives were found to have limitations when transferred at or near the criteria limit. Multimachine simulations indicate that drives can be subjected to more transfer without concern for crack initiation due to torsional fatigue. In most cases, and particularly for high-inertia fan drives, the limiting component of the shaft system is the motor shaft keyway.

Handheld Consumer Electronic Manufacturing Issue—Discoloration was observed on a polished stainless steel part that was being developed for a handheld consumer electronic device. It was found that a lead-free solder was used to attach a bracket and that the residual flux containing chloride had attacked the stainless steel substrate.

Photoelectric Sensor/Emitter Failure—Performed a root cause analysis of a photoelectric sensor/emitter used in exercise equipment. Visual inspection, optical microscopy, and SEM/EDS were used on these sealed devices to determine the likely root cause of failure. No leak path for moisture ingress was found at the transmitter and receiver windows, and moisture likely entered along the power cord.

Thermal Contact Resistance—Methods to reduce thermal contact resistance with thermal greases, phase change materials, soldering, and other methods.

Smoke Detector—Investigated a badly damaged smoke detector. Performed microfocus X-ray radiography to look for the presence of any manufacturing defect.

Stray Current—Various projects involving whether stray current from above-ground and below-ground electrical utilities had affected the corrosion of above-ground or underground steel and copper piping.

Stray Current from Telecom Cables—Investigated external pitting corrosion observed on the copper lateral water supply to private homes. Determined that the cause was stray current from telecommunication cables.

Output Multiplexers (OMUX)—Investigated the low-cycle fatigue life of a copper OMUX component used in communications satellites. Performed a finite element analysis (FEA) and used these results to evaluate the fatigue life via the Coffin-Manson fatigue relationship between cyclic plastic strain and the number of cycles to predict low cycle fatigue life.

Transformer Explosion—International arbitration in Singapore regarding the cause of an explosion of a 500 kV generator step-up transformer (GSUT) at a complex of coal-fired power plants. Issue involved corrosion design and maintenance issues that allowed moisture ingress into the high-voltage bushings. The transformer was in a hot tropical marine environment.

Marine, Maritime, and Shipping Failure Analysis

Metallurgical Issues on Offshore Drilling Platforms—Examined the cause of metallurgical defects and cracks found in large-scale gearing on offshore drilling platforms (jack-up rigs). Presented the findings to the International Center of Dispute Resolution (ICDR) in Houston. The jack-up systems have many gearboxes on each of the three legs of the platform. The pinion is a large forged, quenched, and tempered steel shaft with gear teeth that engage the teeth of a rack affixed to each leg to move the hull up or down. In addition, the gearbox contained many planetary gears and torque plates manufactured by casting. The pinions were not properly heat-treated and/or did not have enough hardenability to achieve the required mechanical properties. The planetary gear components contained excessive aluminum nitride and suffered from aluminum nitride embrittlement. Stress analysis by finite element analysis (FEA) and fracture mechanics were performed to show that the material and heat treatment were not suitable and were responsible for the failures in the shipyard.

Stern Tube Corrosion—Investigated the reasons for a series of stern tube failures on 87-foot boats in a seawater environment. Issues involved the materials selected and inadequate cathodic protection.

Evaluation of Seawater Pump Failure—Investigated two seawater pumps used in an HVAC system. Crevice and deep pitting corrosion was observed in cast duplex stainless steel that occurred in as little as one year of service.

Ship Propulsion Boiler Bolt Failures—Socket head bolts holding the surface blowdown valve bonnet to the valve body failed on a ship operated by the Military Sealift Command. The boiler water chemistries that had been used over the years was investigated. The first boiler water chemistry used was a coordinated phosphate program. This was changed to a continuous chelate treatment consisting of EDTA-hydrazine-phosphate. The boiler water treatment was then changed to a catalyzed hydrazine, disodium phosphate, and sodium hydroxide treatment. Fractography of the bolt fracture surfaces clearly showed that the fracture surface was almost entirely intergranular, indicating that caustic stress corrosion cracking was the reason for the failure. This failure mode was consistent with some of the prior water chemistries used (particularly the ones with high Na/PO4 ratios) since, when concentrated, they can cause concentrated sodium hydroxide solutions to develop.

U.S. Coast Guard Cutter Hull Penetration—A 110-foot patrol boat steel hull was protected by epoxy and anti-fouling paint and an impressed-current cathodic protection (CP) system. Nonetheless, a corrosion hole occurred about eight inches below the waterline. The CP system was found to be in general working order, but the paint in this location had been damaged.

Shipping Container Cargo Crane—Analyzed the reason for cracking observed on a newly build container handling gantry crane. This crane had recently been placed into service at one of the West Coast ports. Cracks developed in the box beam structural elements. Investigated the design, methods of manufacture, and operating history to determine the reason for the cracking.

Fracture of Navy Ship Welds—A probabilistic fracture mechanics (PFM) analysis was performed on U.S. Navy vessel weldments, as described more fully in the section on Welds and Welded Connections.

Pretensioned Monel K-500 Propeller Bolts—Powerheads are used by the marine industry to install pretensioned Monel alloy K-500 ship propeller bolts. The powerhead is manufactured from high-strength steel. The LaQue Center for Corrosion Technology corrosion-fatigue tested the powerhead and bolts in natural seawater. Both the Monel bolts and steel powerheads were cathodically protected with zinc anodes during the corrosion fatigue. The powerhead and bolts were fatigue-cycled till fracture. Exponent investigated to determine the location of the fracture origin and the mode of failure.

Identification of Debris on Ship Hull—Investigated debris that was found on an unpainted area of a ship hull docked in brackish water to determine if it was of a microbiological origin. Optical and scanning electron microscopy (SEM) were used, along with energy-dispersive spectroscopy (EDS), to help

characterize this material. No evidence was found that indicated a microbiological origin. The most likely origin of the debris was from the CP system that resulted in the formation of a calcareous deposit at this location.

Fire and Fire Prevention Investigations

Electric Power Line Arcing—Investigated several fires that have been initiated as the result of arcing from electric power lines. One incident occurred where an aluminum conductor from a high-voltage transmission line had broken and fallen along a road. The origin of the fire was near a tree where the downed line was found. The arc marks were found to be consistent with arcing between the tree limbs and the high-voltage line. Other arcing-initiated fires occurred because of fatigue fractures or fretting/wear-induced failures.

PCB Fire—Investigated an electrical failure that involved rapid thermal damage to the printed circuit board assembly (PCBA) for a medical device that was used in an operating room. Exponent's analysis aimed to understand the cause and origin of the failure and the potential risk of such failures to patients and medical professionals, to offer suggestions for redesigns to minimize future failures, and to evaluate fire and smoke inhalation hazards that may be associated with the electrical failure.

Veterinarian Clinic Fire and Explosion—Investigated a fire and explosion in a mobile veterinarian clinic. Cause and origin were associated with a copper fitting fatigue failure associated with the propane tank.

Arc Damage from Lightning—Investigated the cause of a mercaptan groundwater contamination and soil remediation litigation. A stainless steel mercaptan line, used to inject the odorant to natural gas prior to distribution, was found to be leaking. The leak location on the stainless steel line, which ran underground, was found to be near the grounding rod of a power line. A microstructural investigation of the hole was conducted to determine if the hole was a result of stray current or a lightning strike.

Propane Explosion and House Fire—Investigated the cause and origin of a propane explosion and house fire. Investigated the propane piping and fittings for the cause and origin of their fractures.

Fire Protection Systems (FPSs)—Failure analysis investigations regarding FPSs include the following:

• Investigated leaks in a copper fire sprinkler piping. Corrosion was occurring on the wet side. Investigated allegations that the lubricant used to drill holes or the flux at solder joints was responsible for the leaks.
• Investigated leaks on an FPS. There was corrosion in the inner surface of the steel lines. The issues investigated involved microbiologically influenced corrosion (MIC), defective electrical resistance welds (ERW), grooving corrosion, and corrosion tubercles.
• Investigated the failure of a cast iron elbow in a fire sprinkler system in a food warehouse. Failure was determined to be the result of high pressures formed from an ice plug.
• Failure and flooding from large-diameter fire protection water supply line to a large warehouse. Investigation of the fracture surface and graphitic corrosion indicated failure was associated with initial installation defect.
• Investigated the cause and origin of leaks in an FPS in Hawaii. Issues considered were atmospheric marine corrosion and pipe dope used to seal cut thread in steel pipe.
• Investigated the cause and origin of leaking in FPSs in California. Issues considered were ERW weld defects in seam-welded steel pipe and frequent refilling with fresh water due to operational issues.

Medical Device Investigations

Corrosion Evaluation for Various Implantable Medical Devices—Evaluated a wide range of medical devices and materials for a wide variety of medical device manufacturers. These efforts have included evaluating the medical device's corrosion resistance and surface finish using long-term potential

monitoring, ASTM F3306 Standard Test Method for Ion Release Evaluation of Medical Implants (nickel ion release), ASTM F2129 Standard Test Method for Conducting Cyclic Potentiodynamic Polarization Measurements to Determine the Corrosion Susceptibility of Small Implant Devices, ASTM F3044 Standard Test Method for Evaluating the Potential for Galvanic Corrosion for Medical Implants, transformation temperature determination by differential scanning calorimetry (DSC) in accordance with ASTM F2004 Standard Test Method for Transformation Temperature of Nickel-Titanium Alloys by Thermal Analysis (for instance Af temperature determination), nickel-ion release (leaching) rates, Auger electron spectroscopy, and X-ray photoelectron spectroscopy (XPS) in order to evaluate the chemical composition as a function of depth into the passive/protective oxide layer, and other techniques. Devices and types of corrosion effects evaluated included:

• Passivated stainless steel stents with and without radiopaque markers such as platinum, tantalum, and gold markers.
• Implantable neurostimulator and leads—dissolution rate of platinum.
• Electropolished nitinol (NiTi) coronary stents with and without radiopaque markers.
• Platinum iridium coils.
• Analysis of polymer membrane degradation mechanism for endometrial ablation and suggestions to improve reliability.
• Tungsten dissolution metal release in vivo.
• Cobalt-chromium (CoCr), Elgiloy, Phynox MP35N, stainless steel, and nitinol stents that are overlapped for fretting/wear and galvanic corrosion testing and analysis.
• Nitinol (NiTi) with various organic and inorganic coatings.
• Potential for crevice corrosion from markers or delaminated coatings.
• Metallic components of mitral and aortic heart valves, both mechanical and tissue.
• Annuloplasty rings.
• Inferior vena cava (IVC) filters.
• Various implantable chronic obstructive pulmonary disease (COPD) devices.
• Various implantable devices to mitigate sleep apnea.
• Evaluation of corrosion-fatigue strength of various implantable devices.
• Analysis of the effect of shelf life on the mechanical properties of nitinol.
• Fretting fatigue evaluations.
• Evaluation of the metal ion release (primarily nickel ion release from nitinol and stainless steel) from a variety of implantable medical devices. Measured metal ion leaching from cardiovascular, neural, gynecological, and orthopedic devices and tools manufactured from nitinol, cobalt-chromium alloys, tungsten, MP35N, etc., using ASTM F3306 Standard Test Method for Ion Release Evaluation of Medical Implants.
• Fatigue failure of a CoCrMo (ASTM F1537) modular neck used in total hip arthroplasty (THA).
• Hip implant Ti6Al4V (ASTM F136) femoral neck fatigue fractures.
• Osteointegration of acetabular cup manufactured from beaded CoCrMo (ASTM F75).
• Metal-on-metal (MoM) hip implants: Investigated tribology issues associated with the release of wear debris from MoM and modular tapered junctions used in total hip arthroplasty/replacements (THA/THR).

Electronic Failure in Implantable Device—Performed a failure analysis, and suggested methods to prevent further such failures, for an electronic medical device that failed during clinical trials. The issue involved stress corrosion cracking of glass and laser sealing.

Lung Tissue—Performed an examination of lung tissue with SEM and EDS to determine the size, shape, and composition of particles that were present, if any. Many particles in the tissue were found to have come from various metal alloys as well as silica particles. Most particles were less than 5 microns in size.

Accelerated Life Testing for Active Implantable Medical Devices—Helped a medical device manufacturer design a suite of HASL and accelerated life tests (ALTs) to assure reliability of a new design for an electrically active implantable medical device (AIMD). This effort involved considering potential failure modes and suggesting tests to determine acceleration factors for the ALTs. Mechanical (fatigue, shock, etc.), electrical, and chemical tests were considered.

Implantable Batteries—Various projects involving the testing and manufacture of different types of lithium batteries used for biomedical applications. Destructive and nondestructive failure analysis of primary lithium-silver vanadium oxide (Li-SVO) ICD batteries that exhibited less than expected life including X-ray computed tomography (CT), open circuit voltage (OCV), complex impedance, and swelling measurements.

Leaking Medical Devices, Hermetic Sealing Issues—Helped various implantable medical device manufacturers (cardiovascular and neurological) to determine the reason for moisture ingress. Helium (He) leak checking, dye penetrant testing, metallography, SEM, microfocus X-ray radiography, micro-CT, residual gas analysis (RGA), and accelerated life testing were utilized to solve these problems.

Spinal Rod Failure—Investigated the reason for the failure of the Harrington rod used in the correction of Scheuermann kyphosis. The spinal rod failed because of fatigue. The transconnector had migrated to the end of one rod. The fractured rod, pedicle screws, transconnector, and hooks were examined.

Flexible Reaming System Failure—A patient was undergoing an open reduction internal fixation (ORIF) of a femur fracture. While undergoing the multiple reaming steps to enable the insertion of the intramedullary nail, the reamer head came loose. The allegation was that the flexible reaming system was defective, allowing the reaming head to detach. The surgeon was unable to retrieve the head during this procedure. The patient declined to have the surgeon remove it and had it removed several weeks later by another surgeon after the patient developed an infection. Based on examination of the flexible reaming rod and reaming head, nothing was found wrong with the design or manufacture. There was testimony that the root cause of this failure was that the surgeon had not used the flexible reaming rod during the last reaming operation. The presence of the reaming rod was required for locking the reaming head to the rod, thereby allowing it to detach.

Stainless Steel Bone Plate Failure—Investigated an explanted 316 stainless steel tubular bone plate with seven locking holes that had fractured in situ. The fracture occurred at the middle hole, and fatigue striations were found on the fracture surface. No material or manufacturing defects were found.

Tracheobronchial Stent Failure—A tracheobronchial stent fractured while implanted. Investigated design and manufacturing issues regarding this stent. The adequacy of accelerated life testing for mechanical fatigue (effect of coughing) and corrosion resistance, and submissions to the FDA were reviewed as were product quality management documents. This stent was manufactured from cobalt-chromium-nickel-molybdenum wire. Allegations of improper heat treatment were considered and dismissed based on micro-hardness measurements. It was determined that this stent had failed because of fatigue and the device was found to be free from material or manufacturing defects.

Electronic Control Module for a Medical Procedure—A printed circuit board assembly (PCBA) used in a medical procedure experienced rapid thermal damage due to an electrical failure. Exponent's analysis aimed to understand the cause and origin of the failure, to identify the potential risk to patients and medical professionals from fire and smoke inhalation hazards, and to provide recommendations to minimize future failures.

Pedicle Screw Failure—A patient underwent surgical decompression and fusion that used a pedicle screw system (i.e., a pedicle screw, rod, and locking nut). There was a revision to the original surgery that required the replacement of all locking nuts. Several weeks after the replacement of all locking nuts, the lower-most pedicle screw came off the rod. Investigated the reasons for this failure.

Instrumentation and Data Analysis for In Vivo Loading—Instrumented an implantable medical device (mitral annuloplasty repair device) to collect in vivo biomechanical loading data on a heart repair device for fatigue life analysis.

Trocar Injury Investigation—Evaluated the issues surrounding the reasons for a safety trocar injury.

Retained Objects Post-Surgery—Several investigations regarding the identification of material found in patients after specific surgeries. One instance involved a guidewire that had been left in the patient after the placement of porta-catheter (port-a-cath).

Failure Analysis of Vena Cava Filter—An inferior vena cava (IVC) filter failed to deploy correctly and was successfully retrieved surgically. Reviewed medical device and manufacturing records as well as photographs of the retrieved device within order to determine if a manufacturing defect was responsible for improper deployment.

Failure Analysis of Pacemaker Leads—Investigated the reasons for pacemaker lead failures. Issues included corrosion-fatigue, fretting, how polymer materials were used, manufacturing changes, effects of residual stress, and in vivo loading of the leads.

Failure of Periarticular Screws—Examined the periarticular system including tibial plates and two broken screws with a stereomicroscope and scanning electron microscope (SEM). The subject periarticular screws fractured due to low cycle fatigue crack initiation and growth. The fatigue fracture of the subject screws was due to cyclic in vivo loads that exceeded those for which they were designed.

Safety and Hazard Analysis for Various Medical Devices—Performed safety and hazard analysis such as failure modes and effects analyses (FMEAs) for various medical devices including fertility control devices, brain stem implants, needle incineration devices, plastic surgery devices, septal defect closure device, hearing aid, and a drug inhaler.

Stress and Fatigue Analysis of Various Implantable Medical Devices—Performed stress and fatigue analysis of various implantable medical devices. Stress analysis has included estimating the loading conditions from biomechanical and medical literature reviews, measuring the in vivo loads, modeling device and tissue interactions with finite element analysis (FEA). The calculated stresses, or strains, are then compared to fatigue life data generated from accelerated life testing in physiological solutions such as phosphate-buffered saline (PBS), bile, Hanks salt solution, and Ringer's solution. Devices analyzed include anastomosis fasteners, stents (coronary, iliac, carotid, biliary), abdominal aortic aneurysm (AAA) stent grafts, heart valves, septal defect closure device, vena cava filters, bifurcated stents, COPD devices, and transjugular intrahepatic portosystemic shunt (TIPS). The effect of mean stress is accounted for by the modified Goodman, Gerber, Soderberg, and Haigh type of analysis. These results are generally used for PMA submissions to the FDA.

Great Toe Implant Failure Analysis—Examined the issues regarding the development metallosis in a Ti-6Al-4V great toe joint implant. Device design, manufacture specifications, and quality control during manufacture were examined.

Failure of Electrical Circuit in Defibrillator—Helped a defibrillator manufacturer understand the reasons for a small number of circuit failures that were observed during manufacture.

Intra-aortic Balloon Pump Failure—Examined the reasons for the failure of the balloon used in an intra-aortic balloon pump. The balloon had developed a leak after many days of use. Fatigue, abrasion, and appropriate instructions for use were evaluated.

Laser Cutting of Stents—Evaluated two different laser-cutting processes to cut stents from nitinol tubing. Metallography and SEM were used to characterize the laser-cut surfaces.

Broke Dental Needles—Evaluated several dental needle failures. Needles generally work reliably, but occasionally fine-gauge needles will break in use. Needle breakage in the oral cavity after local anesthesia is a common event, with possible serious complications. In many cases studied, needle fractures happened during inferior alveolar nerve block. It is generally considered to occur because of improper technique or because the needle was too thin. Analysis of the fracture surface of the needle can provide evidence for the presence or absence of material or manufacturing defects.

Examined Components for Possible Corrosion—Used optical microscopy, SEM, EDS, and FTIR to characterize the condition of the stainless steel and nitinol components of a medical device after they were used in animal testing for more than 36 hours. A few spots of reddish-orange deposits were found to be consistent with blood and not corrosion product. No obvious pitting or other corrosion was observed.

Editorships & Editorial Review Boards

Editorial Advisory Board for Engineering Failure Analysis

Appendix B

Deposition and Trial Testimony of Lawrence Eiselstein, Ph.D., P.E., 2020–2024

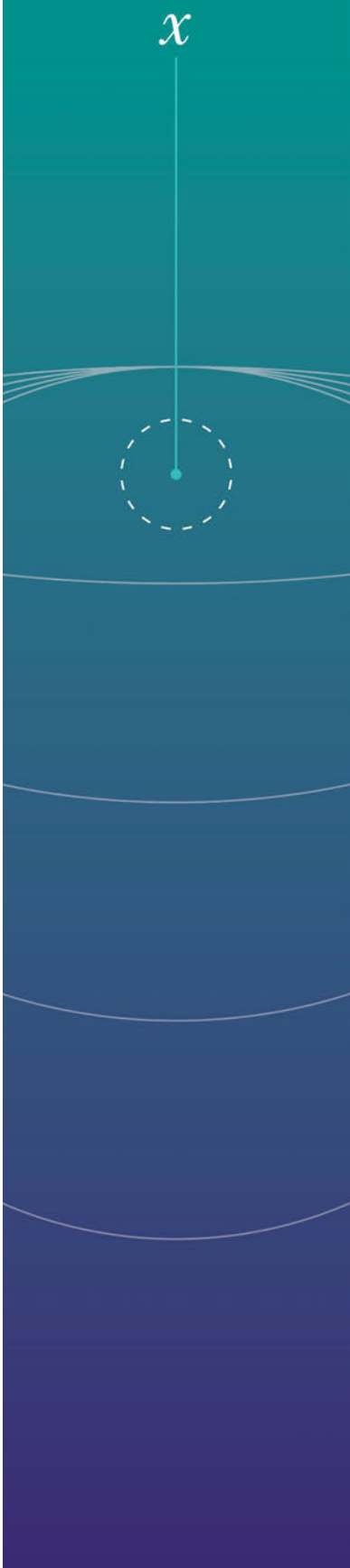

Deposition and Trial Testimony of Lawrence Eiselstein, 2020–2024

Trial or Arbitrations

1. U.S. Well Services, Inc. Plaintiffs, v. Halliburton Company, and Cimarex Energy Co., Defendants, In United States District Court Western District of Texas, Waco Division, Case No. 6:21-cv-00367-ADA, 21-24 August 2023

2. Patrice Sarah & Turner v. Bayer Australia Ltd. (ACN 000 138 714) & ORS, S ECI 2019 02916, Supreme Court of Victoria – Common Law Division – Trial Division, Melbourne, 6 June 2023.

3. In the Matter of the Arbitration Rules of the Singapore Arbitration Centre, between P.T. Paiton Energy (Claimant) and Mitsubishi Heavy Industries (Respondent), SIAC Arbitration No. 050 of 2021, February 23, 2023

4. Tadashi Mitsuoka and Victoria Mitsuoka, individually and on behalf of a class of all persons similarly situated, Plaintiffs, vs. Haseko Homes, Inc, a Hawaii Corporation, Haseko Construction, Inc., a Hawaii Corporation, Ke Noho Kai Development, LLC, Spinnaker Place Development, LLC, Fairway's Edge Development, LLC, and Does 1-10 Defendants, before the Tribunals of Dispute Prevention and Resolution, Inc., State of Hawaii, DPR Case No. 17-0447-A, Panel of Arbitrators: Lou Chang, Jerry M. Hiatt, and Sidney K. Ayabe, October 23, 2020 (Defendant).

Deposition Testimony

1. U.S. Well Services, Inc. Plaintiffs, v. Halliburton Company, and Cimarex Energy Co., Defendants, In United States District Court Western District of Texas, Waco Division, Case No. 6:21-cv-00367-ADA, 28-July 2023

2. Joshua Baker, Plaintiff, v. Suzuki Motor Corporation, Defendant, in the circuit court of the Tenth Judicial Circuit in and for Polk Country, Florida, Case No.: 2016 CA 000780, January 11, 2023

3. Gail Lynn Plaintiffs, vs. Cordis Corporation, Johnson & Johnson, Defendants, in the circuit court of the Sixth Judicial Circuit in and for Pinellas County, Florida, Civil Division, Case No.: 2017-004345-CI, November 9 (2022)

4. U.S. Well Services, Inc. Plaintiffs, v. Halliburton Company, and Cimarex Energy Co., Defendants, In United States District Court Western District of Texas, Waco Division, Case No. 6:21-cv-00367-ADA, October 4, 2022

5. Kincade Fire Cases, JCCP No. 5157, Superior Court of the State of California, in and for the County of San Francisco, September 28, 2022

6. Rene Annette Richards, Plaintiffs, vs. Johnson & Johnson, Inc., Cordis Corporation, Confluent Medical Technologies, Inc. Defendants, Case No.: :17-Cv-00178-Bks-Atb, in the United States District Court for the Northern District of New York, March 4. (2021).

7. Honeywell International Inc., Plaintiff, vs. Forged Metals, Inc., Defendant, in the United States District Court for the District of Arizona, No. 2:19-cv-03730-JAT, December (2020).

8. Tadashi Mitsuoka and Victoria Mitsuoka, Individually and on the Behalf of a Class of All Persons Similarly Situated, Plaintiffs, Vs. Haseko Homes, Inc., a Hawaii Corporation, Haseko Construction, Inc., a Hawaii Corporation et al., Defendants, Case No. 17-0447-a, July 9." (2020).

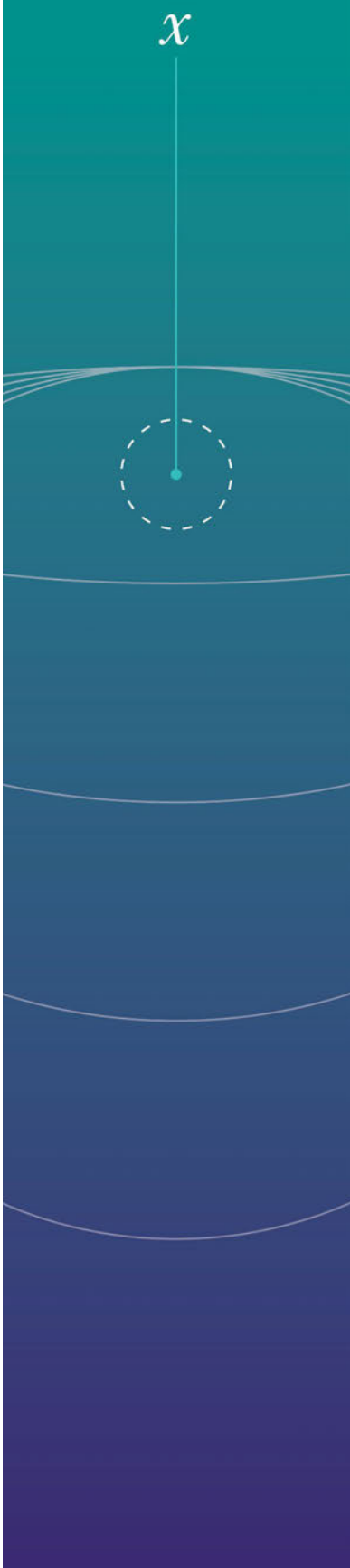

Appendix C

List of Reviewed Photographs Showing Underwater Cables

Appendix C: List of Reviewed Photographs Showing Underwater Cables

BTBMTS0012889	BTBMTS0037645	BTBMTS0039735	BTBMTS0039954
BTBMTS0012890	BTBMTS0037646	BTBMTS0039736	BTBMTS0039956
BTBMTS0012891	BTBMTS0037664	BTBMTS0039738	BTBMTS0039957
BTBMTS0013050	BTBMTS0037665	BTBMTS0039742	BTBMTS0039977
BTBMTS0013051	BTBMTS0037666	BTBMTS0039743	BTBMTS0039979
BTBMTS0013052	BTBMTS0037679	BTBMTS0039744	BTBMTS0040041
BTBMTS0013087	BTBMTS0037681	BTBMTS0039745	BTBMTS0040042
BTBMTS0013088	BTBMTS0037682	BTBMTS0039746	BTBMTS0040043
BTBMTS0013089	BTBMTS0037683	BTBMTS0039747	BTBMTS0040044
BTBMTS0013090	BTBMTS0038163	BTBMTS0039748	BTBMTS0040045
BTBMTS0013091	BTBMTS0039589	BTBMTS0039749	BTBMTS0040046
BTBMTS0013092	BTBMTS0039590	BTBMTS0039750	BTBMTS0040047
BTBMTS0013093	BTBMTS0039591	BTBMTS0039751	BTBMTS0040048
BTBMTS0013095	BTBMTS0039592	BTBMTS0039753	BTBMTS0040049
BTBMTS0013096	BTBMTS0039596	BTBMTS0039766	BTBMTS0040050
BTBMTS0013098	BTBMTS0039640	BTBMTS0039774	BTBMTS0040051
BTBMTS0022822	BTBMTS0039641	BTBMTS0039791	BTBMTS0040084
BTBMTS0023844	BTBMTS0039643	BTBMTS0039793	BTBMTS0040085
BTBMTS0023850	BTBMTS0039644	BTBMTS0039797	BTBMTS0040086
BTBMTS0025225	BTBMTS0039645	BTBMTS0039798	BTBMTS0040087
BTBMTS0025226	BTBMTS0039646	BTBMTS0039800	BTBMTS0040088
BTBMTS0025231	BTBMTS0039654	BTBMTS0039803	BTBMTS0040089
BTBMTS0025232	BTBMTS0039655	BTBMTS0039807	BTBMTS0040090
BTBMTS0025233	BTBMTS0039662	BTBMTS0039810	BTBMTS0040091
BTBMTS0026405	BTBMTS0039669	BTBMTS0039811	BTBMTS0040092
BTBMTS0027272	BTBMTS0039675	BTBMTS0039812	BTBMTS0040097
BTBMTS0028971	BTBMTS0039677	BTBMTS0039814	BTBMTS0040098
BTBMTS0030141	BTBMTS0039683	BTBMTS0039816	BTBMTS0040099
BTBMTS0032551	BTBMTS0039684	BTBMTS0039817	BTBMTS0040101
BTBMTS0032882	BTBMTS0039685	BTBMTS0039819	BTBMTS0040102
BTBMTS0032883	BTBMTS0039686	BTBMTS0039820	BTBMTS0040113
BTBMTS0035842	BTBMTS0039687	BTBMTS0039822	BTBMTS0040516
BTBMTS0035843	BTBMTS0039688	BTBMTS0039823	BTBMTS0040517
BTBMTS0035848	BTBMTS0039690	BTBMTS0039824	BTBMTS0043491
BTBMTS0035892	BTBMTS0039693	BTBMTS0039829	BTBMTS0043498
BTBMTS0035925	BTBMTS0039694	BTBMTS0039837	BTBMTS0043500
BTBMTS0035926	BTBMTS0039695	BTBMTS0039838	BTBMTS0045371
BTBMTS0035927	BTBMTS0039697	BTBMTS0039841	BTBMTS0045372
BTBMTS0035928	BTBMTS0039701	BTBMTS0039842	BTBMTS0045373
BTBMTS0035929	BTBMTS0039704	BTBMTS0039843	BTBMTS0045375
BTBMTS0037398	BTBMTS0039705	BTBMTS0039844	BTBMTS0045377
BTBMTS0037399	BTBMTS0039711	BTBMTS0039845	BTBMTS0045382
BTBMTS0037400	BTBMTS0039712	BTBMTS0039846	BTBMTS0045391
BTBMTS0037448	BTBMTS0039713	BTBMTS0039851	BTBMTS0045393
BTBMTS0037476	BTBMTS0039716	BTBMTS0039853	BTBMTS0045394
BTBMTS0037539	BTBMTS0039717	BTBMTS0039854	BTBMTS0045395
BTBMTS0037596	BTBMTS0039718	BTBMTS0039908	BTBMTS0045396
BTBMTS0037597	BTBMTS0039721	BTBMTS0039909	BTBMTS0045401
BTBMTS0037601	BTBMTS0039728	BTBMTS0039910	BTBMTS0045402
BTBMTS0037637	BTBMTS0039732	BTBMTS0039911	BTBMTS0045403
BTBMTS0037639	BTBMTS0039734	BTBMTS0039913	BTBMTS0045404

Appendix D

Explanation for Apparent Weight Loss vs. Weight Gain During Corrosion Testing

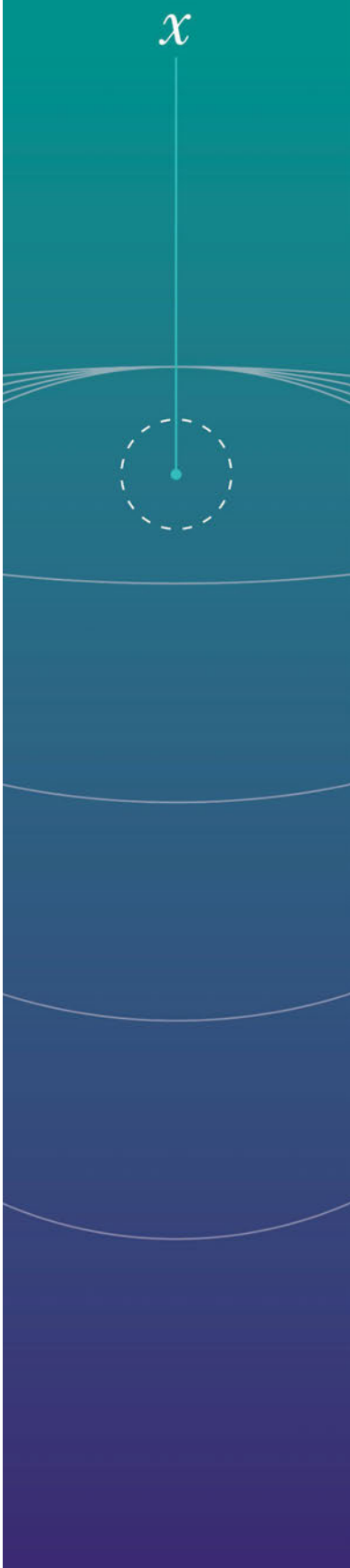

Appendix D: Explanation for Apparent Weight Loss vs. Weight Gain During Corrosion Testing

As described in the main body of the report, some academic literature shows that metals gain weight as they corrode because chemical species from the atmosphere react with the metal and become incorporated in the corrosion product (see the Introduction to Passivation section of this report). However, much of the academic literature discusses weight loss during corrosion testing rather than weight gain. This difference results from how corrosion testing is performed. Academic and engineering studies measuring corrosion rates generally determine corrosion rate by measuring weight loss of the metal that occurs when the metal surface is converted to corrosion product. This testing procedure involves exposing the material to a corrosive environment, deliberately removing the corrosion product or passivating layer after testing, then weighing the remaining metal.[121] This method results in a measured weight loss because the corrosion product or passivating layer is deliberately removed, even if such material would otherwise remain adhered to the metal if it was left undisturbed in the corrosive environment. This test method is useful for engineers who are concerned with how much load-bearing material remains after a certain amount of corrosion occurs rather than how much material has been lost to the environment.

As a practical example, structural engineers designing a steel bridge generally do not consider the amount of iron going into the environment as the bridge corrodes, but rather how the load carrying cross-section has been reduced. They account for this by either designing with thicker members or add a "corrosion allowance" to consider the amount of load bearing capacity that will be reduced during the structure's design life.[122] Therefore, most academic literature reporting experimental corrosion rates remove the corrosion product or passivating layer prior to determining the weight loss to determine the amount of metal surface converted to corrosion product. Consequently, corrosion or release rates based on weight loss measurements overestimate the amount of material that would be released to the surrounding environment, because such measurements involve deliberately removing the corrosion product or passivating layer that may otherwise remain adhered to the metal surface if left undisturbed.

[121] ASTM G1 (2003). Standard Practice for Preparing, Cleaning, and Evaluating Corrosion Test Specimens. ASTM International.

[122] Křivý, V. (2012). Design of corrosion allowances on structures from weathering steel. *Procedia Engineering, 40.*

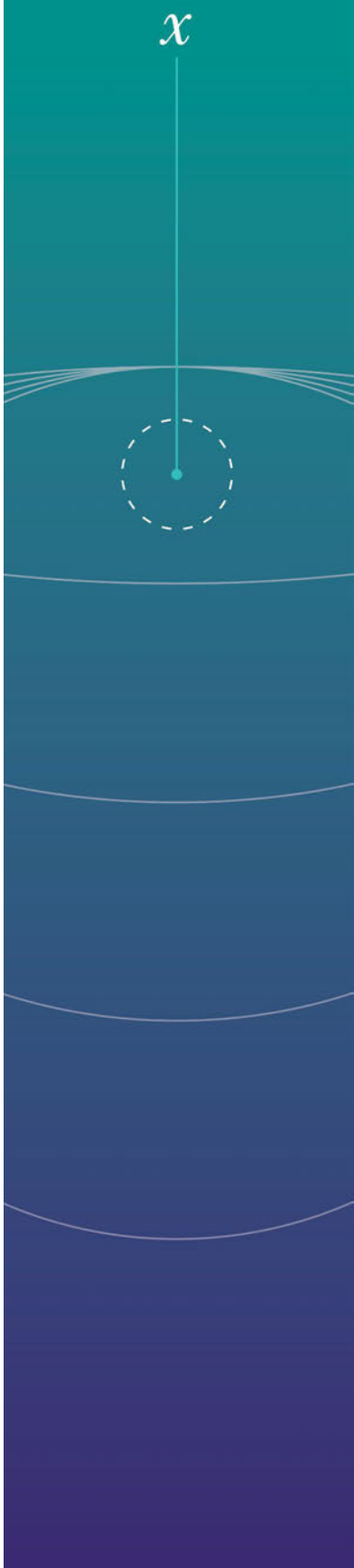

Appendix E

Detailed Examples of Corrosion Reactions and Passivating Layer Development in Lead

Appendix E: Detailed Examples of Corrosion Reactions and Passivating Layer Development in Lead

Figure E1 shows a schematic of the typical corrosion mechanism in a lead sample that is freshly exposed to water. Lead atoms are initially oxidized to a +2-valence state releasing two electrons, which are then consumed at a cathodic reaction site to reduce dissolved oxygen in the water to form a hydroxide ion (OH^-).

The released lead ions can react with anionic species to form corrosion products that can be protective. For example, Figure E2 shows the formation of a typical passivating layer on lead (cerussite $PbCO_3$). Note that corrosion may still occur in the presence of a passivating layer, but the corrosion rate may be much slower since it is limited by diffusion through the passivating layer. In addition, lead can be further oxidized to a +4-valence state.

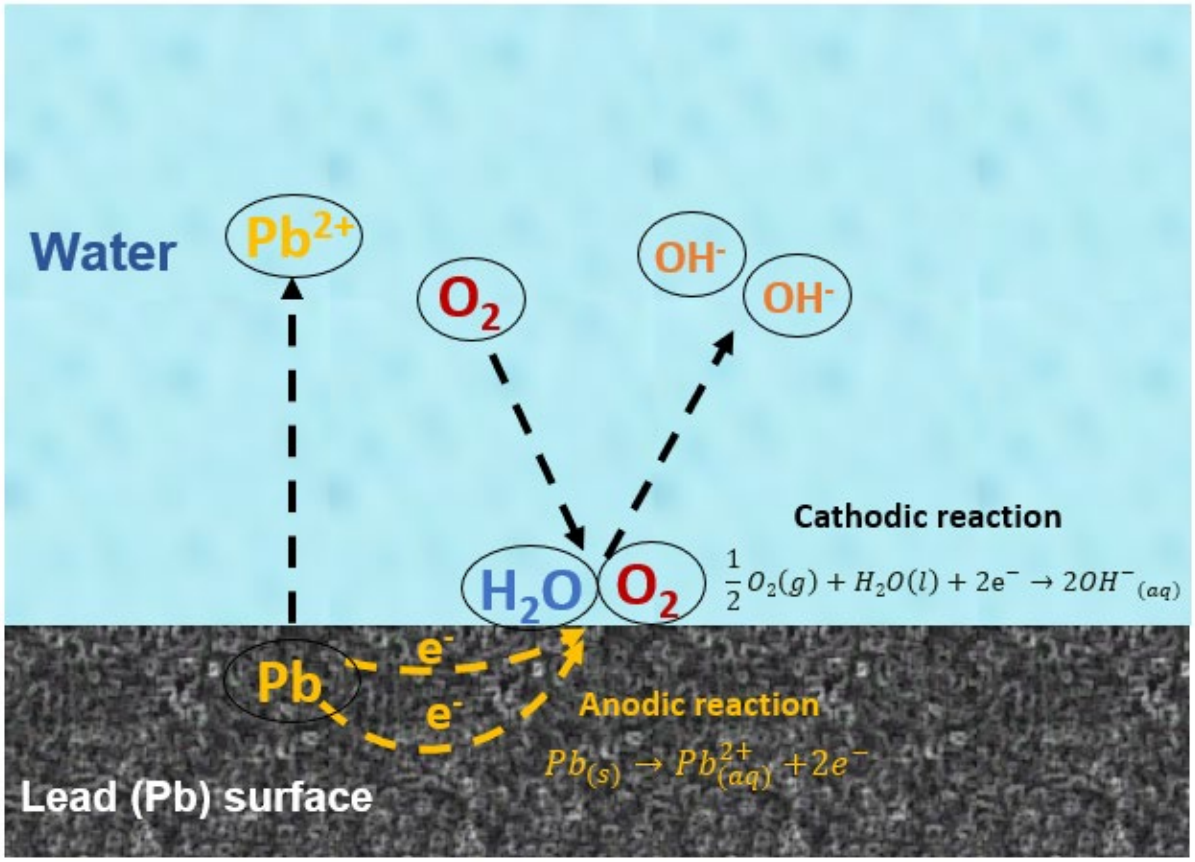

Figure E1. Schematic of corrosion mechanism of lead in an aqueous environment (Figure created by Exponent).

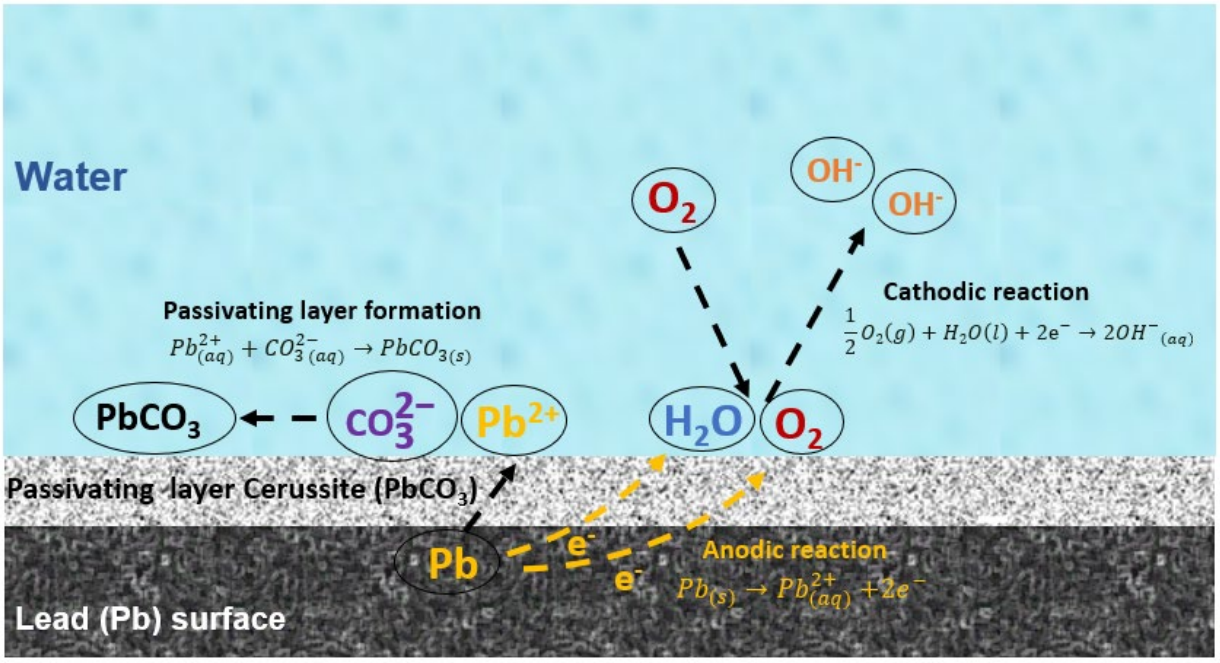

Figure E2. Schematic of a corrosion mechanism and formation of a passivating layer on lead in an aqueous environment (figure created by Exponent).